EUROPEAN Journal of Molecular Biotechnology

Has been issued since 2013.
ISSN 2310-6255. E-ISSN 2409-1332
2014. Vol.(6). № 4. Issued 4 times a year

The journal is registered by Federal Service for Supervision of Mass Media, Communications and Protection of Cultural Heritage (Russia). Registration Certificate **ПИ № ФС77-55114** 26.08.2013.

Journal is indexed by: **CiteFactor** – Directory of International Reseach Journals (Canada), **Cross Ref** (UK), **EBSCOhost Electronic Journals Service** (USA), **Global Impact Factor** (Australia), **International Society of Universal Research in Sciences** (Pakistan), **Journal Index** (USA), **Electronic scientific library** (Russian Federation), **Open Academic Journals Index** (Russian Federation), **Sherpa Romeo** (Spain), **ULRICH's WEB** (USA), **Universal Impact Factor** (Australia).

All manuscripts are peer reviewed by experts in the respective field. Authors of the manuscripts bear responsibility for their content, credibility and reliability.

Editorial board doesn't expect the manuscripts' authors to always agree with its opinion.

Postal Address: 26/2 Konstitutcii, Office 6
354000 Sochi, Russian Federation

Website: http://ejournal8.com/
E-mail: ejm2013@mail.ru

Founder and Editor: Academic Publishing House *Researcher*

Passed for printing 16.12.14.
Format 21 × 29,7/4.
Enamel-paper. Print screen.
Headset Georgia.
Ych. Izd. l. 4,5. Ysl. pech. l. 4,2.

Circulation 500 copies. Order № 6.

European Journal of Molecular Biotechnology

2014

№ 4

Европейский журнал молекулярных биотехнологий

2014

№ 4

Европейский журнал молекулярных биотехнологий

Издается с 2013 г. ISSN 2310-6255. E-ISSN 2409-1332
2014. № 4 (6). Выходит 4 раза в год.

Журнал зарегистрирован Федеральной службой по надзору в сфере массовых коммуникаций, связи и охраны культурного наследия (Российская Федерация). Свидетельство о регистрации средства массовой информации ПИ № ФС77-55114 от 26.08.2013 г.

Журнал индексируется в: **CiteFactor** – Directory of International Reseach Journals (Канада), **Cross Ref** (Великобритания), **EBSCOhost Electronic Journals Service** (США), **Global Impact Factor** (Австралия), **International Society of Universal Research in Sciences** (Пакистан), **Journal Index** (США), **Научная электронная библиотека** (Россия), **Open Academic Journals Index** (Россия), **Sherpa Romeo** (Испания), **ULRICH's WEB** (США), **Universal Impact Factor** (Австралия).

Адрес редакции: 354000, Российская Федерация, г. Сочи, ул. Конституции, д. 26/2, оф. 6
Сайт журнала: http://ejournal8.com/
E-mail: ejm2013@mail.ru

Учредитель и издатель: ООО «Научный издательский дом "Исследователь"» - Academic Publishing House *Researcher*

Подписано в печать 16.12.14.
Формат 21 × 29,7/4.
Бумага офсетная.
Печать трафаретная.
Гарнитура Georgia.
Уч.-изд. л. 4,5. Усл. печ. л. 4,2.
Тираж 500 экз. Заказ № 6.

CONTENTS

Published in the Russian Federation
European Journal of Molecular Biotechnology
Has been issued since 2013.
ISSN: 2310-6255
E-ISSN 2409-1332
Vol. 6, No. 4, pp. 160-169, 2014

DOI: 10.13187/ejmb.2014.6.160
www.ejournal8.com

UDC 553

Extraction, Identification and Quantitative HPLC Analysis of Flavonoids From Fruit Extracts of *Arbutus unedo* L from Tiaret Area (Western Algeria)

[1] Khadidja Bouzid
[1] Fouzia Toumi Benali
[2] Rabah Chadli
[2] Mohamed Bouzouina
[2] Aman Bouzid
[1] Amal Benchohra
[1] Mustapha Mahmoud Dif

[1] Djillali Liabes University, Algeria
Laboratory of Spaces Eco-development, Faculty of Natural and Life Sciences
Sidi Bel Abbes 22000
E-mail: bouzid_khadidja@yahoo.com
[2] University of Mostaganem, Algeria
Faculty of Sciences and the Natural Sciences and Life, BP300, Mostaganem 27000

Abstract

The aim of the current study was to evaluate the total phenolic, flavonoid content and to investigate the antioxidant capacities of the fruit extracts of *Arbutus unedo* L. that grows in Tiaret area (Western Algeria). First we have extracted the fruit by some non-polar solvent (chloroform, ethyl acetate, 1-butanol).

Total phenolic content and total flavonoid content were evaluated according to the Folin-Ciocalteu procedure, and a colorimetric method, respectively. Extracts content was determined by using a high-performance liquid chromatography (HPLC)-UV method. The total phenolic contents of *A.unedo* L. varied between 12.75±0.06 to 34.17±1.36 mg gallic acid equivalent/g of dry weight of extract. The total flavonoid varied from 2.18±0.10 to 6.54±1.14 mg catechin equivalent/g.

The antioxidant potential of all extracts was evaluated using 1,1-diphenyl-2-picrylhydrazyl (DPPH) free radical scavenging activity, the IC50 of acetate ethyl was the best by 0,009 mg/ml may due to the phenolic compound, in the second was the chloroform extract by IC50=0,015mg/ml, in the third was butanol extract by IC50= 0,022 mg/ml and in the last was water extract by IC50= 0,048mg/ml. the antioxidant activity of all extracts was better than ascorbic acid. The extract obtained under optimum conditions was analyzed by HPLC and five flavonoid compounds were identified; they are catechin, apiginin, silybin, fisetine and naringin.

Keywords: antioxidant activity; *Arbutus unedo* L.; fruit; flavonoids; phenols; HPLC; Western Algeria.

Introduction

The fruits of the strawberry tree (Arbutus unedo L.) are consumed mainly as processed product, but may be a good source of antioxidants if consumed as fresh fruit (Pallauf et al, 2008).

A. unedo, the strawberry tree, belongs to the Ericaceae family, and it is native of the Mediterranean climate (Celikel et al., 2008). It grows wildly in Mediterranean basin from sea level to about 600 m above sea level (Ayaz et al., 2000).

This species have been traditionally used as food, by using the arbutus berries in the production of alcoholic beverages, jams, jellies and marmalades (Alarcao-e-Silva et al., 2001; Pallauf et al., 2008); and as phytopharmaceuticals. The fruits are well known in folk medicine as antiseptic, diuretic, and laxative, while the leaves are used as astringent, diuretic, urinary antiseptic, antidiarrheal, depurative and more recently in the therapy of hypertension, diabetes and in the treatment of inflammatory diseases (Ziyyat et al., 1997; Ziyyat and Boussairi, 1998; Mariotto et al., 2008; Afkir et al., 2008). It is therefore of considerable interest to validate the bioactivities of *A. unedo* fruits in cell/organism-based assays to assess their potential therapeutic effect against a wide range of human diseases.

Polyphenolic compounds, such as phenolic acids and flavonoids, are important constituents in many plants, and their identification and quantification can give vital information relating to antioxidant function, food quality, and potential health benefits (Vesna et al, 2004). Wild fruits have been for a long time part of the human diet. In rural areas, wild fruits are consumed because of economic reasons not only as vitamin sources but also for medicinal purposes. Recent studies have focused on the description of phenolic compounds, such as flavonoids, phenolic acids and anthocyanins, as a part of the antioxidant compositions of these fruits (Pawlowska et al., 2006; Barros., 2008).

This paper is concerned with high performance liquid chromatography (HPLC) qualitative analysis of in *A.unedo* L. extracts obtained by successive extraction with solvents of different polarities (chloroform, ethyl acetate,1-butanol). Total phenolic and flavonoid contents as well as antioxidant activity of different extracts were investigated.

Materiel and methods:

Sample preparation and extraction

Biological material

Fruits of *A.unedo* L. (Ericaceae) were collected, in November 2013, from Guezoul djebel located at the end in North of the wilaya of Tiaret (latitude 35°22'26" N, longitude 1°10'30" E, altitude 1150 m), characterized by a semi-arid climate at fresh variant.

Powder preparation

Fruits randomly collected were oven dried (<40 ° C) until a constant dry weight, then ground to a fine powder using an electric grinder and finally stored at darkness at 25 ° C.

Extraction

100 g of fine powder of the dried fruit were macerated in a hydro-alcoholic mixture (methanol / water 80/20: v/v) for 72 hours, in the dark at room temperature, with renewal of solvent every 24 hours (350 ml x 3). Macerate was filtered through filter paper to obtain a clear extract, and then solvent was evaporated under vacuum at a temperature of 40° C, 200 ml of distilled water was added to the residue, extract was kept for 48 h in a refrigerator, then decanted, and was filtered again through filter paper (Lim et al., 2012).

The liquid-liquid extraction has been then carried out with three organic solvent system of increasing polarity: 200 ml of petroleum ether, 200 ml of chloroform, 200 ml of ethyl acetate and finally 200 ml of 1-butanol **(**Benhammou et al., 2007**)**. The residue of each solvent extract was dissolved in water, frozen and lyophilized. Chloroform, ethyl acetate, 1-butanol and aqueous crude extract powder were used for investigate phytochemical compounds, determination of total phenols, flavonoids content, antioxidant screening and for HPLC.

Determination of total phenolic contents

Total soluble phenolics of each fraction (chloroform, ethyl acetate, 1-butanol, aqueous) were determined with Folin-Ciocalteu reagent according to the method of (Singleton et al, 1999) using gallic acid as a standard phenolic compound. A volume of 40 µL of each fraction and standard was transferred into separate test tubes and to each added 3.16 mL water and 200 µL of Folin-Ciocalteu's reagent. The mixture was mixed well, waited for 8 min and then added 600 µL of sodium carbonate solution with continuous stirring. The solution was allowed to stand for 1 hour at

room temperature in a dark place and the absorption was measured at 750 nm using a spectrophotometer. The concentration of total phenolic compounds of all fractions of *A.unedo* fruit was determined as milligrams of gallic acid equivalent (GAE).

Determination of Flavonoid Content

The total flavonoid content of different fractions was analyzed by using catechin as standard (Kim et al., 2003). To 1 ml of extract solution (each of 100 µg/ml concentration), 4 ml of distilled water, 300 µl of sodium nitrite and aluminium chloride were added. The mixture was incubated at room temperature for 5 min. After the completion of incubation, 2 ml of sodium hydroxide was added and final volume of solution was raised to 10 ml by addition of distilled water. The absorbance of samples was measured at 510 nm. The total flavonoid content for all the fractions was expressed in terms of catechin equivalents (mg/g).

DPPH free radical-scavenging activity assay

The DPPH radical scavenging activity of extract was measured according to the slightly modified method of Liyana-Pathirana and Shahidi (2005). Sample extracts at various concentrations were taken and the volume was adjusted to 100 µl with methanol. 900 µl of 0.1 mM methanolic solution of DPPH was added and shaken vigorously. The tubes were allowed to stand for 20 min at 27 °C. The absorbance of the sample was measured at 517 nm. Radical scavenging activity was expressed as the inhibition percentage of free radical by the sample and was calculated using the formula: % DPPH radical scavenging activity = (control OD – sample OD/control OD) × 100.

Qualitative HPLC Analysis:

Analysis of extracts and standards were performed by Liquid chromatography was performed using a Shimadzu HPLC apparatus equipped with two LC-6A Vp pumps, an UV- VIS SPD-10A Module, an SLC-6B system controller, a Rheodyne injector 20 µL loop with RP-8 LiChroCart column (125 mm × 4.60 mm, 5 µm particle size). Chromatograms were obtained and analyzed using the software Class-VP ® (Shimadzu, Tokyo, Japan). The mobile phase consisted of a binary mixture of methanol- water (50:50 v/v) adjusted to pH 2.8 with phosphoric acid (Kuntić et al 2007) at isocratic flow rate of 1.0 mL min^{-1}. The absorbance was monitored at λ = 280 and 350 nm.

The need to know and identify flavonoidy individual compounds in the samples requires the replacement of traditional methods of separation techniques. High performance liquid chromatography is probably the most widely used analytical technique for characterizing the polyphenolic compounds (Gomez-Caravaca et al., 2006). This technique is used for the qualitative analysis of different extracts of the fruit of *A.unedo* L. taken from Tiaret area.

Statistical analysis

All tests were performed in triplicate and the results are presented as mean±standard deviation (SD). Differences with P values of <0.05 were considered significant.

Results and discussion

The yields of the extracts obtained per 100 g of dry plant material with the different solvents are given in Table 1.

Extract	Total extract (g/100 g of dry plant material)
Chloroform	0.25 ± 0.06
Aqueous	1.75 ± 0.16
1-butanol	0.34 ± 0.09
Ethyl acetate	0.44 ±0.09

The yield of aqueous extract was higher than yield of ethyl acetate,1-butanol and chloroform extract.

Total phenolic and flavonoid content

Total phenolic content of four crude extracts was determined by Folin-Ciocalteu method (Figure 1). Total phenols of *A.unedo* L. extracts were calculated according to the equation y= 0.001x + 0.0015 (r^2= 0.995) as Gallic Acid Equivalent (GAE, mg/g dry material), while total flavonoid contents were determined in accordance with the equation y= 0.002 x - 0.003 (r^2= 0.993) obtained by calibration curves as Catechin Equivalent (CE, mg/g dry material).

Total phenolic varied in different extracts was reported in Table 1: 29.46, 12.75, 34.17 and 32.84 mg Gallic Acid Equivalent /g of the dry extract in chloroform, aqueous, 1-butanol and ethyl acetate extract, respectively. Among the four crude extracts, 1-butanol extract contained the highest (34.17 mg GAE g of dry extract) amount of phenol compounds.

Figure 1: Gallic acid standard curve.

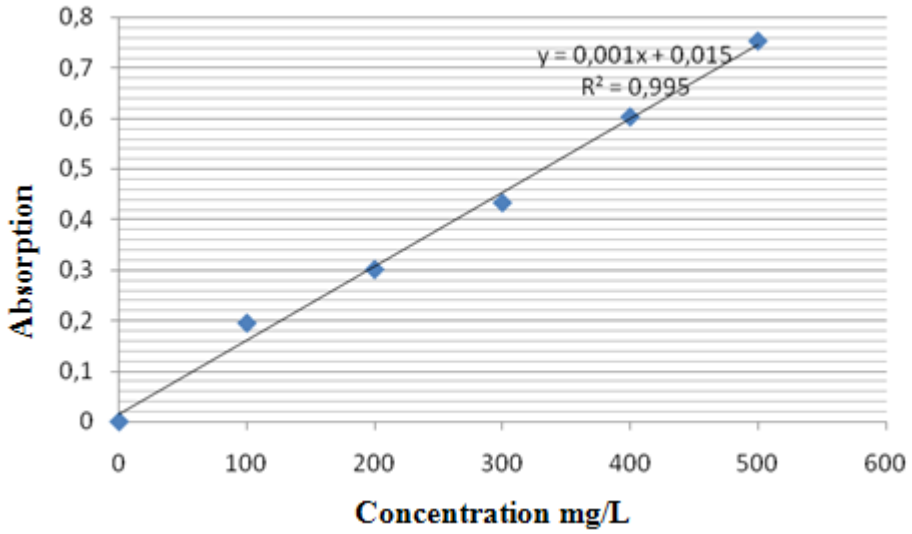

Table 1: Total phenolic content in *A.unedo* L. extracts

Extract	Total phenolic content (GAE mg/g extract)
Chloroform	29.46 ± 0.34
Aqueous	12.75 ± 0.06
1-butanol	34.17 ± 1.36
Ethyl acetate	32.84 ±0.53

In regard to the amount of flavonoids in the different crude extracts varied from 2.18 to 6.54 mg catechin equivalent/g (Tableau 2), chloroform extract contained a higher content of flavonoids (6.54 mg CE/g of the dry material), compared to ethyl acetate (5.59 mg CE/g), 1-butanol (3.61 mg CE/g) and aqueous extracts (2.18 mg CE/g) (figure 2).

Figure 2: Calibration cruve of quercetin standard.

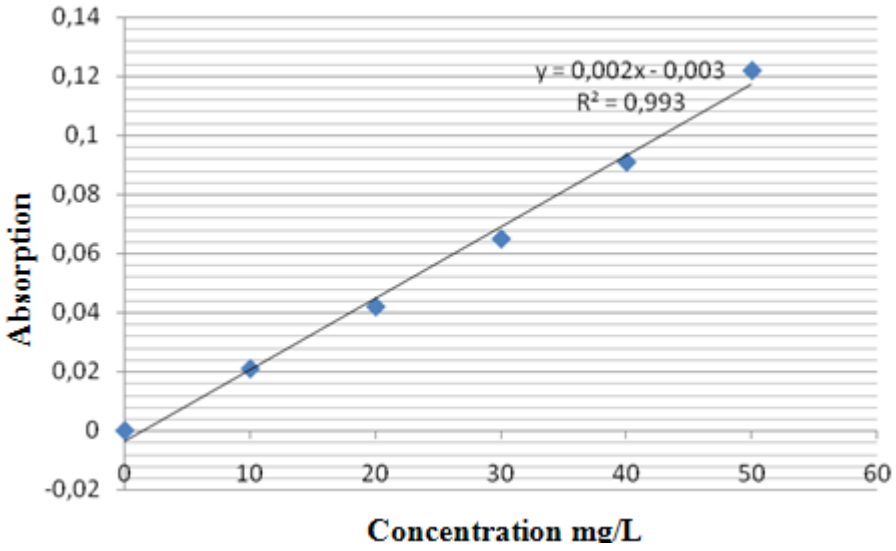

Table 2: Total flavonoid content in *A.unedo* L. extracts

Extract	Total flavonoid content (CE mg/g extract)
Chloroform	6.54 ± 1.14
Aqueous	2.18 ± 0.10
1-butanol	3.61 ± 0.59
Ethyl acetate	5.59 ± 0.82

Figure 2: IC50 (µg/mL) values of the DPPH assay in A.*unedo* L. fruit fractions

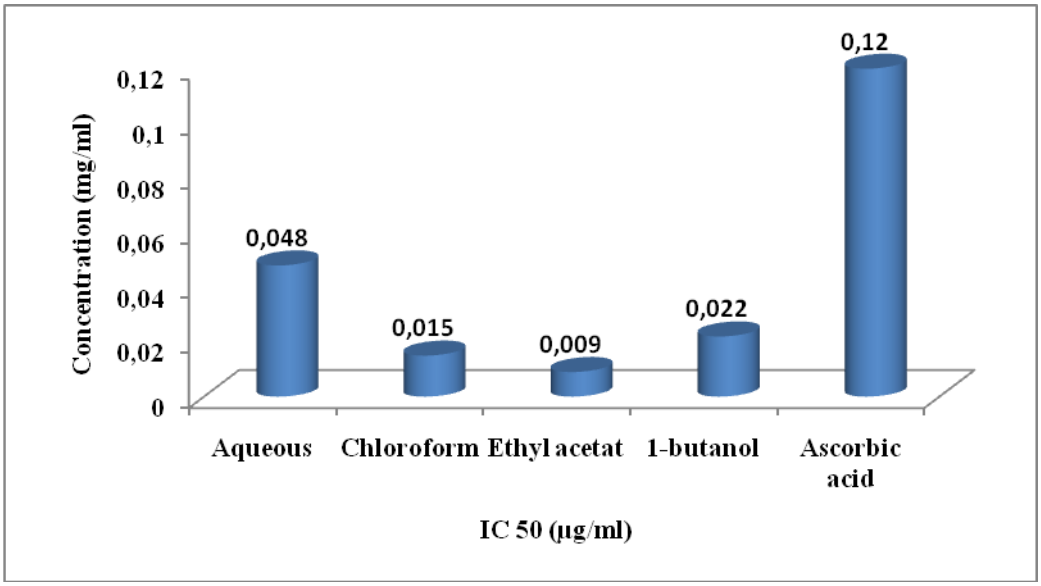

The IC50 value is a widely used parameter to measure the free radical scavenging activity. A lower IC50 indicates a higher antioxidant activity (Maisuthisakul et al., 2007). IC50 values for 1-butanol, aqueous, chloroform and ethyl acetate extract were: 0.022, 0.048, 0.015 and 0.009 mg/ml respectively, compared to the other work carried out by (Bouzid and Toumi, 2014). Several studies provide evidence to the fact that DPPH-scavenging ability is a reliable index of antioxidant

potential. The difference in the antioxidant activity of extracts may be attributed to the difference in the total phenolic and flavonoid content as well as the composition of these bioactive phytochemicals (sing et al., 2007). Reveals that fruits and vegetables have high values of important nutrients and phytochemicals which exhibit antioxidant functions (Hamza et al., 2013).

Identification of Various Phenolic Acids and Flavonoids in *A.unedo* L.

Based on these results, HPLC analysis was employed to define qualitative content of phenolic acids in A.*unedo* L extracts. HPLC Chromatograms of standards and different extracts are represented in Figure 4. (Naringin, Catechin, Apiginin, Fisetin, Taxifolin, Silybin) were identified in the investigated extracts by comparing spectra with those of standards (Figure 3).

Figure 3: HPLC chromatogram of part of phenolic standards at 280 nm

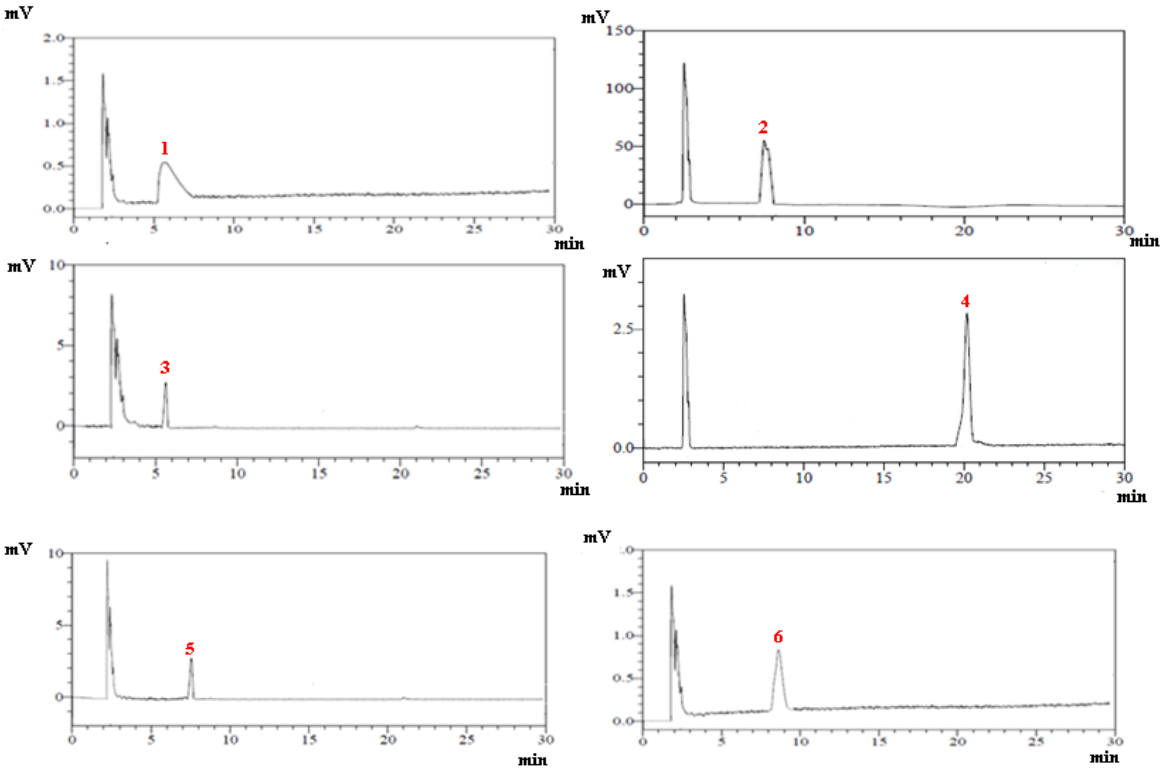

Peaks: **1**, Naringin; **2**, Catechin; **3**, Apiginin; **4**, Fisetin; **5**, Taxifolin; **6**, Silybin.

Figure 4: HPLC profiles of four fruit extract at 280 nm.

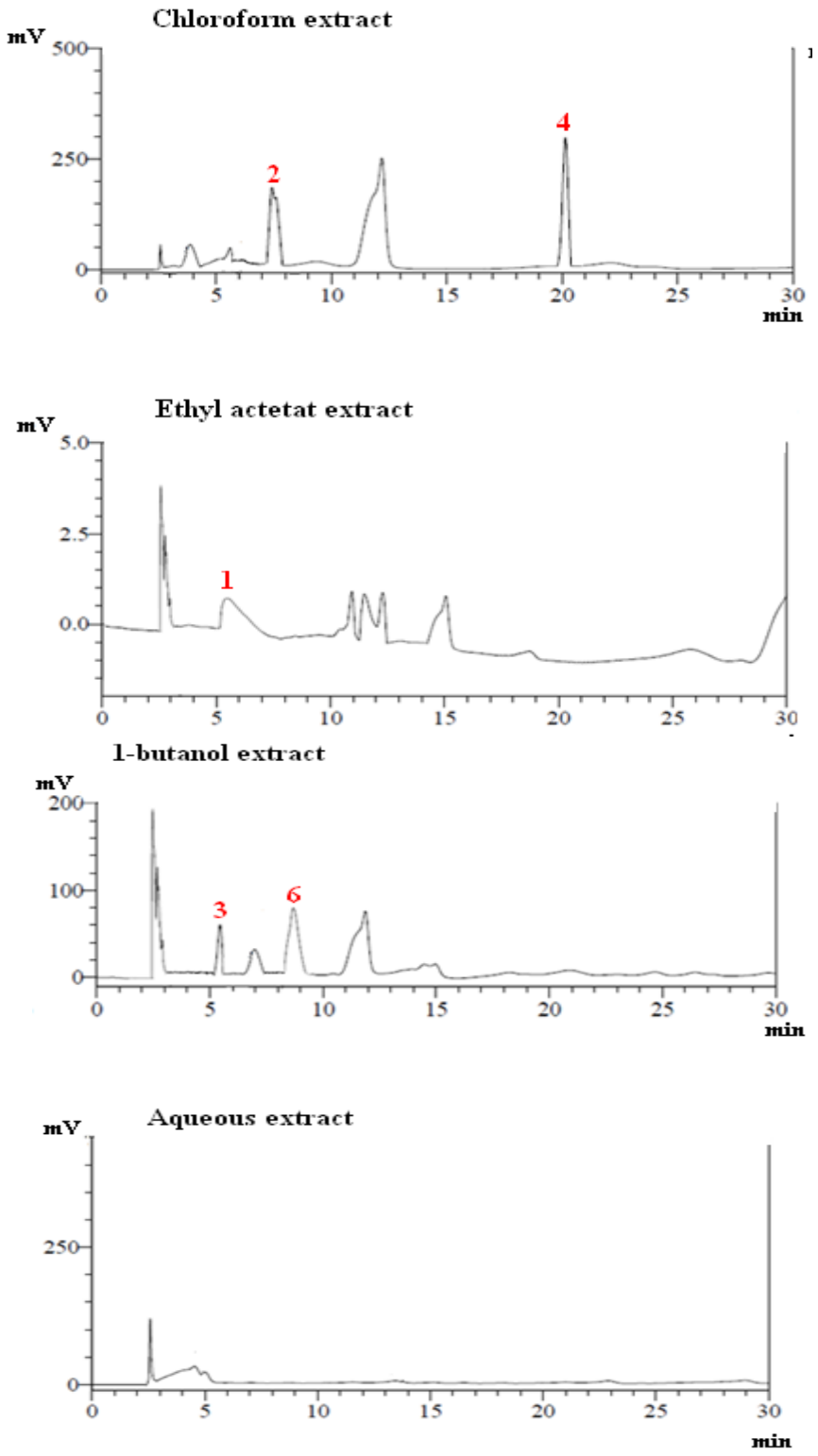

Peaks: **1**, Naringin; **2**, Catechin; **3**, Apiginin; **4**, Fisetin; **6**, Silybin

The results of qualitative HPLC analysis showed that Taxifolin was absent in all the fruit extract. Catechin and fisetin are present in chloroform extract, apeginin and silybin in 1-butanol

extract. These phenolic acids were not detected in aqueous extract, while ethyl acetate extract contained only naringin.

Peaks 1, 2, 3, 4 and 6 were positively identified as Naringin, Catechin, Apiginin, Fisetin and Silybin respectively, by comparing the retention time, absorption and mass spectra with that of standards (Figure 3 and 4). Figure 5 shows the chemical structures of phenolic compounds positively identified by comparison with standards.

Figure 5: Structures of phenolic compounds detected in fruit extracts.

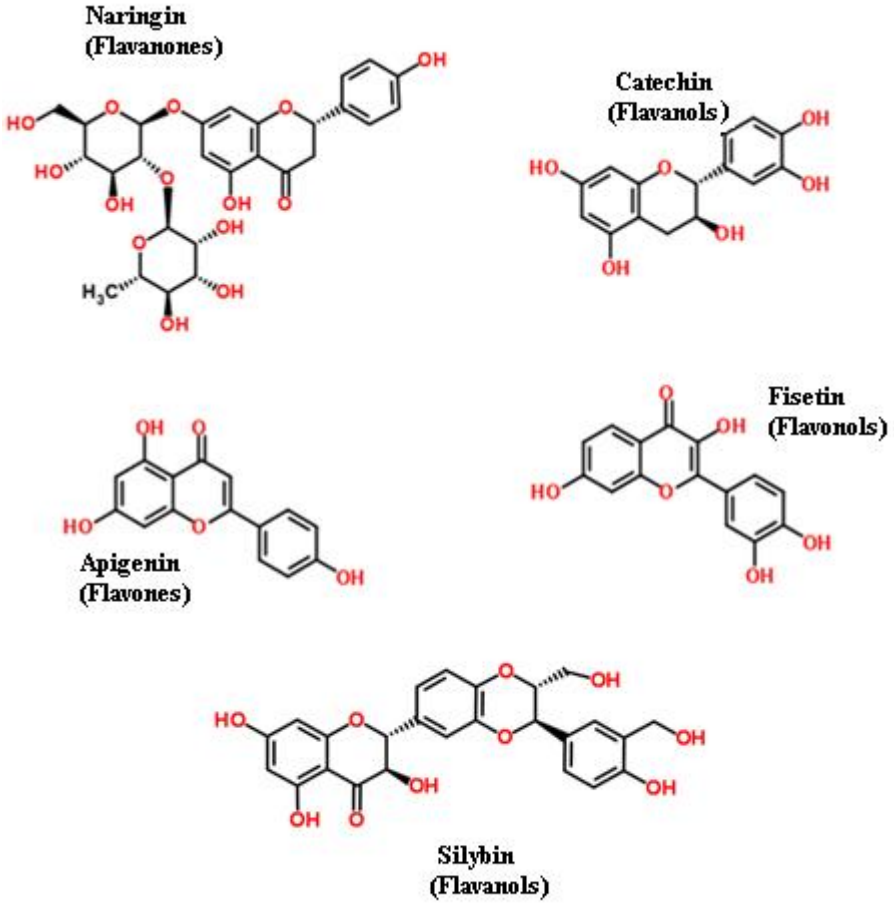

Conclusion

In conclusion, this study indicates that the extracts obtained from the fruit of *A. unedo* L. have significant free radical scavenging activity on stable DPPH• and high reactive hydroxyl radical. The data suggest that aqueous, ethyl acetate and chloroform extracts of *A.unedo* L. from Tiaret area are a potential source of natural antioxidants.

References

1. Pallauf K, Rivas-Gonzaloa JC, del Castilloc MD, Canob MP, de Pascual-Teresa S. Characterization of the antioxidant composition of strawberry tree (*Arbutus unedo* L.) fruits. J Food Compos Anal. 2008;21 (4):273–281.

2. Celikel G, Demirsoy L, Demirsoy H. The strawberry tree (*Arbutus unedo* L.) selection in Turkey. Sci. Hortic. 2008;118:115-119.

3. F.A. Ayaz, M. Kucukislamoglu, M. Reunanen, Sugar, nonvolatile and phenolic acids composition of strawberry tree (*Arbutus unedo* L. var. ellipsoides) fruits. J. Food Compos. Anal., 13 (2000), pp. 171–177

4. Alarcao-E-Silva ML, Leitao AEB, Azinheira HG, Leitao MCA (2001).The Arbutus Berry: studies on its color and chemical characteristics at two mature stages. J. Food Comp. Anal. 14:27-35.

A. Ziyyat, E. Boussairi, Cardiovascular effects of *Arbutus unedo* L; in spontaneously hypertensive rats, Phytother. Res., 12 (1998), pp. 110–113

A. Ziyyat, A. Legssyer, H. Mekhfi, A. Dassouli, M. Serhrouchni, W. Benjelloun

5. Phytotherapy of hypertension and diabetes in oriental Morocco, J. Ethnopharmacol., 58 (1997), pp. 45–54

6. S. Mariotto, E. Esposito, R. Di Paola, A. Ciampa, E. Mazzon, A. Carcereri de Parti, E. Darra, E. Vinzenzo, G. Cucinotta, R. Caminiti, H. Suzuki, S. Cuzzocrea,Protective effect of *Arbutus unedo* aqueous extract in carrageenan-induced lung inflammation in mice, Pharmacol. Res., 57 (2008), pp. 110–124

7. S.T. Afkir, B. Nguelefack, M. Aziz, J. Zoheir, G. Cuisinaud, M. Bnouham, H. Mekhfi, A. Legssyer, S. Lahlou, A. Ziyyat, *Arbutus unedo* prevents cardiovascular and morphological alterations in L-NAME-induced hypertensive rats, part I: cardiovascular and renal hemodynamic effects of *Arbutus unedo* L. in L-NAME-induced hypertensive rats, J. Ethnopharmacol., 116 (2008), pp. 288–295

8. Vesna T. Tumbas, Anamarija I. Mandić, Gordana S. Ćetković, Sonja M. Đilas and Jasna M. Čanadanović-Brunet, HPLC ANALYSIS OF PHENOLIC ACIDS IN MOUNTAIN GERMANDER (Teucrium montanum L.) EXTRACTS. APTEFF, 35, 1-280 (2004).

9. Pawlowska, A.M., Leo, M., Braca, A. Phenolics of Arbutus unedo L. (Ericaceae) Fruits: Identification of anthocyanins and gallic acid derivatives. Journal of Agricultural and Food Chemistry, 2006, 54, 10234-10238

10. Barros, L., Carvalho, A.M., Morais, J.S., Ferreira, I. Strawberry-tree, blackthorn and rose fruits: Detailed characterisation in nutrients and phytochemicals with antioxidant properties. Food Chemistry, 2010, 1, 247–254.

11. Benhammou N, Atik F, Bekkara and Kadifkova Panovska T (2007). Antiradical capacity of the phenolic compounds of Pistacia lentiscus L and Pistacia atlantica Desf. *Adv Food Sci*, 29(3):155-16.

12. Lim T.K (2012). Edible Medicinal and non-medicinal plants, volume 2, fruits. pp1088

13. Singleton, V.L., R. Orthofer and R.M. Lamuela-Raventos, 1999. Analysis of total phenols and other oxidation substrates and antioxidants by means of folin-ciocalteu reagent. Methods Enzymol., 299: 152-178.

14. Kim, D., O. Chun, Y. Kim, H. Moon and C. Lee, 2003. Quantification of phenolics and their antioxidant capacity in fresh plums. J. Agric. Food Chem., 51: 6509-6515.

15. Liyana-Pathirana, C.M. and F. Shahidi, 2005. Antioxidant activity of commercial soft and hard wheat (*Triticum aestivum* L.) as affected by gastric pH conditions. J. Agric. Food Chem., 53: 2433-2440.

16. Kuntic V., Pejic N., Ivkovic B. (2007). Isocratic RP-HPLC method for rutin determinationin solid oral dosage forms. J Pharm Biomed Anal,43(2),718–721.

17. Gómez-Caravaca, A. M., Gómez-Romero, M., Arráez-Román, D., Segura-Carretero, A., & Fernández-Gutiérrez, A. (2006). Advances in the analysis of phenolic compounds in products derived from bees. Journal of Pharmaceutical and Biomedical Analysis, 41, 1220-1234. PMid:16621403.

18. Maisuthisakul P, Suttajit M, Pongsawatmanit R (2007). Assessment of phenolic content and free radical scavenging capacity of some Thai indigenous plants. Food Chem., 100(4): 1409-1418.

19. Singh R, Singh S, Kumar S, Arora S (2007) Evaluation of antioxidant potential of ethyl acetate extract/fractions of Acacia auriculiformis A Cunn. Food ChemToxicol 45, 1216–23.

20. Bouzid K, Benali Toumi F (2014) Influences géo-climatiques sur les constituants et effets antioxydants du fruit *Arbutus unedo* L. Phytothérapie, Volume 12, Issue 4, pp 229-233.

Published in the Russian Federation
European Journal of Molecular Biotechnology
Has been issued since 2013.
ISSN: 2310-6255
E-ISSN 2409-1332
Vol. 6, No. 4, pp. 169-179, 2014

DOI: 10.13187/ejmb.2014.6.169
www.ejournal8.com

UDC 735.29: 573.552

Modeling of Possible Conditions for Origin of First Organic Forms in hot Mineral Water

[1] Ignat Ignatov
[2] Oleg Mosin

[1] Scientific Research Center of Medical Biophysics (SRC MB), Bulgaria
Professor, D. Sc., director of SRC MB
1111, Sofia, N. Kopernik street, 32
E-mail: mbioph@dir.bg
[2] Moscow State University of Applied Biotechnology, Russian Federation
Senior research Fellow of Biotechnology Department, Ph. D. (Chemistry)
103316, Moscow, Talalihina ulitza, 33
E-mail: mosin-oleg@yandex.ru

Abstract

The composition of water, its temperature and pH value was analyzed in experiments with modelling of primary hydrosphere and possible conditions for origin of first organic forms in hot mineral water. For this aim the authors performed experiments with hot mineral and seawater from Bulgaria by IR-spectrometry (DNES-method). As model systems were used cactus juice of *Echinopsis pachanoi* and Mediterranean jellyfish *Cotylorhiza tuberculata*. It was considered the reactions of condensation and dehydration in alkaline aqueous solutions with pH = 9–10, resulting in synthesis from separate molecules larger organic molecules as polymers and short polipeptides. It was shown that hot alkaline mineral water with temperature from +65 °C to +95 °C and pH value from 9 to 11 is more suitable for the origination of life and living matter than other analyzed water samples. The pH value of seawater on contrary is limited to the range of 7,5 to 8,4 units. Two common local maximums were observed in the IR-spectra of jellyfish and seawater, which were more pronouncedly expressed in IR-spectra of jellyfish.

Keywords: deuterium; hydrosphere; evolution; origin of life; IR-spectrometry.

Introduction

Previous biological experiments with D_2O and structural-conformational studies with deuterated molecules, performed by us, enable to modeling conditions under which the first living forms of life might be evolved [1–3]. The content of deuterium in hot mineral water may be increased due to the physical chemical processes of the deuterium accumulation. It can be presumed that primary water might contain more deuterium at early stages of evolution of first living structures, and deuterium was distributed non-uniformly in the hydrosphere and atmosphere [4]. The primary reductive atmosphere of the Earth consisted basically of gas mixture CO, H_2, N_2, NH_3, CH_4, lacked O_2–O_3 layer protecting the Earth surface from rigid short-wave solar radiation carrying huge energy capable to cause radiolysis and photolysis of water. The processes accompanying accumulation of deuterium in the hydrosphere are solar radiation, volcanic

geothermal processes and electric discharges in the atmosphere. These natural processes could lead to the enrichment of the hydrosphere by deuterium in the form of HDO which evaporates more slowly then H_2O, and condenses faster. If this is true, this is a significant fact regarding thermal stability of deuterated macromolecules in the preservation of life under thermal conditions, because chemical bonds with participation of deuterium are stronger than those ones formed of hydrogen.

Natural prevalence of deuterium makes up approximately 0,015–0,020 at.%, and depends strongly on the uniformity of substance and the total amount of matter formed in the course of early Galaxy evolution [5]. Constant sources of deuterium are explosions of nova stars and thermonuclear processes frequently occurring inside the stars. Probably, it could explain a known fact, why the amount of deuterium is slightly increased during the global changes of climate in warming conditions. The gravitational field of the Earth is insufficiently strong for the retaining of lighter hydrogen, and our planet is gradually losing hydrogen as a result of its dissociation into interplanetary space. Hydrogen evaporates faster than heavy deuterium, which can be collected by the hydrosphere. Therefore, as a result of this natural process of fractionation of H/D isotopes throughout the process of Earth evolution there should be an accumulation of deuterium in the hydrosphere and surface waters, while in the atmosphere and in water vapour deuterium content tends to be low. Thus, on the planet there occurs a natural process of separation of H and D isotopes, playing an essential role in the maintenance of life on the planet.

The second point regards the influence of temperature on the processes in living matter. Recent studies have shown that the most favorable for the origin of life and living matter seem to be hot alkaline mineral waters interacting with $CaCO_3$ [6, 7]. According to the law for conservation of energy the process of self-organization of primary organic forms in water solutions may be supported by thermal energy of magma, volcanic activity and solar radiation. According to J. Szostak, the accumulation of organic compounds in open lakes is more possible compared to the ocean [8]. Life began near a hydrothermal vent: an underwater spout of hot water. Geothermal activity gives more opportunities for the origination of life. In 2009 A. Mulkidjanian and M. Galperin demonstrate that the cell cytoplasm contains potassium, zinc, manganese and phosphate ions, which are not particularly widespread in the sea aquatorium [9]. J. Trevors and G. Pollack proposed in 2005 that the first cells on the Earth assembled in a hydrogel environment [10]. Gel environments are capable of retaining water, oily hydrocarbons, solutes, and gas bubbles, and are capable of carrying out many functions, even in the absence of a membrane. Hydrocarbons are an organic compounds consisting entirely of hydrogen and carbon. The data presented in this paper show that the origination of living matter most probably occurred in hot mineral water. This occurred in ponds and hydrothermal vents in seawater or hot mineral water. An indisputable proof of this is the presence of stromatolites fossils. They lived in warm and hot water in zones of volcanic activity, which could be heated by magma and seem to be more stable than other first sea organisms [11].

The purpose of the research was studying the conditions of primary hydrosphere (temperature, pH, isotopic composition) for possible processes for origin of life and living matter in hot mineral water. Various samples of water from Bulgaria were studied within the frames of the research.

Materials and methods

The research by the IR-spectrometry (DNES-method) was carried out with samples of water taken from various water springs of Bulgaria:

1 – mineral water (Rupite, Bulgaria);
2 – seawater (Varna resort, Bulgaria);
3 – mountain water (Teteven, Bulgaria);
5 – deionized water (the control).

As two model systems were used cactus juice of *Echinopsis pachanoi* and Mediterranean jellyfish *Cotylorhiza tuberculata* (Chalkida (Greece), Aegean Sea), which were both investigated by the IR-spectrometry.

IR-spectra of water samples were registered on Brucker Vertex ("Brucker", Germany) Fourier-IR spectrometer (spectral range: average IR – 370–7800 cm^{-1}; visible – 2500–8000 cm^{-1};

permission – 0,5 cm^{-1}; accuracy of wave number – 0,1 cm^{-1} on 2000 cm^{-1}); Thermo Nicolet Avatar 360 Fourier-transform IR (M. Chakarova); Differential Non-equilibrium Spectrum (DNES).

A device for high-frequency coronal electric discharge was used in this study, constructed by I. Ignatov and Ch. Stoyanov [12]. The frequency of the applied saw-tooth electric voltage was 15 kHz, and the electric voltage – 15 кV. The electric discharge was obtained using a transparent firm polymer electrode on which a liquid sample of water (2–3 mm) was placed. The spectral range of the photons released upon electric discharge was from λ = 400 to λ = 490 nm and from λ = 560 to λ = 700 nm.

Results and discussion

We have carried out the research of various samples of mineral water from mineral springs and seawater from Bulgaria (Fig. 1, curves *1–5*). For this aim we employed the IR-spectrometry and DNES method relative to the control – deionized water. Cactus juice was also investigated by the DNES method (Fig. 1, *curve 1*). The cactus was selected as a model system because this plant contains approximately 90 % of water. The closest to the spectrum of cactus juice was the spectrum of mineral water contacting with Ca^{2+} and HCO_3^- ions (Fig. 1, *curve 2*). DNES-spectra of cactus juice and mineral water have magnitudes of local maximums at –0,1112; -0,1187; -0,1262; -0,1287 and –0,1387 eV. Similar local maximums in the DNES-spectrum between cactus juice and seawater were detected at -0,1362 eV. The spectrum of the control sample of deionized water (Fig. 1, *curve 5*) was substantially different from the spectra of seawater and mineral water. Another important parameter was measured by the DNES method – the average energy ($\Delta E_{H...O}$) of hydrogen H...O-bonds among individual molecules H_2O, which makes up -0,1067±0,0011 eV. When the water temperature is changed, the average energy of hydrogen H...O-bonds alternates. This testified about the restructuring of average energies among individual H_2O molecules with a statistically reliable increase of local maximums in DNES-spectra.

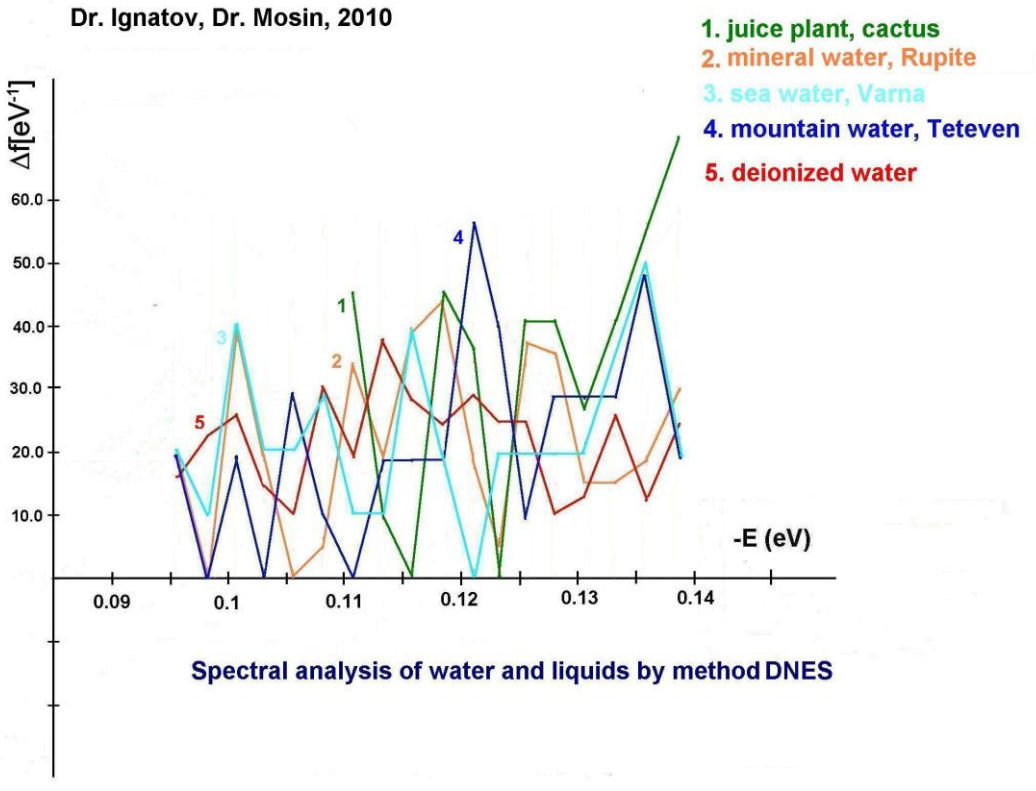

Figure 1. DNES-spectra of water samples of various origin: 1 – cactus juice; 2 – mineral water from Rupite village (Bulgaria); 3 – seawater (Varna, Bulgaria); 4 – mountain water (Teteven, Bulgaria); 5 – deionized water (the control)

As shown from these data, the closest to the IR-spectrum of cactus juice was mineral water from Rupite Village (Bulgaria), which DNES and IR spectrum is shown in Fig. 2 and Fig. 3 (Thermo

Nicolet Avatar 360 Fourier-transform IR). IR-spectra of cactus juice and mineral water with HCO_3^- (1320–1488 mg/l), Ca^{2+} (29–36 mg/l), pH (6,85–7,19), have local maximums at 8,95; 9,67; 9,81; 10,47 and 11,12 μm (Fourier-IR spectrometer Brucker Vertex). Common local maximums in the IR-spectrum between cactus juice and seawater are detected at 9.10 μm. The local maximums obtained with IR method at 9,81 μm (1019 cm^{-1}) and 8,95 μm (1117 cm^{-1}) (Thermo Nicolet Avatar 360 Fourier-transform IR) are located on the spectral curve of the local maximum at 9,7 μm (1031 cm^{-1}) (Fig. 3). With the DNES method were obtained the following results – 8,95; 9,10; 9,64; 9,83; 10,45 and 11,15 μm, or 897; 957; 1017; 1037; 1099 and 1117 wave numbers.

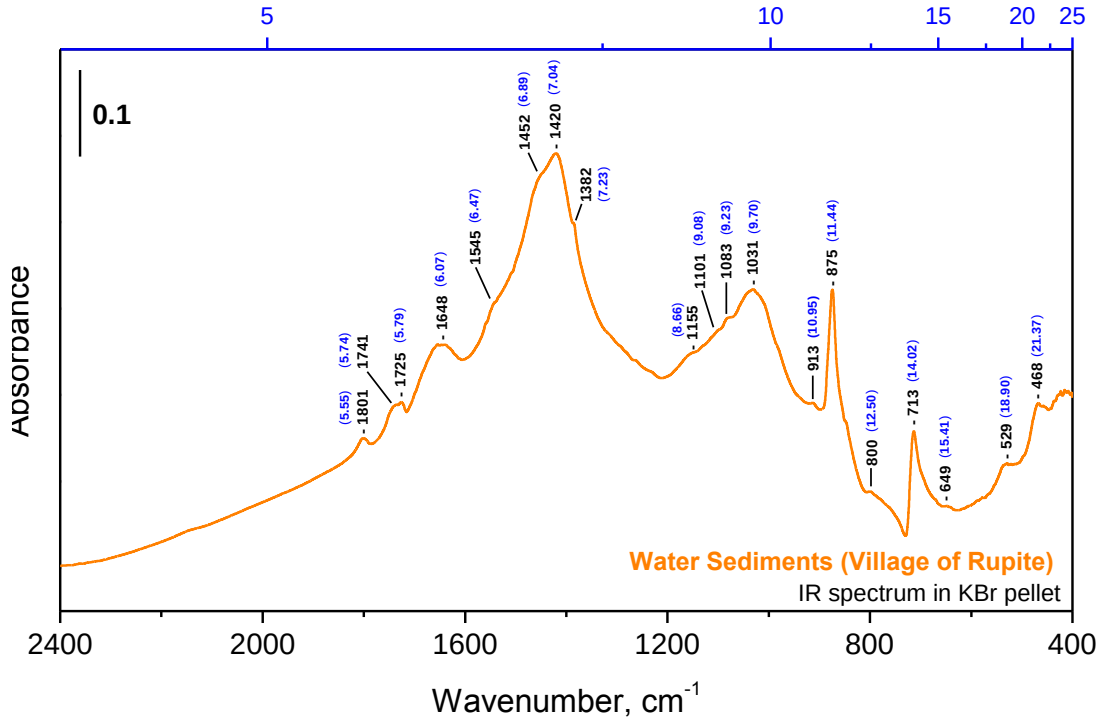

Figure 2. IR-spectrum of water obtained from Rupite Village (Bulgaria)

Table: Characteristics of spectra of water of various origin obtained by DNES-method*

-E, eV			λ, μm	k, cm^{-1}
Cactus juice	Mineral water from Rupite Village (Bulgaria)	Seawater		
0,1112	0,1112	–	11,15	897
0,1187	0,1187	–	10,45	957
0,1262	0,1262	–	9,83	1017
0,1287	0,1287	–	9,64	1037
0,1362	–	0,1362	9,10	1099
0,1387	0,1387	–	8,95	1117

The note:
*The function of the distribution of energies Δf was measured in reciprocal electron volts (eV^{-1}). It is shown at which values of the spectrum -E (eV) are observed the biggest local maximums of this function; λ – wave length; κ – wave number.

The results with Mediterranean jellyfish *Cotylorhiza tuberculata* indicated that jellyfish has local maximums in IR-spectra at 8,98 and 10,18 μm (Fig. 3). Before measurements the jellyfish was kept in seawater for several days. On comparison seawater has a local maximum at 8,93 μm in IR-spectra. These results were obtained with Thermo Nicolet Avatar 360 Fourier-transform IR. With

DNES method the local maximums in spectra for jellyfish are at 8,95 and 10,21 μm, and for seawater at 9,10 μm. A differential spectrum was recorded between jellyfish and seawater by using the Thermo Nicolet Avatar 360 Fourier-transform IR method. In IR-spectrum of jellyfish are observed more pronouncedly expressed local maximums, detected by Thermo Nicolet Avatar 360 Fourier-transform IR and DNES method. Measurements demonstrate that two common local maximums are observed in IR-spectra of jellyfish and seawater. These maximums are not observed in the IR-spectrum of cactus juice and mineral water from Rupite (Bulgaria). Jellyfish contains approximately 97 (w/w) % of water and is more unstable living organism compared to those ones formed stromatolites. The explanation for this is the smaller concentration of salts and, therefore, the smaller number of local maximums in the IR-spectrum in relation to seawater.

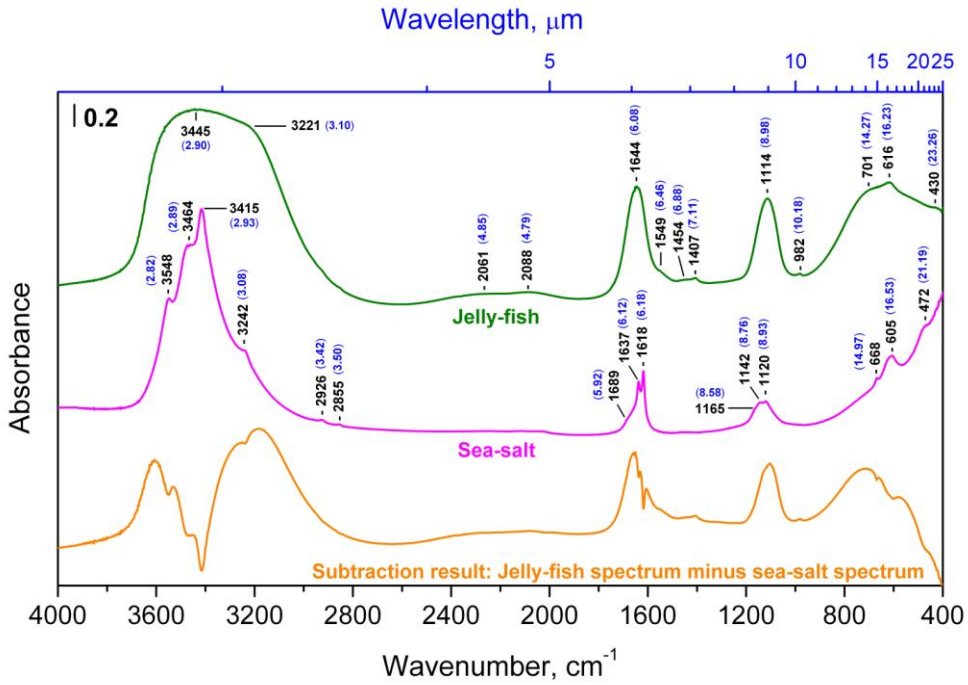

Figure 3. IR-spectrum of seawater obtained from Varna (Bulgaria) and jellyfish *Cotylorhiza tuberculata*, Chalkida (Greece), Aegean Sea

Such a character of IR- and DNES-spectra and distribution of local maximums may prove that hot mineral alkaline water is preferable for origin and maintenance of life compared to other types of water analyzed by these methods. Thus, in hot mineral waters the local maximums in the IR-spectrum are more manifested compared to the local maximums obtained in IR-spectrum of the same water at a lower temperature. The difference in the local maximums from +20 °C to +95 °C at each 5 °C according to Student t-criterion – $p < 0,05$. These data indicate that the origination of life and living matter depends on the structure and physical chemical properties of water, as well as its temperature and pH value. The most closed to the IR- and DNES-spectrum of water, which contains bicarbonates and calcium ions typical for the formation of stromatolites is the IR-spectrum of cactus juice. For this reason cactus juice was applied as a model system. The most closed to local maximums in IR-spectrum of cactus juice are local maximums in IR-spectra of alkaline mineral water interacting with $CaCO_3$ and then seawater. In connection with these data the following reactions participating with $CaCO_3$ in aqueous solutions are important:

$$CO_2 + 4H_2S + O_2 = CH_2O + 4S + 3H_2O, \quad (1)$$

$$CaCO_3 + H_2O + CO_2 = Ca(HCO_3)_2, \quad (2)$$

$$CO_2 + OH^- = HCO_3^- \quad (3)$$

$$2HCO_3^- + Ca^{2+} = CaCO_3 + CO_2 + H_2O \quad (4)$$

The equation (1) shows how some chemosynthetic bacteria use energy from the oxidation of H_2S and CO_2 to S and formaldehyde (CH_2O). The equation (2) is related to one of the most common

processes in nature: in the presence of H_2O and CO_2, $CaCO_3$ transforms into $Ca(HCO_3)_2$. In the presence of hydroxyl OH^- ions, CO_2 transforms into HCO_3^- (equation (3)). Equation (4) is valid for the process of formation of the stromatolites – the dolomite layered acretionary structures formed in shallow seawater by colonies of cyanobacteria. In 2010 D. Ward described fossilized stromatolites in the Glacier National Park (USA) [13]. Stromatolites aged 3,5 billion years had lived in warm and hot water in zones of volcanic activity, which could be heated by magma. This suggests that the first living forms evidently evolved in hot geysers [14]. It is known that water in geysers is rich in carbonates, while the temperature is ranged from +100 °C to +150 °C. In 2011 a team of Japanese scientists under the leadership of T. Sugawara showed that life originated in warm or, more likely, hot water [15]. From aqueous solution of organic molecules, DNA and synthetic enzymes were created proto cells. For this the initial solution was heated to a temperature close to water's boiling point +95 °C. Then its temperature was lowered to +65 °C with formation of proto cells with primitive membrane. This laboratory experiment is an excellent confirmation of the possibility that life originated in hot water.

The above-mentioned data can predict a possible transition from synthesis of small organic molecules under high temperatures to more complex organic molecules as proteins. There are reactions of condensation-dehydration of amino acids into separate blocks of peptides that occur under alkaline conditions, with pH = 9–11. The important factor in reaction of condensation of two amino acid molecules into dipeptide is allocation of H_2O molecule when a peptide chain is formed. As reaction of polycondensation of amino acids is accompanied by dehydration, the H_2O removal from reaction mixture speeds up the reaction rates. This testifies that formation of early organic forms may have occured nearby active volcanoes, because at early periods of geological history volcanic activity occurred more actively than during subsequent geological times. However, dehydratation accompanies not only amino acid polymerization, but also association of other small blocks into larger organic molecules, and also polymerization of nucleotides into nucleic acids. Such association is connected with the reaction of condensation, at which from one block a proton is removed, and from another – a hydroxyl group with the formation of H_2O molecule.

In 1969 the possibility of existence of condensation-dehydration reactions under conditions of primary hydrosphere was proven by M. Calvin [16]. From most chemical substances hydrocyanic acid (HCN) and its derivatives – cyanoamid (CH_2N_2) and dicyanoamid ($HN(CN)_2$) possess dehydration ability and the ability to catalyze the process of linkage of H_2O from primary hydrosphere [17]. The presence of HCN in primary hydrosphere was proven by S. Miller's early experiments [18]. Chemical reactions with HCN and its derivatives are complex with a chemical point of view; in the presence of HCN, CH_2N_2 and $HN(CN)_2$ the condensation of separate blocks of amino acids accompanied by dehydration, can proceed at normal temperatures in strongly diluted H_2O-solutions. These reactions show the results of synthesis from separate smaller molecules to larger organic molecules of polymers, e.g. proteins, polycarboxydrates, lipids, and ribonucleic acids (Fig. 4). Furthermore, polycondensation reactions catalyzed by HCN and its derivatives depend on acidity of water solutions in which they proceed [19]. In acid aqueous solutions with pH = 4–6 these reactions do not occur, whereas alkaline conditions with pH = 9–10 promote their course. There has not been unequivocal opinion, whether primary water was alkaline, but it is probable that such pH value possessed mineral waters adjoining with basalts, i.e. these reactions could occur at the contact of water with basalt rocks, that testifies our hypothesis.

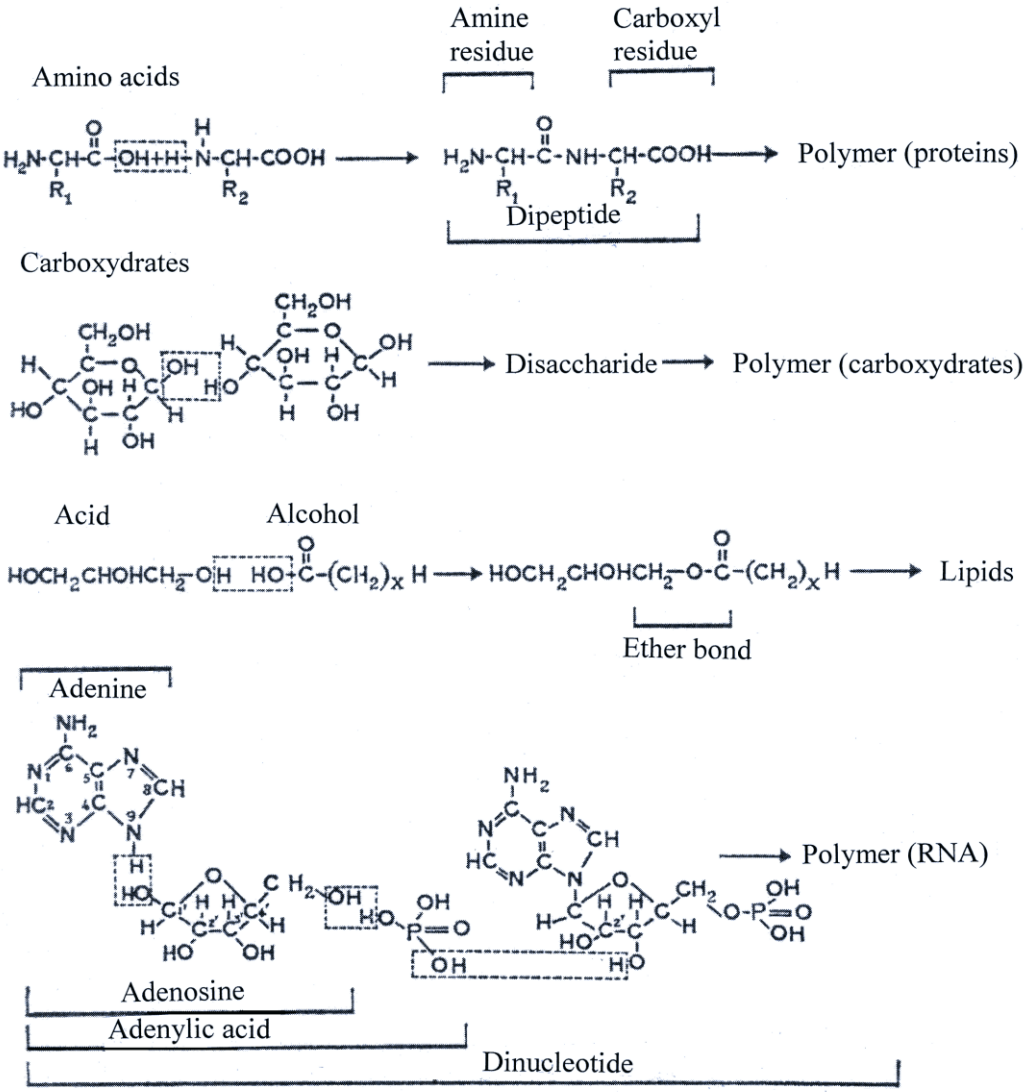

Figure 4. Reactions of condensation and dehydration in alkaline conditions with pH = 9–10 catalyzed by HCN and its derivatives, resulting in synthesis from separate molecules larger organic molecules of polymers. The top three equations: condensation and the subsequent polymerization of amino acids in proteins; carbohydrates – in polycarboxydrates and acids and ethers – into lipids. The bottom equation – condensation of adenine with ribose and H_3PO_4, leading to formation of dinucleotide

It should be noted, that geothermal sources might be used for synthesis of various organic molecules. Thus, amino acids were detected in solutions of formaldehyde CH_2O with hydroxylamine NH_2OH, formaldehyde with hydrazine (N_2H_4) in water solutions with HCN, after heating of a reactionary mixture to +95 °C [20]. In model experiments reaction products were polymerized into peptide chains that is the important stage towards inorganic synthesis of protein. In a reactionary mixture with a HCN–NH_3 solution in water were formed purines and pyrimidines (Fig. 5). In other experiments amino acid mixtures were subjected to influence of temperatures from +60 °C up to +170 °C with formation of short protein-like molecules resembling early evolutionary forms of proteins subsequently designated as thermal proteinoids. They consisted of 18 amino acids usually occurring in protein hydrolyzates. The synthesized proteinoids are similar to natural proteins on a number of other important properties, e. g. on linkage by nucleobases and ability to cause the reactions similar to those catalyzed by enzymes in living organisms as decarboxylation, amination, deamination, and oxidoreduction. Proteinoids are capable to

catalytically decompose glucose [21] and to have an effect similar to the action of α-melanocyte-stimulating hormone [22]. The best results on polycondensation were achieved with the mixes of amino acids containing aspartic and glutamic acids, which are essential amino acids occurring in all modern living organisms.

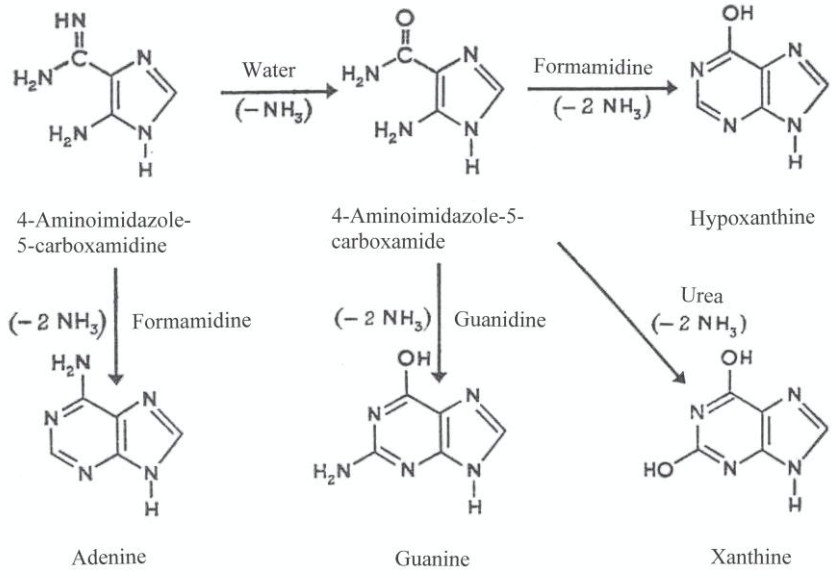

a)

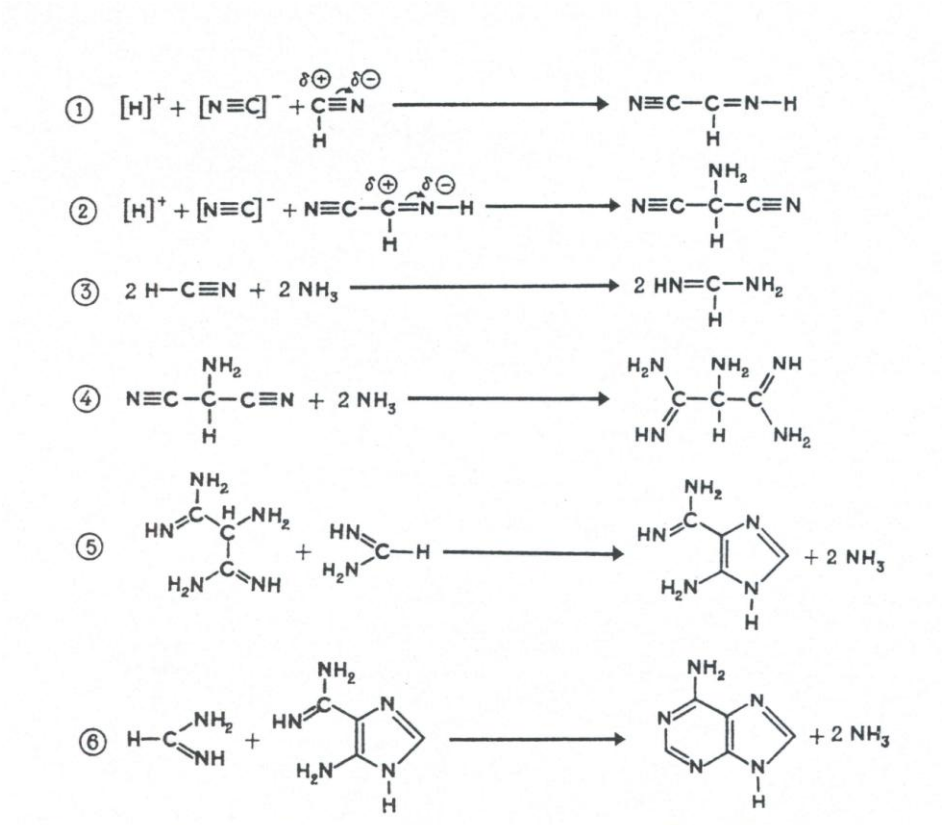

b)

Figure 5. Prospective mechanisms of thermal (+95 °C) synthesis of purines in aqueous solutions: *a)* – synthesis of hypoxanthine, adenine, guanine and xanthine from 4-aminoimidazole-5-carboxamidine, 4-aminoimidazole-5-carboxamide, water, NH_3, formamidine and urea; *b)* – synthesis of adenine from NH_3 and HCN (total reaction: 5HCN = adenine)

Under certain conditions in hot mixture of proteinoids in water solutions are formed elementary structures like proteinoid microspheres with diameter 5–10 μm [23]. Gas electric discharge with color coronal spectral analyses was applied in this type of experiment analogous to S. Miller's experiments [24]. In S. Miller's experiments one of the basic conditions is electric gas discharge. The analogous experiment was conducted by the authors under laboratory conditions. The first living structures were most probably formed in warm and hot mineral water with more bicarbonate and metal ions (Na, Ca, Mg, Zn, K, etc.). There occurred gas electric discharge (lightning) in the primordial atmosphere close to the water surface. In the course of experiment was used the similar gas coronal electric discharge on water drops placed on the electrode of the device for gas coronal electric discharge formation. Water drops were heated to the boiling point in an electric field of high frequency and voltage and an electric discharge was applied, analogious as in the primordial atmosphere. As a result, an organized structure with a size of 12–14 mm was formed in interelectrode space (Fig. 6). It was formed as a result of the self-organization of elementary structures sized 5–10 μm in the biggest structure with size 1,2–1,4 mm and concentrated in a large structure where the basic electric voltage is applied. On its form it resembles a small jellyfish.

Figure 6. Organized structure in water on an electrode, which is heated to boiling point in an electric field of high frequency and voltage

It should be noted that no structure was organized in a control sample of water placed on the electrode. Before its placement on the electrode, the water was heated to boiling point and then cooled. The structure organization increased with the increase of the duration of the gas electric discharge. Moreover, in experiments was observed formation of small structures and their further "adjoining" to the larger structure. It should be noted that the large structure was preserved with original unchanged size for 2 years in the absence of electric discharge.

This experiment shows that the organization of structures in water under certain external conditions as the temperature takes place. Water in natural conditions was heated by the magma. The structure formed from heated water was evidently a result of self-organization. Living organisms are complex self-organizing systems. They are open because they constantly exchange substances and energy with the environment. The changes in the open systems are relatively stable in time. The stable correlation between components in an open system is called a dissipative structure. According to I. Prigozhin, the formation of dissipative structures and the elaboration to living cells is related to changes in entropy [25].

The initial stage of evolution, apparently, was connected with formation at high temperature of the mixtures of amino acids and nitrogenous substances – analogues of nucleic acids. Such synthesis is possible in aqueous solutions under thermal conditions in the presence of H_3PO_4. The next stage is polycondensation of amino acids into thermal proteinoids at temperatures 65–95 °C. After that in a mix of proteinoids in hot water solutions were formed membrane like structures. In 2011 T. Sugawara (Japan) created membrane like proto cells from aqueous solution of organic molecules, DNA and synthetic enzymes under temperature close to water's boiling point

+95 °C [26] (Sugawara, 2011). These experiments are excellent confirmation of the possibility that life and living matter originated in hot water.

Conclusions

The data obtained testify that origination of life and living matter depends on physical-chemical properties of water and external factors – temperatures, pH, electric discharges and isotopic composition. Hot mineral alkaline water interacting with $CaCO_3$ is closest to these conditions. Next in line with regard to quality is seawater. For chemical reaction of dehydration-condensation to occur in hot mineral water, water is required to be alkaline with pH range 9–11. In warm and hot mineral waters the local maximums in IR-spectra from 8 to 14 μm were more expressed in comparison with the local maximums measured in the same water samples with lower temperature.

Acknowledgements

The authors wish to thank M. Chakarova from Bulgarian Academy of Sciences for registering IR-spectra.

References:

1. Ignatov I. Color coronal (Kirlian) spectral analysis in modeling of nonequilibrioum conditions with the gas electric discharges simulating primary atmosphere. S. Miller's experiments / I. Ignatov, O.V. Mosin // Naukovedenie. 2013. № 3(16). P. 1–15 [in Russian] [Online] Available: URL: http://naukovedenie.ru/PDF/05tvn313.pdf (May 10, 2013).

2. Ignatov I. Isotopic composition of water and its temperature in the evolutionary origin of life and living matter / I. Ignatov, O.V. Mosin // Naukovedenie. 2013. № 1(14). P. 1–16 [in Russian] [Online] Available: URL: http://naukovedenie.ru/PDF/42tvn113.pdf (February 13, 2013).

3. Ignatov I. Possible processes for origin of life and living matter with modeling of physiological processes of bacterium *Basillus subtilis* as model system in heavy water / I. Ignatov, O.V. Mosin // Journal of Natural Sciences Research. 2013. Vol. 3, № 9. P. 65–76.

4. Ignatov I. Isotopic composition of water and its temperature in modeling of primordial hydrosphere experiments / I. Ignatov, O.V. Mosin. Euro-Eco, Hanover. 2012. P. 62.

5. Linsky J.L. D/H and nearby interstellar cloud structures / Ed. J.I. Linsky. Space Science Reviews, NY: Springer Science, Business Media. 2007. Vol. 130. 367 p.

6. Ignatov I. Which water is optimal for the origin (generation) of life? / I. Ignatov. Euromedica, Hanover. 2010. P. 34–37.

7. Ignatov I. Modeling of possible processes for origin of life and living matter in hot mineral and seawater with deuterium / I. Ignatov, O.V. Mosin // Journal of Environment and Earth Science. 2013. Vol. 3, № 14. P. 103–118.

8. Szostak J.W. An optimal degree of physical and chemical heterogeneity for the origin of life? / J.W. Szostak // Philos. Trans. Royal Soc. Lond. Biol. Sci. 2011. Vol. 366, № 1580. P. 2894–901.

9. Mulkidjanian A.Y. On the origin of life in the Zinc world. Validation of the hypothesis on the photosynthesizing zinc sulfide edifices as cradles of life on Earth / A.Y. Mulkidjanian, M.Y. Galperin // Biology Direct. 2009. Vol. 4. P. 26.

10. Trevors J.I. Hypothesis: origin of live in hydrogel environment / J.I. Trevors, G.H. Pollack // Progress in biophysics and molecular biology. 205. Vol. 89, № 1. P. 1–8.

11. Ignatov I. Origin of life and living matter in hot mineral water. Conference on the Physics, Chemistry and Biology of Water, Vermont Photonics, USA. 2012. P. 67.

12. Ignatov I. Method for colour coronal (Kirlian) spectral analysis // I. Ignatov, O.V. Mosin // Biomedical Radio electronics. 2013. Vol. 1. P. 38–47 [in Russian].

13. Schirber M. First fossil-makers in hot water / M. Schirber M. // Astrobiology magazine. 2010 [Online] Available: URL: http://www.astrobio.net/exclusive/3418/first-fossil-makers-in-hot-water (January 3, 2010).

14. Ponsa M.L. Early archean serpentine mud volcanoes at Isua, Greenland, as a niche for early life / M.L. Pons, G. Quitte, T. Fujii, M.T. Rosingc, B. Reynarda, F. Moynierd, Ch. Doucheta, F. Albaredea // Proc. Natl. Acad. Sci. U.S. 2011. Vol. 108. P. 17639–17643.

15. Kurihara K. Self-Reproduction of supramolecular giant vesicles combined with the amplification of encapsulated DNA / K. Kurihara, M. Tamura, K. Shohda, T. Toyota, K. Suzuki, T. Sugawara // Nature Chemistry. 2011. Vol. 4, № 10. P. 775–781.

16. Calvin M. Chemical evolution / Ed. M. Calvin. Oxford: Clarendon. 1969. 278 p.

17. Mathews C.N. Peptide synthesis from hydrogen-cyanide and water / C.N. Mathews, R. Moser // Nature. 1968. Vol. 215. P. 1230–1234.
18. Miller S.L. A production of amino acids under possible primitive Earth conditions / S.L. Miller // Science. 1953. Vol. 117, № 3046. P. 528–529.
19. Abelson P. Chemical events on the “primitive” earth / P. Abelson // Proc. Natl. Acad. Sci. U.S. 1966. Vol. 55. P. 1365–1372.
20. Harada I. Thermal synthesis of natural ammo-acids from a postulated primitive terrestrial atmosphere / I. Harada, S.W. Fox, S.W. // Nature. 1964. Vol. 201. P. 335–336.
21. Fox S.W. Catalytic decomposition of glucose in aqueous solution by thermal proteinoids / S.W. Fox, G. Krampitz // Nature. 1964. Vol. 203. P. 1362–1364.
22. Fox S.W. Melanocytestimulating hormone: Activity in thermal polymers of alpha-ammo acids / S.W. Fox, C.T. Wang // Science. 1968. Vol. 160. P. 547–548.
23. Nakashima T. (1987) Metabolism of proteinoid microspheres / Ed. T. Nakashima. In: Origins of life and evolution of biospheres. 1987. Vol 20, № (3–4). P. 269–277.
24. Ignatov I. Water for the origin of life and informationability of water. Kirlian (electric images) of different types of water / I. Ignatov, V. Tsvetkova. Euromedica, Hanover. 2011. P. 32–35.
25. Nikolis P. Self-organization in non-equilibrium systems / Ed. P. Nikolis, I. Prigozhin. Moscow: Mir. 1979. P. 1–512 [in Russian].
26. Sugawara T. (2011) Self-reproduction of supramolecular giant vesicles combined with the amplification of encapsulated DNA / T. Sugawara // Nature Chemistry. 2011. Vol. 1127. P. 775–780.

УДК 735.29: 573.552

Моделирование возможных условий происхождения первых органических форм жизни в горячей минеральной воде

[1] Игнат Игнатов
[2] Олег Викторович Мосин

[1] Научно-исследовательский центр медицинской биофизики (РИЦ МБ), Болгария
Профессор, доктор наук Европейской академии естественных наук (ФРГ), директор НИЦ МБ.
1111, София, ул. Н. Коперника, 32/6
[2] Московский государственный университет прикладной биотехнологии, Российская Федерация
Старший научный сотрудник кафедры биотехнологии, канд. хим. наук.
103316, Москва, ул. Талалихина, 33
E-mail: mosin-oleg@yandex.ru

Аннотация. Изучен состав воды, температура и значение pH в экспериментах по моделированию первичной гидросферы и возможных условий возникновения органических форм жизни в горячей минеральной воде. Для этой цели авторы провели исследования горячей минеральной и морской воды из Болгарских источников ИК-спектрометрией (ДНЭС-метод). В качестве модельных систем использовали сок кактуса *Echinopsis pachanoi* и средиземноморскую медузу *Cotylorhiza tuberculata*. Рассмотрены реакции конденсации-дегидратации в щелочных водных растворах со значением pH 9–10, результатом которых является синтез из мелких молекул более крупных органических молекул полимеров как короткие полипептиды. Показано, что горячие минеральные воды с температурой от +65 °C до +95 °C и значением pH от 9 до 11 более пригодны для возникновения жизни, чем другие исследованные образцы воды. Напротив, значение pH для морской воды лимитируется значениями от 7,5 до 8,4. В ИК-спектрах морской воды и медузы детектировались два локальных максимума, которые лучше экспрессировались в ИК-спектре медузы.

Ключевые слова: дейтерий; гидросфера; эволюция; возникновение жизни; ИК-спектрометрия.

Published in the Russian Federation
European Journal of Molecular Biotechnology
Has been issued since 2013.
ISSN: 2310-6255
E-ISSN 2409-1332
Vol. 6, No. 4, pp. 180-209, 2014

DOI: 10.13187/ejmb.2014.6.180
www.ejournal8.com

UDC 579.871.08

Studying of Phenomenon of Biological Adaptation to Heavy Water

[1] Oleg Mosin
[2] Ignat Ignatov
[3] Dmitry Skladnev
[4] Vitaly Shvets

[1] Moscow State University of Applied Biotechnology, Russian Federation
Senior research Fellow of Biotechnology Department, Ph. D. (Chemistry)
103316, Moscow, Talalihina ulitza, 33
E-mail: mosin-oleg@yandex.ru
2 The Scientific Research Center of Medical Biophysics (SRC MB), Bulgaria
Professor, D. Sc., director of SRC MB
1111, Sofia, N. Kopernik street, 32
E-mail: mbioph@dir.bg
[3] Scientific Center of Russian Federation Research Institute for Genetics and Selection of Industrial Microorganisms “Genetika”, Russian Federation
Professor, D. Sc (Biology), leading scientist of “Genetika”
117545, Moscow, 1st Dorozhniy proezd, 1
E-mail: genetika@genetika.ru
[4] M.V. Lomonosov Moscow University of Fine Chemical Technology, Russian Federation
Academician of Russian Academy of Sciences, D. Sc. (Chemistry), head of the department of biotechnology and nanobiotechnology
119571, Moscow, Vernadskogo avenue, 86
E-mail: mitht@mitht.ru

Abstract

Biological influence of deuterium on cells of various taxonomic groups of prokaryotic and eucaryotic microorganisms realizing methylotrophic, chemoheterotrophic, photo-organotrophic, and photosynthetic ways of assimilation of carbon substrates (methylotrophic bacteria *Brevibacterium methylicum*, chemoheterotrophic bacteria *Bacillus subtilis*, photo-organotrophic halobacteria *Halobacterium halobium*, and green micro algae *Chlorella vulgaris*) was investigated at the growth on media with heavy water (^2H_2O). For investigated microorganisms are submitted the data on growth and adaptation on the growth media containing as sources of deuterated substrates ^2H_2O, [^{2}H]methanol and hydrolisates of deutero-biomass of methylotrophic bacteria *B. methylicum*, obtained after multistage adaptation to ^2H_2O. The qualitative and quantitative composition of intra- and endocellular amino acids, proteins, carbohydrates and fatty acids in conditions of adaptation to ^2H_2O is investigated. It is shown, that the effects observed at adaptation to ^2H_2O, possess a complex multifactorial character and connected to cytological, morphological and physiological changes – the magnitude of the lag- period, time of cellular generation, output of

biomass, a parity ratio of synthesized amino acids, proteins, carbohydrates and lipids, and also with an evolutionary level of the organization of the investigated object and the pathways of assimilation of carbon substrates as well.

Keywords: deuterium; heavy water; adaptation; isotopic effects; bacteria; micro algae.

Introduction

The most interesting biological phenomenon is the ability of some microorganisms to grow on heavy water (^2H_2O) media in which all hydrogen atoms are replaced with deuterium [1, 2]. ^2H_2O has high environmental potential in biomedical studies due to the absence of radioactivity and poccebility of detecting the deuterium label in the molecule by high-resolution methods as NMR, IR, and mass spectrometry that facilitates its use as a tracer in biochemical and biomedical research [3].

The average ratio of $^1H/^2H$ in nature makes up approximately 1:5700 [4]. In natural waters, the deuterium is distributed irregularly: from 0,02–0,03 mol.% for river water and sea water, to 0,015 mol.% for water of Antarctic ice – the most purified from deuterium natural water containing in 1,5 times less deuterium than that of seawater. According to the international SMOW standard isotopic shifts for ^2H and ^{18}O in sea water: $^2H/^1H = (155{,}76\pm0{,}05)\cdot10^{-6}$ (155,76 ppm) and $^{18}O/^{16}O = (2005{,}20\pm0{,}45)\cdot10^{-6}$ (2005 ppm). For SLAP standard isotopic shifts for ^2H and ^{18}O in seawater make up $^2H/^1H = 89\cdot10^{-6}$ (89 ppm) and for a pair of $^{18}O/^{16}O = 1894\cdot10^{-6}$ (1894 ppm). In surface waters, the ratio $^2H/^1H = \sim(1{,}32–1{,}51)\cdot10^{-4}$, while in the coastal seawater – $\sim(1{,}55–1{,}56)\cdot10^{-4}$. The natural waters of CIS countries are characterized by negative deviations from SMOW standard to $(1{,}0–1{,}5)\cdot10^{-5}$, in some places up to $(6{,}0–6{,}7)\cdot10^{-5}$, but however there are also observed positive deviations at $2{,}0\cdot10^{-5}$.

The chemical structure of ^2H_2O molecule is analogous to that one for H_2O, with small differences in the length of the covalent H–O-bonds and the angles between them. The molecular mass of ^2H_2O exceeds on 10% that one for H_2O. The difference in nuclear masses stipulates the isotopic effects, which may be sufficiently essential for the $^1H/^2H$ pair [5]. As a result, physical-chemical properties of ^2H_2O differ from H_2O: ^2H_2O boils at 101,44 °C, freezes at 3,82 °C, has maximal density at 11,2 °C (1,106 g/cm^3) [6]. In mixtures of ^2H_2O with H_2O the isotopic exchange occurs with high speed with the formation of semi-heavy water ($^1H^2HO$): $^2H_2O + H_2O = {}^1H^2HO$. For this reason deuterium presents in smaller content in aqueous solutions in form of $^1H^2HO$, while in the higher content – in form of ^2H_2O. The chemical reactions in ^2H_2O are somehow slower compared to H_2O. ^2H_2O is less ionized, the dissociation constant of ^2H_2O is smaller, and the solubility of the organic and inorganic substances in ^2H_2O is smaller compared to these ones in H_2O [7]. Due to isotopic effects the hydrogen bonds with the participation of deuterium are slightly stronger than those ones formed of hydrogen.

For a long time it was considered that heavy water was incompatible with life. Experiments with the growing of cells of different organisms in ^2H_2O show toxic influence of deuterium. The high concentrations of ^2H_2O lead to the slowing down the cellular metabolism, mitotic inhibition of the prophase and in some cases – somatic mutations [8]. This is observed even while using natural water with an increased content of ^2H_2O or $^1H^2HO$ [9]. Bacteria can endure up to 90 % (v/v) ^2H_2O, plant cells can develop normally in up to 75 % (v/v) ^2H_2O, while animal cells – up to not more than 30 % (v/v) ^2H_2O [10]. Further increase in the concentration of ^2H_2O for these groups of organisms leads to the cellular death [11], although isolated cell's cultures suspended in pure ^2H_2O exert a strong radioprotective effect in ^2H_2O-solutions towards γ–radiation [12, 13]. On the contrary, deuterium depleted water with decreased deuterium content has benefitial effects on organism and stimulates the cellular metabolism [14].

With the development of new microbiological approaches, there appears an opportunity to use adapted to deuterium cells for preparation of deuterated natural compounds. The traditional method for production of deuterium labelled compounds consists in the growth on media containing maximal concentrations of ^2H_2O and deuterated substrates as [^2H]methanol, [^2H]glucose etc. [15, 16]. During growth of cells on ^2H_2O are synthesized molecules of biologically important natural compounds (DNA, proteins, amino acids, nucleosides, carbohydrates, fatty acids), which hydrogen atoms at the carbon backbones are completely substituted with deuterium. They are isolated from deuterated biomass obtained on growth media with high ^2H_2O content and deuterated substrates with using a combination of physico-chemical methods of separation –

hydrolysis, precipitation, extraction with organic solvents and chromatographic purification by column chromatography on different adsorbents. These deuterated molecules evidently undergo structural adaptational modifications necessary for the normal functioning in ^2H_2O.

The adaptation to ^2H_2O is interested not only from scientific point, but allows to obtain the unique biological material for the studying of molecular structure by ^{1}H-NMR [17]. Trend towards the use of deuterium as an isotopic label are stipulated by the absence of radioactivity and possebility of determination the deuterium localization in the molecule by high resolution NMR spectroscopy [18], IR spectroscopy [19] and mass spectrometry [20]. The recent advances in technical and computing capabilities of these analytical methods have allowed to considerable increase the efficiency of *de novo* biological studies, as well as to carry out structural-functional biophysical studies with deuterated molecules on a molecular level.

This study is a continuation of our research into the adaptation to deuterium of various procaryotic and eucaryotic organisms. The purpose of our research was studying the influence of deuterium on the cells of different taxonomic groups of microorganisms and microalgae realizing methylotrophic, chemoheterotrophic, photo-organotrophic and photosynthetic pathways of carbon assimilation.

Material and methods

Biological objects

The objects of the study were various microorganisms, realizing methylotrophic, chemoheterotrophic, photo-organotrophic, and photosynthetic ways of assimilation of carbon substrates. The initial strains were obtained from the State Research Institute of Genetics and Selection of Industrial Microorganisms (Moscow, Russia):

1. *Brevibacterium methylicum B-5652*, a leucine auxotroph Gram-positive strain of facultative methylotrophic bacterium, L-phenylalanine producer, assimilating methanol via the NAD^+ dependent methanol dehydrogenase variant of ribulose-5-monophosphate cycle (RuMP) of carbon fixation.
2. *Bacillus subtilis B-3157*, a polyauxotrophic for histidine, tyrosine, adenine, and uracil spore-forming aerobic Gram-positive chemoheterotrophic bacterium, inosine producer, realizing hexose-6-mono-phosphate (GMP) cycle of carbohydrates assimilation.
3. *Halobacterium halobium ET-1001*, photo-organotrophic carotenoid-containing strain of extreme halobacteria, synthesizing the photochrome transmembrane protein bacteriorhodopsin.
4. *Chlorella vulgaris B-8765*, photosynthesizing single-cell blue-green alga.

Chemicals

For preparation of growth media was used ^2H_2O (99,9 atom.%), ^{2}HCl (95,5 atom.%) and [^{2}H]methanol (97,5 atom% ^{2}H), purchased from the "Isotope" Russian Research Centre (St. Petersburg, Russian Federation). Inorganic salts and D- and L-glucose ("Reanal", Hungary) were preliminary crystallized in ^2H_2O and dried in vacuum before using. ^2H_2O was distilled over $KMnO_4$ with the subsequent control of isotope enrichment by ^{1}H-NMR-spectroscopy on a Brucker WM-250 device ("Brucker", Germany) (working frequency: 70 MHz, internal standard: Me_4Si). According to ^{1}H-NMR, the level of isotopic purity of growth media usually was by ~8–10 atom% lower than the isotope purity of the initial ^2H_2O.

Adaptation technique

The initial microorganisms were modified by adaptation to deuterium by plating individual colonies onto 2 % (w/v) agarose growth media with stepwise increasing gradient of ^2H_2O concentration and subsequent selection of individual cell colonies stable to the action of ^2H_2O. As a source of deuterated growth substrates for the growth of chemoheterotrophic bacteria and chemoorganoheterotrophic bacteria was used the deuterated biomass of facultative methylotrophic bacterium *B. methylicum*, obtained via a multi-stage adaptation on solid 2 % (w/v) agarose M9 media with an increasing gradient of ^2H_2O (from 0; 24,5; 49,0; 73,5 up to 98 % (v/v) ^2H_2O). Raw deuterated biomass (output, 100 gram of wet weight per 1 liter of liquid culture) was suspended in 100 ml of 0,5 N ^{2}HCl (in ^2H_2O) and autoclaved for 30–40 min at 0,8 atm. The suspension was neutralized with 0,2 N KOH (in ^2H_2O) to pH = 7,0 and used as a source of growth substrates while

adaptation and growing the chemoheterotrophic bacterium *B. sublilis* and the photo-organotrophic halobacterium *H. halobium*.

Growth media

The following growth media were used (concentratioin of components are given in g/l):

1. Minimal salt medium M9 for growth of the facultative methanol assimilating methylotrophic bacterium *B. methylicum B-5662*, supplemented with 2 % (v/v) [^{2}H]methanol and increasing gradient of ^2H_2O concentration from 0; 24,5; 49,0; 73,5 up to 98 % (v/v) ^2H_2O: KH_2PO_4 – 3; Na_2HPO_4 – 6; NaCl – 0,5; NH_4Cl – 1,0; L-leucine – 0,01.

2. Hydrolysated medium HM1 for growth of the aerobic Gram-positive chemoheterotrophic bacterium *B. subtilis B-3157*, based on ^2H_2O (89–90 atom% ^{2}H) and 2 % (w/v) hydrolysate of deuterated biomass of *B. methylicum B-5662* as a source of ^{2}H-labeled growth substrates: L-glucose – 120; hydrolysate of deuterated biomass of *B. methylicum* – 20, NH_4NO_3 – 20; $MgSO_4 \cdot 7H_2O$ – 10; $CaCO_3$ – 20; adenine – 0,01; uracil – 0,01. As a control was used protonated medium containing 2 % (w/v) yeast protein–vitamin concentrate (PVC).

3. Hydrolysated medium HM2 for the growth of the extreme aerobic halobacterium *Halobacterium halobium ET-1001* (based on 99,9 atom% ^2H_2O): NaCl – 250; $MgSO_4 \cdot 7H_2O$ – 20; KCl – 2; $CaCl_2 \cdot 6H_2O$ – 0,065; sodium citrate – 0,5; hydrolyzate of deuterated biomass of *B. methylicum B-5662* – 20; biotin – $1 \cdot 10^{-4}$; folic acid – $1{,}5 \cdot 10^{-4}$, vitamin B_{12} – $2 \cdot 10^{-5}$.

4. Tamiya medium for the growth of the photosynthetic green microalgae *C. vulgaris B-8765* (based on 99,9 atom% ^2H_2O): KNO_3 – 5,0; $MgSO_4 \cdot 7H_2O$ – 2,5; KH_2PO_4 – 1,25; $FeSO_4$ – 0,003; $MnSO_4 \cdot 2H_2O$ – $3 \cdot 10^{-4}$; $CaCl_2 \cdot 6H_2O$ – 0,065; $ZnSO_4 \cdot 7H_2O$ – $4 \cdot 10^{-5}$; $CuSO_4 \cdot 5H_2O$ – $5 \cdot 10^{-5}$, $CoCl_2 \cdot 6H_2O$ – $5 \cdot 10^{-6}$).

Growth conditions

The cells were grown in 500 ml Erlenmeyer flasks containing 100 ml of the growth medium at 32–34 °C and vigorously aerated on an orbital shaker Biorad ("Biorad Labs", Poland). Photo-organotrophic bacteria and blue-green algae were grown at illumination by fluorescent monochromatic lamps LDS-40-2 (40 W) ("Alfa-Electro", Russia). Growing of microalgae *C. vulgaris* was carried out at 32 °C in a photoreactor with CO_2 bubbling. The bacterial growth was monitored on the ability to form individual colonies on the surface of solid 2 % (w/v) agarose media, as well as on the optical density of the cell suspension measured on a Beckman DU-6 spectrophotometer ("Beckman Coulter", USA) at λ = 620 nm. After 6–7 days the cells were harvested and separated by centrifugation (10000 g, 20 min) on T-24 centrifuge ("Heracules", Germany). The biomass was washed with ^2H_2O and extracted with a mixure of organic solvents: chloroform–methanol–acetone = 2:1:1, % (v/v) for isolating lipids and pigments. The resulting precipitate (10–12 mg) was dried in vacuum and used as a protein fraction, while the liquid extract – as a lipid fraction. The exogenious deuterated amino acids and ribonucleosides were isolated from culture liquids (CL) of appropriate strain-producers. Inosine was isolated from the CL of *B. subtilis* by adsorption/desorption on activated carbon as adsorbent with following extraction with 0,3 M NH_4-formate buffer (pH = 8,9), subsequent crystallization in 80 % (v/v) ethanol, and ion exchange chromatography (IEC) on a column with cation exchange resin AG50WX 4 equilibrated with 0,3 M NH_4-formate buffer and 0,045 M NH_4Cl (output – 3,1 g/l (80 %); $[\alpha]_D^{20}$ = 1,61 (ethanol)). Bacteriorhodopsin was isolated from the purple membranes of photo-organotrophic halobacterium *H. halobium* by the method of D. Osterhelt, modificated by the authors, with using SDS as a detergent [21].

Protein hydrolysis

Dry biomass (10 g) was treated with a chloroform–methanol–acetone mixture (2:1:1, % (v/v)) and supplemented with 5 ml of 6 N ^{2}HCl (in ^2H_2O). The ampules were kept at 110 °C for ~24 h. Then the reaction mixture was suspended in hot ^2H_2O and filtered. The hydrolysate was evaporated at 10 mm Hg. Residual ^{2}HCl was removed in an exsiccator over solid NaOH.

Hydrolysis of intracellular policarbohydrates

Dry biomass (50 mg) was placed into a 250 ml round bottomed flask, supplemented with 50 ml distilled ^2H_2O and 1,6 ml of 25 % (v/v) H_2SO_4 (in ^2H_2O), and boiled in a reflux water evaporator

for ~90 min. After cooling, the reaction mixture was suspended in one volume of hot distilled ^2H_2O and neutralized with 1 N $Ba(OH)_2$ (in ^2H_2O) to pH = 7,0. $BaSO_4$ was separated by centrifugation (1500 g, 5 min); the supernatant was decanted and evaporated at 10 mm Hg.

Amino acid analysis

The amino acids of the hydrolyzed biomass were analyzed on a Biotronic LC-5001 (230×3,2) column ("Eppendorf–Nethleler–Hinz", Germany) with a UR-30 sulfonated styrene resin ("Beckman–Spinco", USA) as a stationary phase; the temperature – 20±25 °C; the mobile phase – 0,2 N sodium–citrate buffer (pH = 2,5); the granule diameter – 25 μm; working pressure – 50–60 atm; the eluent input rate – 18,5 ml/h; the ninhydrin input rate – 9,25 ml/h; detection at λ = 570 and λ = 440 nm (for proline).

Analysis of carbohydrates

Carbohydrates were analyzed on a Knauer Smartline chromatograph ("Knauer", Germany) equipped with a Gilson pump ("Gilson Inc.", USA) and a Waters K 401 refractometer ("Water Associates", USA) using Ultrasorb CN column (250×10 mm) as a stationary phase; the temperature – 20±25 °C; the mobile phase – acetonitrile–water (75:25, % (w/w); the granule diameter – 10 μm; the input rate – 0,6 ml/min.

Analysis of fatty acids

Fatty acids were analyzed on a Beckman Gold System (USA) chromatograph (250×4.6 mm), equiped with Model 126 UV-Detector (USA), 20±25 °C . Stationary phase – Ultrasphere ODS 5 μm; mobile phase – linear gradient of 5 mM KH_2PO_4–acetonitrile; elution rate – 0,5 ml/min, detection at λ = 210 nm.

Mass spectrometry

For evaluation of deuterium enrichment levels EI and FAB mass spectrometry was used. EI mass spectra were recorded on MB-80A device ("Hitachi", Japan) with double focusing (the energy of ionizing electrons – 70 eV; the accelerating voltage – 8 kV; the cathode temperature – 180–200 °C) after amino acid modification into methyl esters of N-5-dimethylamino(naphthalene)-1-sulfonyl (dansyl) amino acid derivatives according to an earlier elaborated protocol. FAB-mass spectra were recorded on a VG-70 SEQ chromatograph ("Fisons VG Analytical", USA) equipped with a cesium Cs^+ source on a glycerol matrix with accelerating voltage 5 kV and ion current 0,6–0,8 mA. Calculation of deuterium enrichment of the molecules was carried out using the ratio of contributions of molecular ion peaks of deuterated compounds extracted on ^2H_2O-media relative to the control obtained on H_2O.

Scanning electron microscopy (SEM)

SEM was carried out on JSM 35 CF (JEOL Ltd., Korea) device, equiped with SE detector, thermomolecular pump, and tungsten electron gun (Harpin type W filament, DC heating); working pressure – 10^{-4} Pa (10^{-6} Torr); magnification – ×150,000, resolution – 3,0 nm, accelerating voltage – 1–30 kV; sample size – 60–130 mm.

IR-spectroscopy

IR-spectroscopy was performed on Brucker Vertex spectrometer ("Brucker", Germany) (spectral range: average IR – 370–7800 cm^{-1}; visible – 2500–8000 cm^{-1}; the permission – 0,5 cm^{-1}; accuracy of wave number – 0,1 cm^{-1} on 2000 cm^{-1}).

Results

Adaptation to deuterium the methylotrophic bacterium B. methylicum.

Numerous studies with various biological objects in ^2H_2O, proved that when biological objects being exposed to water with different deuterium content, their reaction varies depending on the isotopic composition of water (the content of deuterium in water) and magnitude of isotope effects determined by the difference of constants of chemical reactions rates k_H/k_D in H_2O and ^2H_2O. The maximum kinetic isotopic effect observed at ordinary temperatures in chemical reactions leading to rupture of bonds involving hydrogen and deuterium atoms lies in the range k_H/k_D = 5–8 for C–H

versus C–^{2}H, N–^{2}H versus N–^{2}H, and O–^{2}H versus O–^{2}H-bonds [22]. Isotopic effects have an impact not only on the physical and chemical properties of deuterated macromolecules in which H atoms are substituted with ^{2}H atoms, but also on the biological behaviour of biological objects in ^2H_2O. Experiments with ^2H_2O (Table 1) have shown, that green-blue algae is capable to grow on 70 % (v/v) ^2H_2O, methylotrophic bacteria – 75 % (v/v) ^2H_2O, chemoheterotrophic bacteria – 82 % (v/v) ^2H_2O, and photo-organotrophic halobacteria – 95 % (v/v) ^2H_2O.

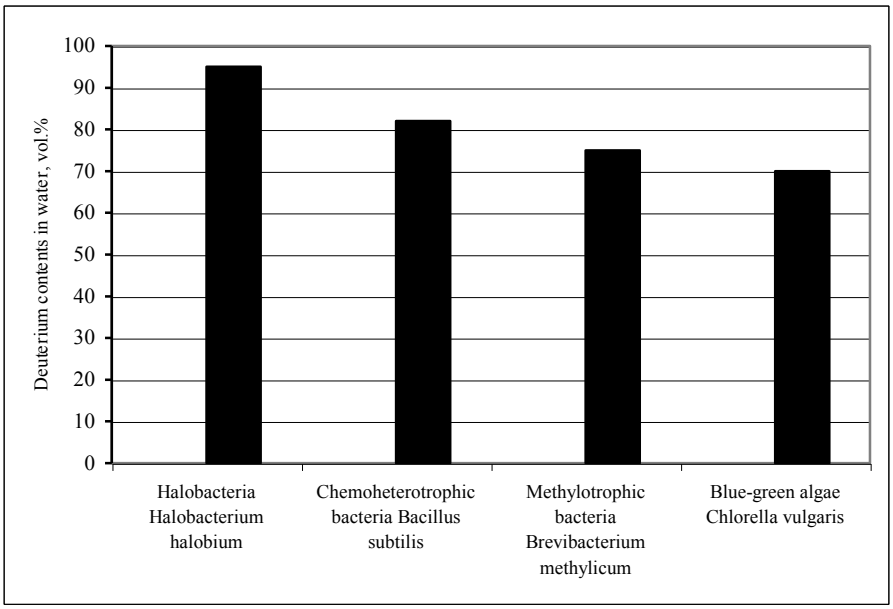

Figure 1. Cell survival of various microorganisms in water with different deuterium content (%, v/v)

In the course of the experiment were obtained adapted to the maximum concentration of ^2H_2O cells belonging to different taxonomic groups of microorganisms, realizing methylotrophic, chemoheterotrophic, photo-organotrophic and photosynthetic pathways of assimilation of carbon substrata, as facultative methylotrophic bacterium *B. methylicum*, chemoheterotrophic bacterium *B. subtilis*, halobacterium *H. halobium* and blue-green algae *C. vulgaris*.

Selection of methanol-assimilating facultative methylotrophic bacterium *B. methylicum* was connected with the development of new microbiological strategies for preparation of deuterated biomass via bioconversion of [^{2}H]methanol and ^2H_2O and its further use as a source of deuterated growth substrates for the growing other strains-producers in ^2H_2O.

Choosing of photo photo-organotrophic halobacterium *H. halobium* was stipulated by the prospects of further isolation of retinal containing transmembrane protein bacteriorhodopsin (BR) – chromoprotein of 248 amino acid residues, containing as a chromophore an equimolar mixture of 13-*cis*-and 13-*trans* C20 carotenoid associated with a protein part of the molecule via a Lys-216 residue [23]. BR performs in the cells of halobacteria the role of ATP-dependent translocase, which creates an electrochemical gradient of H^+ on the surface of the cell membrane, which energy is used by the cell for the synthesis of ATP in the anaerobic photosynthetic phosphorylation.

Using chemoheterotrophic bacterium *B. subtilis* was determined by preparative isolation produced by this bacterium deuterated ribonucleoside – inosine (total deuteration level 65,5 atom.% ^{2}H) for biomedical use [24], and the use of photosynthetic blue-green *C. vulgaris* was stipulated by the study of biosynthesis of deuterated chlorophyll and carotenoid pigments (deuteration level 95–97 atom.% ^{2}H) on growth media with high ^2H_2O-content.

We used stepwise increasing gradient concentration of ^2H_2O in growth media, because it was assumed that the gradual accustoming of micorganisms to deuterium would have a beneficial effect upon the growth and physiological parameters. The strategy of adaptation to ^2H_2O is shown in Table. 1 on an example of methylotrophic bacterium *B. methylicum*, which deuterated biomass was used in further experiments as a source of deuterated growth substrates for growing of chemoheterotrophic and photo-organotrophic bacteria. For this, deuterium enrichment technique

was applied *via* plating cell colonies on 2 % (w/v) agarose M9 media supplemented with 2 % (v/v) [U-^{2}H]MeOH with an increase in the ^2H_2O content from 0; 24,5; 49,0; 73,5 up to 98 % (v/v) ^2H_2O, combined with subsequent selection of cell colonies which were resistant to deuterium. The degree of cell survive on maximum deuterated medium was approx. 40 %. The data on the yield of biomass of initial and adapted *B. methylicum*, magnitude of lag-period and generation time on protonated and maximum deuterated M9 medium are shown in Figure 2. The yield of biomass for adapted methylotroph (*c*) was decreased approx. on 13 % in comparison with control conditions (*a*) at an increase in the time of generation up to 2,8 h and the lag-period up to 40 h (Figure 1). As is shown from these data, as compared with the adapted strain, the growth characteristics of initial strain on maximally deuterated medium were inhibited by deuterium.

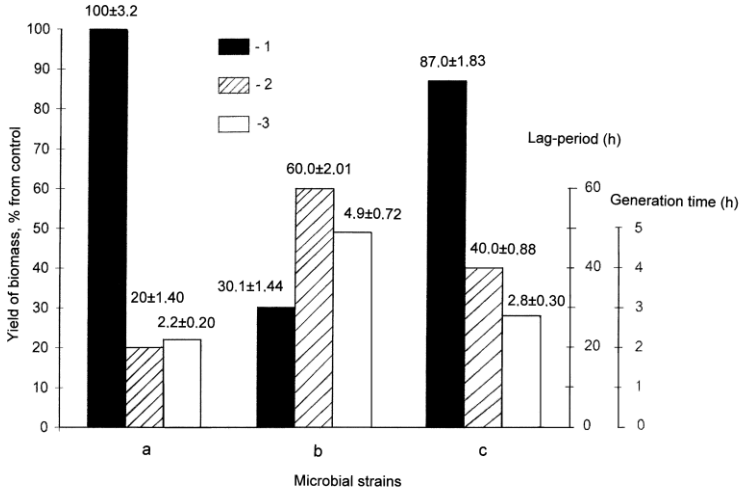

Figure 2. Yield of microbial biomass of *B. methylicum*, magnitude of lag-period and generation time in various experimental conditions: initial strain on protonated M9 medium (control) with water and methanol (*a*); initial strain on maximally deuterated M9 medium (b); adapted to deuterium strain on maximally deuterated M9 medium (c): 1 – yield of biomass, % from the control; 2 – duration of lag-period, h; 3 – generation time, h.

Experimental conditions are given in Table 1 (expts. 1–10) relative to the control (expt. 1) on protonated medium M9 and to the adapted bacterium (expt. 10'). Various compositions of [U-^{2}H]MeOH and ^2H_2O were added to growth media M9 as hydrogen/deuterium atoms could be assimilated both from MeOH and H_2O. The maximum deuterium content was under conditions (10) and (10') in which we used 98 % (v/v) ^2H_2O and 2 % (v/v) [U-^{2}H]MeOH. The even numbers of experiment (Table 1, expts. 2, 4, 6, 8, 10) were chosen to investigate whether the replacement of MeOH by its deuterated analogue affected growth characteristics in presence of ^2H_2O. That caused small alterations in growth characteristics (Table 1, expts. 2, 4, 6, 8, 10) relative to experiments, where we used protonated methanol (Table 1, expts. 3, 5, 7, 9). The gradual increment in the concentration of ^2H_2O into growth medium caused the proportional increase in lag-period and yields of microbial biomass in all isotopic experiments. Thus, in the control (Table 1, expt. 1), the duration of lag-period did not exceed 20,2 h, the yield of microbial biomass (wet weight) and production of phenylalanine were 200,2 and 0,95 gram per 1 liter of growth medium. The adding gradually increasing concentrations of ^2H_2O into growth media caused the proportional increasing of *lag*-period and yield of microbial biomass in all isotopic experiments. The results suggested, that below 49 % (v/v) ^2H_2O (Table 1, expts. 2–4) there was a small inhibition of bacterial growth compared with the control (Table 1, expt. 1). However, above 49 % (v/v) ^2H_2O (Table 1, expts. 5–8), growth was markedly reduced, while at the upper content of ^2H_2O (Table 1, expts. 9–10) growth got 3,3-fold reduced. With increasing content of ^2H_2O in growth media there was a simultaneous increase both of lag-period and generation time. Thus, on maximally deuterated growth medium (Table 1, expt. 10) with 98 % (v/v) ^2H_2O and 2 % (v/v) [U-^{2}H]MeOH, lag-period was 3 fold higher with an increased generation time to 2,2 fold as compared to protonated growth medium with protonated water and methanol which serve as control (Table 1, expt. 1). While on comparing

adapted bacterium on maximally deuterated growth medium (Table 1, expt. 10') containing 98 % (v/v) ^2H_2O and 2 % (v/v) [U-^{2}H]MeOH with non adapted bacterium at similar concentration showed 2,10 and 2,89 fold increase in terms of phenylalanine production and biomass yield due to deuterium enrichment technique, while, the lag phase as well as generation time also got reduced to 1,5 fold and 1,75 fold in case of adapted bacterium.

The adapted bacterium of *B. methylicum* eventually came back to normal growth at placing over in protonated growth medium after some lag-period that proves phenotypical nature of a phenomenon of adaptation that was observed for others adapted by us strains of methylotrophic bacteria and representatives of other taxonomic groups of microorganisms [25]. Literature reports clearly reveal that the transfer of deuterated cells to protonated medium M9 eventually after some lag period results in normal growth that could be due to the phenomenon of adaptation wherein phenotypic variation was observed by the strain of methylotrophic bacteria [26]. The improved growth characteristics of adapted methylotroph essentially simplify the scheme of obtaining the deutero-biomass which optimum conditions are M9 growth medium with 98 % ^2H_2O and 2 % [^{2}H]methanol with incubation period 3–4 days at temperature 35 ^{0}C.

Table 1: Effect of variation in isotopic content (0–98 % ^2H_2O, v/v) present in growth medium M9 on bacterial growth of *B. methylicum* and phenylalanine production

Bacterial strains	Exp. number	Media components, % (v/v)				Lag-period (h)	Yield in terms of wet biomass (g/l)	Generation time (h)	Phenylalanine production (g/l)
		H_2O	^2H_2O	MeOH	[U-^{2}H] MeOH				
Non adapted	1(control)	98,0	0	2	0	20,2±1,40	200,2±3,20	2,2±0,20	0,95±0,12
Non adapted	2	98,0	0	0	2	20,3±1,44	184,6±2,78	2,4±0,23	0,92±0,10
Non adapted	3	73,5	24,5	2	0	20,5±0,91	181,2±1,89	2,4±0,25	0,90±0,10
Non adapted	4	73,5	24,5	0	2	34,6±0,89	171,8±1,81	2,6±0,23	0,90±0,08
Non adapted	5	49,0	49,0	2	0	40,1±0,90	140,2±1,96	3,0±0,32	0,86±0,10
Non adapted	6	49,0	49,0	0	2	44,2±1,38	121,0±1,83	3,2±0,36	0,81±0,09
Non adapted	7	24,5	73,5	2	0	45,4±1,41	112,8±1,19	3,5±0,27	0,69±0,08
Non adapted	8	24,5	73,5	0	2	49,3±0,91	94,4±1,74	3,8±0,25	0,67±0,08
Non adapted	9	98,0	0	2	0	58,5±1,94	65,8±1,13	4,4±0,70	0,37±0,06
Non adapted	10	98,0	0	0	2	60,1±2,01	60,2±1,44	4,9±0,72	0,39±0,05
Adapted	10'	98,0	0	0	2	40,2±0,88	174,0±1,83	2.8±0,30	0,82±0,08

Notes:
* The date in expts. 1–10 described the growth characteristics for non-adapted bacteria in growth media, containing 2 % (v/v) MeOH/[U-^{2}H]MeOH and specified amounts (%, v/v) ^2H_2O.
** The date in expt. 10' described the growth characteristics for bacteria adapted to maximum content of deuterium in growth medium.
***As the control used exprt. 1 where used ordinary protonated water and methanol

Adaptation, which conditions are shown in experiment 10' (Table 1) was observed by investigation of growth dynamics (expts. 1*a,* 1*b,* 1*c*) and accumulation of L-phenylalanine into growth media (expts. 2*a,* 2*b,* 2*c*) by initial (*a*) and adapted to deuterium (*c*) strain *B. methylicum* in maximum deuterated growth medium M9 (Figure 3, the control (*b*) is obtained on protonated growth medium M9). In the present study, the production of phenylalanine (Figure 2, expts. 1b, 2b,

3b) was studied and was found to show a close linear extrapolation with respect to the time up to exponential growth dynamics (Figure 3, expts. 1a, 2a, 3a). The level of phenylalanine production for non-adapted bacterium on maximally deuterated medium M9 was 0,39 g/liter after 80 hours of growth (Figure 2, expt. 2b). The level of phenylalanine production by adapted bacterium under those growth conditions was 0,82 g/liter (Figure 3, expt. 3b). Unlike to the adapted strain the growth of initial strain and production of phenylalanine in maximum deuterated growth medium were inhibited. The important feature of adapted to ^2H_2O strain *B. methylicum* was that it has kept its ability to synthesize and exogenously produce L-phenylalanine into growth medium. Thus, the use of the adapted bacterium enabled to improve the level of phenylalanine production on maximally deuterated medium by 2,1 times with the reduction in the lag phase up to 20 h. This is an essential achievement for this strain of methylotrophic bacteria, because up till today there have not been any reports about production of phenylalanine by leucine auxotrophic methylotrophs with the NAD^+ dependent methanol dehydrogenase (EC 1.6.99.3) variant of the RuMP cycle of carbon assimilation. This makes this isolated strain unique for production of deuterated phenylalanine and other metabolically related amino acids.

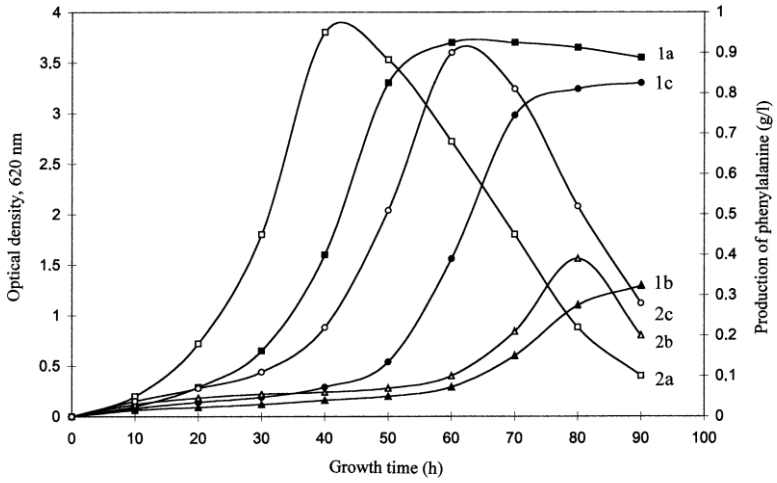

Figure 3. Growth dynamics of *B. methylicum* (1a, 2a, 3a) and production of phenylalanine (1b, 2b, 3b) on media M9 with various isotopic content: 1a, 1b – non-adapted bacterium on protonated medium (Table 1, expt. 1); 2a, 2b – non-adapted bacterium on maximally deuterated medium (Table 1, expt. 10); 3a, 3b – adapted bacterium on maximally deuterated medium (Table 1, expt. 10')

The general feature of phenylalanine biosynthesis in $H_2O/^2H_2O$-media was increase of its production at early exponential phase of growth when outputs of a microbial biomass were insignificant (Figure 3). In all the experiments it was observed that there was a decrease in phenylalanine accumulation in growth media at the late exponential phase of growth. Microscopic research of growing population of microorganisms showed that the character of phenylalanine accumulation in growth media did not correlate with morphological changes at various stages of the cellular growth. Most likely that phenylalanine, accumulated in growth media, inhibited enzymes of its biosynthetic pathways, or it later may be transformed into intermediate compounds of its biosynthesis, e.g. phenylpyruvate [27]. It is necessary to notice, that phenylalanine is synthesised in cells of microorganisms from prephenic acid, which through a formation stage of phenylpiruvate turns into phenylalanine under the influence of cellular transaminases. However, phenylalanine was not the only product of biosynthesis; other metabolically related amino acids (alanine, valine, and leucine/isoleucine) were also produced and accumulated into growth media in amounts of 5–6 μmol in addition to phenylalanine. This fact required isolation of [^{2}H]phenylalanine from growth medium, which was carried out by extraction of lyophilized LC with iso-PrOH and the subsequent crystallization in EtOH. Analytical separation of [^{2}H]phenylalanine and metabolically related [^{2}H]amino acids was performed using a reversed-

phase HPLC method on Separon SGX C_{18} Column, developed for methyl esters of N-DNS-[^{2}H]amino acids with chromatographic purity of 96–98 % and yield of 67–89 %.

With increasing ^2H_2O content in growth media, the levels of deuterium enrichment in exogenous [^{2}H]amino acids (phenylalanine, alanine, valine, and leucine/isoleucine), secreted by *B. methylicum*, were varied proportionally. The similar result on proportional specific increase of levels of deuterium enrichment into [^{2}H]phenylalanine and other metabolically related [^{2}H]amino acids was observed in all isotopic experiments where used increasing concentration ^2H_2O in growth media (Table 2). Predictably, enrichment levels of [^{2}H]phenylalanine related to the family of aromatic amino acids synthesised from shikimic acid and metabolically related [^{2}H]amino acids of pyruvic acid family – alanine, valine and leucine at identical ^2H_2O concentration in growth media are correlated among themselves. Such result is fixed in all isotope experiments with ^2H_2O (Table 2). Unlike [^{2}H]phenylalanine, deuterium enrichment levels in accompanying [^{2}H]amino acids – Ala, Val and Leu/Ile keep a stable constancy within a wide interval of ^2H_2O concentration: from 49 % (v/v) to 98 % (v/v) ^2H_2O (Table 2). Summarizing these data, it is possible to draw a conclusion on preservation of minor pathways of the metabolism connected with biosynthesis of leucine and metabolic related amino acids of pyruvic acid family – alanine and valine, which enrichment levels were in correlation within identical concentration of H_2O in growth media (phenylalanine is related to the family of aromatic amino acids synthesized from shikimic acid). Since leucine was added into growth media in protonated form, another explanation of this effect, taking into consideration the various biosynthetic pathways of Leu and Ileu (Ileu belongs to the family of aspartic acid, while Leu belongs to the pyruvic acid family), could be cell assimilation of protonated leucine from growth media. Since Leu and Ileu could not be clearly estimated by EI MS method, nothing could be said about possible biosynthesis of [^{2}H]isoleucine. Evidently, higher levels of deuterium enrichment can be achieved by replacement of protonated leucine on its deuterated analogue, which may be isolated from hydrolysates of deuterated biomass of this methylotrophic bacterium.

Table 2: Effect of deuterium enrichment levels (atom.%) in the molecules of [^{2}H]amino acids excreted by *B. methylicum**

[^{2}H]amino acid	Concentration of ^2H_2O in growth media, % (v/v)**			
	24,5	49,0	73,5	98,0
Alanine	24,0±0,70	50,0±0,89	50,0±0,83	50,0±1,13
Valine	20,0±0,72	50,0±0,88	50,0±0,72	62,5±1,40
Leucine/isoleucine	20,0±0,90	50,0±1,38	50,0±1,37	50,0±1,25
Phenylalanine	17,0±1,13	27,5±0,88	50,0±1,12	75,0±1,40

Notes:
* At calculation of enrichment levels protons (deuterons) at COOH- and NH_2-groups of amino acids were not considered because of dissociation in H_2O (^2H_2O).
*** The data on enrichment levels described bacteria grown on minimal growth media M9 containing 2 % (v/v) [U-^{2}H]MeOH and specified amounts (%, v/v) ^2H_2O.*

It should be noted that the yields of biomass on deuterated growth media were varried 85–90 % for different taxonomic groups of microorganisms. All adapted microorganisms had a slightly reduced levels of microbial biomass accumulation and increased cell generation times on maximal deuterated media.

Adaptation to deuterium the chemoheterotrophic bacterium *B. subtillis*

The result obtained in experiments on the adaptation of methylotrophic bacterium *B. methylicum* to ^2H_2O allowed to use hydrolysates of biomass of this bacterium obtained in the process of multi-stage adaptation to ^2H_2O, as a source of deuterated growth substrates for the

growing of the chemoheterotrophic bacterium *B. subtillis* and the photoorganotrophic halobacterium *H. halobium*.

The assimilation rate of methylotrophic biomass by protozoa and eukaryotic cells amounts to 85–98 %, while the productivity calculated on the level of methanol bioconversion into cell components makes up 50–60 % [28]. While developing the composition of growth media on the basis of deutereted biomass of methylotrophic bacteria *B. methylicum* it was taken into account the ability of methylotrophic bacteria to synthesize large amounts of protein (output, 50 % (w/w) of dry weight), 15–17 % (w/w) of polysaccharides, 10–12 % (w/w) of lipids (mainly, phospholipids), and 18% (w/w) of ash [29]. To provide high outputs of these compounds and minimize the isotopic exchange ($^1H-^2H$) in amino acid residues of protein molecules, the biomass was hydrolyzed by autoclaving in 0,5 N ^2HCl (in ^2H_2O) and used for the growing of the chemoheterotrophic bacterium *B. subtillis* and the photoorganoheterotrophic halobacterium *H. halobium*.

The methylotrophic hydrolysate, obtained on the maximally deuterated medium M9 with 98 % (v/v) ^2H_2O and 2 % (v/v) [^{2}H]methanol, contains 15 identified amino acids (except for proline detected at λ = 440 nm) with tyrosine and histidine content per 1 gram of dry methylotrophic hydrolysate 1,82 % and 3,2 % (w/w), thereby satisfying the auxotrophic requirements of the inosine producer strain for these amino acids (Table 3). The content of other amino acids in the hydrolysate is also comparable with the needs of the strain in sources of carbon and amine nitrogen. The indicator determining the high efficiency of deuterium incorporation into the synthesized product is high levels of deuterium enrichment of amino acid molecules, varied from 50 atom% ^{2}H for leucine/isoleucine to 98,5 atom% ^{2}H for alanine (Table 3).

Table 3: Amino acid composition of hydrolyzed biomass of the facultative methylotrophic bacterium *B. methylicum* obtained on maximally deuterated M9 medium with 98 % (v/v) ^2H_2O and 2 % (v/v) [^{2}H]methanol and levels of deuterium enrichment*

Amino acid	Yield, % (w/w) dry weight per 1 gram of biomass	Number of deuterium atoms incorporated into the carbon backbone of a molecule**	Level of deuterium enrichment of molecules, % of the total number of hydrogen atoms***
Glycine	9,55	2	92,5±1,86
Alanine	13,30	4	98,5±1,96
Valine	4,21	4	52,2±1,60
Leucine	8,52	5	50,0±1,52
Isoleucine	4,01	5	50,0±1,55
Phenylalanine	3,89	8	96,0±1,85
Tyrosine	2,10	7	95,5±1,82
Serine	3,60	3	86,7±1,55
Threonine	4,89	–	–
Methionine	2,62	–	–
Asparagine	10,02	2	68,5±1,62
Glutamic acid	10,31	4	70,0±1,65
Lysine	3,53	5	59,0±1,60
Arginine	4,65	–	–
Histidine	3,98	–	–

Notes: *The data were obtained for methyl esters of N-5-dimethylamino(naphthalene)-1-sulfonyl (dansyl) chloride amino acid derivatives.

** At calculation the level of deuterium enrichment, the protons (deuterons) at COOH- and NH_2-groups of amino acid molecules were not taken into account because of the dissociation in $H_2O/^2H_2O$.

*** A dash denotes the absence of data.

Taking into account the pathways of assimilation of carbon substrates, the adaptation of chemoheterotrophic bacterium *B. subtilis* was carried out via plating of initial cells to separate colonies on solid 2 % (w/v) agarose HM1 media based on 99,9 atom% ^2H_2O and deuterated hydrolyzate biomass of B. methylicum, with the following subsequent selection of the colonies resistant to ^2H_2O. On contrary to ^2H_2O, ^2H-substrates in composition of deuterated biomass hydrolyzate had no significant negative effect on the growth parameters of the studied microorganisms. The growth and biosynthetic characteristics of inosine-producing strain *B. subtilis* were studied on protonated yeast PVC medium with H_2O and 2 % (w/v) yeast PVC and on HW medium with 89 % (v/v) ^2H_2O and 2 % (w/w) hydrolysate of deuterated biomass of *B. methylicum* (Figure 4). Experiments demonstrated a certain correlation between the changes of growth dynamics of *B. subtilis* (Figure 4, curves *1*, *1*'), output of inosine (Figure 4, curves *2*, *2*'), and glucose assimilation (Figure 4, curves *3*, *3*'). The maximal output of inosine (17 g/l) was observed on protonated PVC medium at a glucose assimilation rate 10 g/l (Figure 4, curve *2*). The output of inosine in the HW medium decreased in 4,4-fold, reaching 3,9 g/l (Figure 4, curve *2*'), and the level of glucose assimilation – 4-fold, as testified by the remaining 40 g/l non-assimilated glucose in CL (Figure 4, curve *3*'). The experimental data demonstrate that glucose is less efficiently assimilated during growth in the HW medium as compared to the control conditions in H_2O.

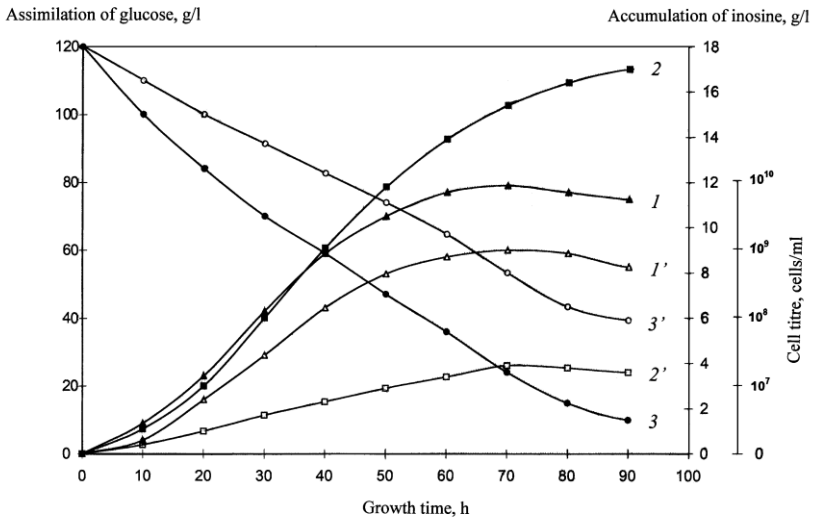

Figure 4. Growth dynamics of *B. subtilis* (*1*, *1*') (cells/ml), inosine accumulation in LC (*2*, *2*') (g/l), and glucose assimilation (*3*, *3*') (g/l) under different experimental conditions: (*1–3*) – protonated yeast PVC medium; (*1*'–*3*') – HW medium with 2% (w/v) hydrolysate of deuterated biomass of *B. methylicum*.

The isolation of inosine from the CL consisted in low-temperature precipitation of high molecular weight impurities with organic solvents (acetone and methanol), adsorption/desorption on the surface of activated carbon, extraction of the end product, crystallization, and ion exchange chromatography. The proteins and polysaccharides were removed from the CL by precipitation with acetone at 4 °C with subsequent adsorption/desorbtion of total ribonucleosides on activated carbon. The desorbed ribonucleosides were extracted from the reacted solid phase by eluting with EtOH-NH_3-solution at 60 °C; inosine – by extracting with 0,3 M ammonium–formate buffer (pH = 8,9) and subsequent crystallization in 80% (v/v) ethanol. The final purification consisted in column ion exchange chromatography on AG50WX 4 cation exchange resin equilibrated with 0,3 M ammonium–formate buffer containing 0,045 M NH_4Cl with collection of fractions at R_f = 0,5. The curves *1–3* in Figure 5 shows UV-absorption spectra of inosine isolated from the CL at various stages of isolation procedure. The presence of major absorbance band I, corresponding to natural inosine (λ_{max} = 249 nm, ε_{249} = 7100 M^{-1} cm^{-1}), and the absence of secondary metabolites II and III in the analyzed sample (Figure 5, curve *3*), demonstrates the homogeneity of the isolated product and the efficiency of the isolation method.

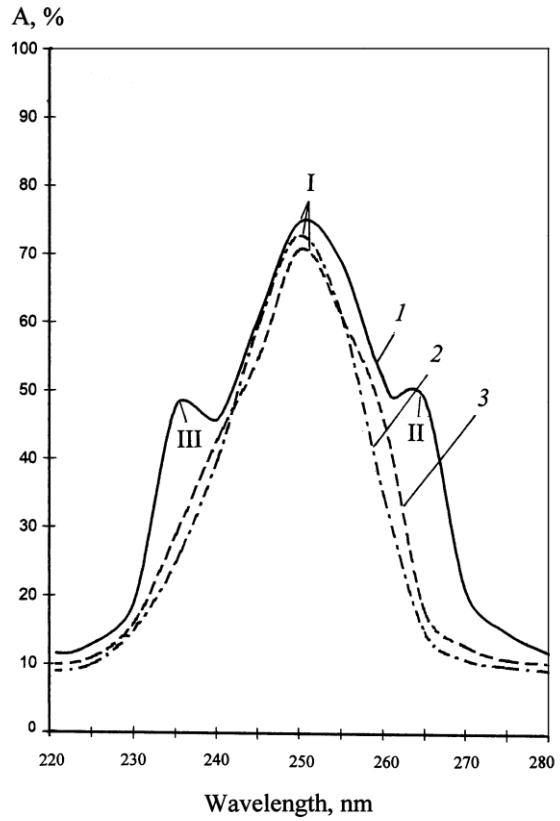

Figure 5. UV-absorption spectra of inosine (0,1 N HCl): (*1*) – initial LC after the growth of *B. subtilis* on HW medium; (*2*) – natural inosine, and (*3*) – inosine extracted from the LC. Natural inosine (*2*) was used as a control: (I) – inosine, (II, III) – secondary metabolites

The level of deuterium enrichment of [^{2}H]inosine was determined by FAB mass spectrometry, the high sensitivity of which allows to detect 10^{-8} to 10^{-10} moles of a substance in a sample. The formation of a molecular ion peak for inosine in FAB mass spectrometry was accompanied by the migration of H^+. Biosynthetically ^{2}H-labeled inosine**,** which FAB mass-spectrum represented in Figure 6*b* regarding the control (natural protonated inosine, Figure 6*a*), represented a mixture of isotope-substituted molecules with different numbers of hydrogen atoms replaced by deuterium. Correspondingly, the molecular ion peak of inosine $[M+H]^+$, was polymorphically splintered into individual clusters with admixtures of molecules with statistical set of mass numbers *m/z* and different contributions to the total level of deuterium enrichment of the molecule. It was calculated according to the most intensive molecular ion peak (the peak with the largest contribution to the level of deuterium enrichment) recorded by a mass spectrometer under the same experimental conditions. These conditions are satisfied the most intensive molecular ion peak $[M+H]^+$ at *m/z* 274 with 38 % (instead of $[M+H]^+$ at *m/z* 269 with 42 % under the control conditions; Figure 6*a*). That result corresponds to five deuterium atoms incorporated into the inosine molecule (Figure 6b). The molecular ion peak of inosine also contained less intensive peaks with admixtures of molecules containing four (*m/z* 273, 20 %), five (*m/z* 274, 38 %), six (*m/z* 275, 28 %), and seven (*m/z* 276, 14 %) deuterium atoms (Table 4).

Table 4: Values of peaks $[M+H]^+$ in the FAB mass spectra and levels of deuterium enrichment of inosine isolated from HW-medium

Value of peak $[M+H]^+$	Contribution to the level of deuterium enrichment, mol.%	The number of deuterium atoms	Level of deuterium enrichment of molecules, % of the total number of hydrogen atoms*
273	20	4	20,0±0,60
274	38	5	62,5±1,80
275	28	6	72,5±1,96
276	14	7	87,5±2,98

Notes: *At calculation of the level of deuterium enrichment, the protons(deuterons) at the hydroxyl (OH^-) and imidazole protons at NH^+ heteroatoms were not taken into account because of keto–enol tautomerism in $H_2O/^2H_2O$.

Taking into account the contribution of the molecular ion peaks $[M]^+$, the total level of deuterium enrichment (TLDE) of the inosine molecule calculated using the below equation was 65,5 % of the total number of hydrogen atoms in the carbon backbone of the molecule:

$$TLDE = \frac{[M]^+_{r1} \cdot C_2 + [M]^+_{r2} \cdot C_2 + ... + [M]^+_{rn} \cdot C_n}{\sum C_n}$$

where $[M]^+_r$ - the values of the molecular ion peaks of inosine; C_n - the contribution of the molecular ion peaks to TLDE (mol %).

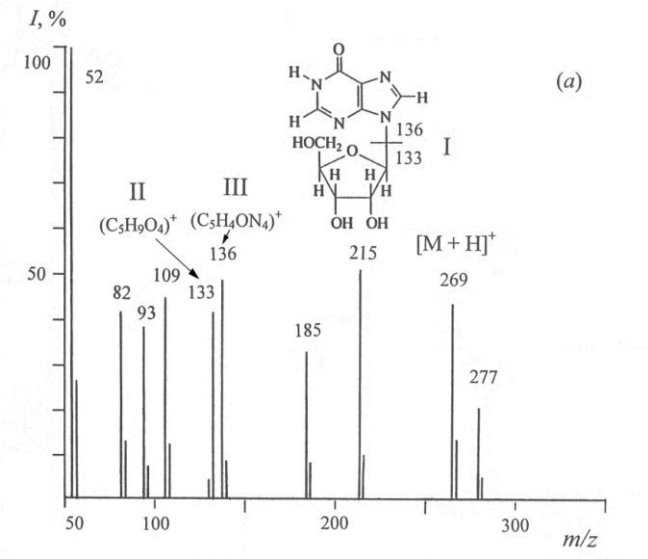

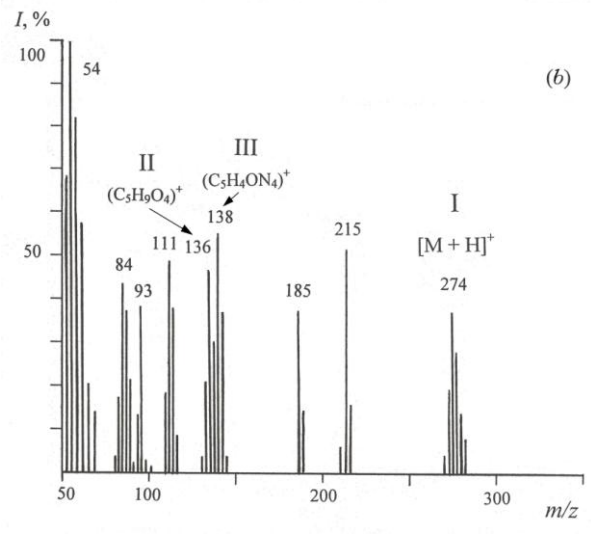

Figure 6. FAB mass spectra of inosine (glycerol as a matrix) under different experimental conditions: (*a*) – natural inosine; (*b*) – [^{2}H]inosine isolated from HW medium (scanning interval at *m/z* 50–350; major peaks with a relative intensity of 100 % at *m/z* 52 and *m/z* 54; ionization conditions: cesium source; accelerating voltage, 5 kV; ion current, 0,6–0,8 mA; resolution, 7500 arbitrary units): *I* – relative intensity of peaks (%); (I) – inosine; (II) – ribose fragment; (III) – hypoxanthine fragment

The fragmentation of the inosine molecule, shown in Figure 7, gives more precise information on the deuterium distribution in the molecule. The FAB fragmentation pathways of the inosine molecule (I) lead to formation of ribose $(C_5H_9O_4)^+$ fragment (II) at *m/z* 133 and hypoxanthine $(C_5H_4ON_4)^+$ fragment (III) at *m/z* 136 (their fragmentation is accompanied by the migration of H^+), which in turn, later disintegrated into several low-molecular-weight splinter fragments at *m/z* 109, 108, 82, 81, and 54 due to HCN and CO elimination from hypoxanthine (Figure 7). Consequently, the presence of two "heavy" fragments of ribose II $(C_5H_9O_4)^+$ at *m/z* 136 (46 %) (instead of *m/z* 133 (41 %) in the control) and hypoxanthine III $(C_5H_4ON_4)^+$ at *m/z* 138 (55 %) (instead of *m/z* 136 (48 %) in the control), as well as the peaks of low molecular weight splinter fragments formed from FAB-decomposition of hypoxanthine fragment at *m/z* 111 (49 %) (instead of *m/z* 109 (45 %) in the control) and *m/z* 84 (43 %) (instead of 82 (41 %) in the control) suggests that three deuterium atoms are incorporated into the ribose residue, and two other deuterium atoms – into the hypoxanthine residue of the inosine molecule (Figure 7). Such selective character of the deuterium inclusion into the inosine molecule on specific locations of the molecule was confirmed by the presence of deuterium in the smaller fission fragments.

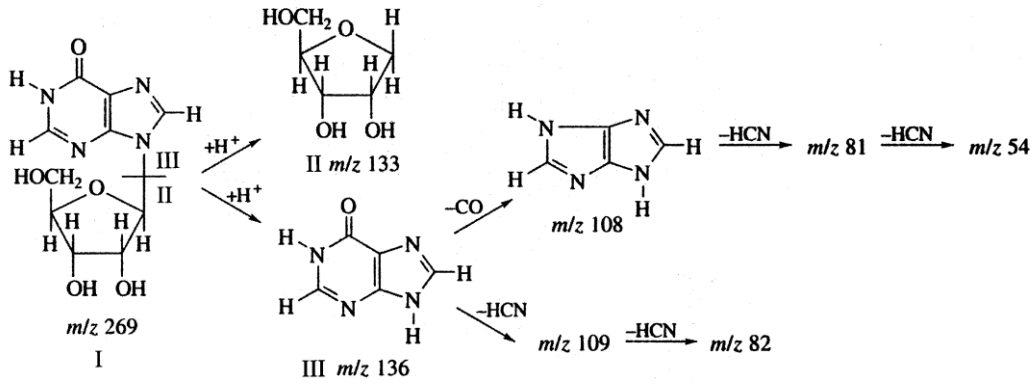

Figure 7. The fragmentation pathways of the inosine molecule leading to formation of smaller fragments by the FAB-method

When analyzing the level of deuterium enrichment of the inosine molecule we took into account the fact that the character of deuterium incorporation into the molecule is determined by the pathways of carbon assimilation. The carbon source was glucose as a main substrate and a mixture of deuterated amino acids from deuterated hydrolizate of methylotrophic bacterium *B. methylicum* as a source of deuterated substrated and amine nitrogen. Since the protons (deuterons) at positions of the ribose residue in the inosine molecule could have been originated from glucose, the character of deuterium inclusion into the ribose residue is mainly determined by hexose monophosphate (HMP) shunt, associated with the assimilation of glucose and other carbohydrates. HMP shunt is a complex of 12 reversible enzymatic reactions resulting in the oxidation of glucose to CO_2 to form reduced NADPH, and H^+, and the synthesis of phosphorylated sugars containing from 3 to 7 carbon atoms. Since glucose in our experiments was used in a protonated form, its contribution to the level of deuterium enrichment of the ribose residue was neglected.

However, as the investigation of deuterium incorporation into the molecule by FAB method showed that deuterium was incorporated into the ribose residue of the inosine molecule owing to the preservation in this bacterium the minor pathways of *de novo* glucose biosynthesis in ^2H_2O-medium. Evidently the cell uses its own resources for intracellular biosynthesis of glucose from intracellular precursors. It should be noted that numerous isotopic $^1H–^2H$ exchange processes could also have led to specific incorporation of deuterium atoms at certain positions in the inosine molecule. Such accessible positions in the inosine molecule are hydroxyl (OH^-)- and imidazole protons at NH^+ heteroatoms, which can be easily exchanged on deuterium in ^2H_2O *via* keto–enol tautomerism. Three non-exchangeable deuterium atoms in the ribose residue of inosine are synthesized *de novo* and could have been originated from HMP shunt reactions, while two other deuterium atoms at C2,C8-positions in the hypoxanthine residue could be synthesized *de novo* at the expense of [^{2}H]amino acids, primarily glutamine and glycine, that originated from deuterated hydrolysate of the methylotrophic bacterium *B. methylicum* obtained on 98 % of ^2H_2O medium. In particular, the glycoside proton at β-N_9-glycosidic bond could be replaced with deuterium *via* the reaction of CO_2 elimination at the stage of ribulose-5-monophosphate formation from 3-keto-6-phosphogluconic acid with subsequent proton (deuteron) attachment at the C1-position of ribulose-5-monophosphate. Two other protons at C2(C3) and C4 positions in ribose residue could be replaced with deuterium *via* further enzimatic isomerization of ribulose-5-monophosphate into ribose-5-monophosphate. In general, our studies confirmed this scheme. However, it should be noted that the level of deuterium enrichment of inosine molecule is determined by isotopic purity of ^2H_2O and deuterated substrates and, therefore, for the total administration of the deuterium label into the inosine molecule instead of protonated glucoce it must be used its deuterated analogue. Deuterated glucose may be isolated in gram-scale quntities from deuterated biomass of the methylotrophic bacterium *B. methylicum*.

Adaptation to deuterium of microalgae C. vulgaris

For adaptation of microalgae *C. vulgaris* was used Tamiya liquid mineral medium containing 25; 50; 75 and 98 % (v/v) ^2H_2O. The levels of deuterium enrichment of carotenoids were In the case of C. vulgaris and H. halobium used fluorescent illumination, as both microorganisms grown in the presence of light. Individual colonies of cells of these microorganisms resistant to ^2H_2O, allocated by selection were grown on liquid growth media of the same composition with 99,9 atom% ^2H_2O for producing the deuterated biomass.

Adaptation to deuterium the photoorganotrophic halobacterium H. halobium

The cell membrane of extreme aerobic photo-organotrophic halobacterium *Halobacterium halobium* contains a chromoprotein trans-membrane protein – bacteriorhodopsin (BR) with the molecular weight ~26,5 kDa, determining the purple-red culour of halophilic bacteria. BR contains as chromophore group an equimolar mixture of 13-*cis*- and 13-*trans*-retinol C20 carotenoid, bound by aldemine bond schiff base (as in the visual animal pigments) with Lys-216 residue of the protein. In halobacteria BR functions as a light-driven transmembrane proton pump pumping a proton accros the membrane. Along with the BR the cell membrane of halobacteria contains a small amount of other related carotenoid pigments, the main of which bakterioruberin determining the stability of halobacteria to solar radiation.

The adaptation of photo-organotrophic halobacterium *Halobacterium halobium* was carried out via plating of initial cells to separate colonies on solid 2 % (w/v) agarose HM2 media based on 99,9 atom% ^2H_2O and deuterated hydrolyzate biomass of *B. methylicum*, with the following subsequent selection of the colonies resistant to ^2H_2O. The growing of halobacteria was carried out under illumination by light fluorescent lamps LDS-40-2 (40 W) with monochromatic light with λ = 560 nm for 4–5 days at 35 °C as swoun in Figure 8. While growing of *H. halobium* on HM2 growth medium cells synthesized the purple carotenoid pigment, identified as a native BR on the the spectral ratio of protein and chromophore fragments in the molecule (D_{280}/D_{568} = 1,5:1,0). The growth of this bacterium on ^2H_2O medium was slightly inhibited as compared with the control on protonated growth medium that simplifies the optimization of conditions for the production of microbial biomass, which consists in the growing of the halobacterium on deuterated growth medium with 2 % (w/v) of deuterated biomass hydrolyzate of *B. methylicum*, cell disintegration and lysis; isolation of purple membrane (PM) fraction; purification of PM from the low and high-molecular weight impurities, cellular RNA, carotenoids and phospholipids; solubilization of PM in 0,5 % (w/v) solution of ionic detergent SDS–Na to form a microemulsion; fractionation of solubilized BR by MeOH; gel permeation chromatography (GPC) on Sephadex G-200 and electrophoresis in 12,5 % (w/v) PAAG in 0,1 % (w/v) SDS -Na.

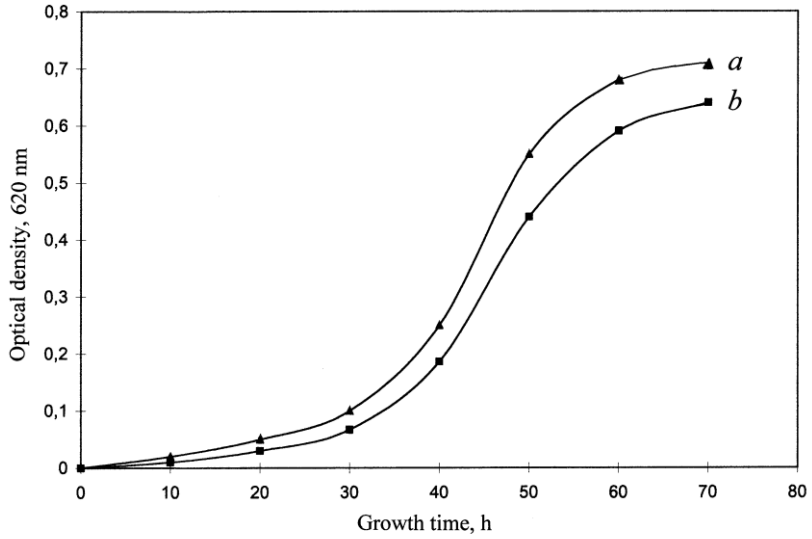

Figure 8. Growth dynamics of *H. halobium* under various experimental conditions: *a*) – HW2-medium; *b*) – peptone medium. Growing conditions: the incubation period: 4–5 days, temperature: 35 °C, illumination under monochrome light at λ = 560 nm

In an attempt to remove a large fraction of the carotenoids and phospholipids from the membrane by column GPC, PM fraction was washed by 50 % (v/v) of EtOH before stabilization by SDS-Na. Removing of carotenoids, consisting in repeated treatment of PM with 50 % (v/v) EtOH at 0 °C, was a routine but necessary step, in spite of the significant loss of the chromoprotein. It was used five treatments by 50 % (v/v) EtOH to obtain the absorption spectrum of PM suspension purified from carotenoids (4) and (5) (degree of chromatographic purity of 80-85 %), as shown in Figure 9 at various processing stages (*b*) and (*c*) relative to the native BR (a). Figure 9 shows a dark-adapted absorption maximum at λ = 548 nm. Formation of retinal-protein complex in the BR molecule leads to a bathochromic shift in the absorption spectrum of PM (Figure 9*c*) - the main bandwith (1) with the absorption maximum at λ = 568 nm caused by the light isomerization of the chromophore by the C13=C14 bond is determined by the presence of 13-*trans*-retinal residue in BR_{568}; additional low-intensity bandwith (2) at λ = 412 nm characterizes a minor impurity of a spectral form of *meta*-bacteriorhodopsin M_{412} (formed in the light) with deprotonated aldimine bond between 13-*trans*-retinal residue and protein; the total bandwith (3) with λ = 280 nm is determined by the absorption of aromatic amino acids in the polypeptide chain of the protein (for native BR D_{280}/D_{568} = 1,5:1,0). Upon the absorption of light, the maximum absorbance of PM shifts to λ = 556 nm with 6-8 % increase in extinction. The 280/568 nm absorbance ratio of BR is directly

related to the ratio of total protein (native BR) and is a convenient indicator for BR stability and integrity. Identical absorbance ratios are monitored using the conventional optics on a Beckman DU-6 spectrophotometer ("Beckman Coulter", USA) for detergent-solubilized BR or purified BR-solubilized in detergent.

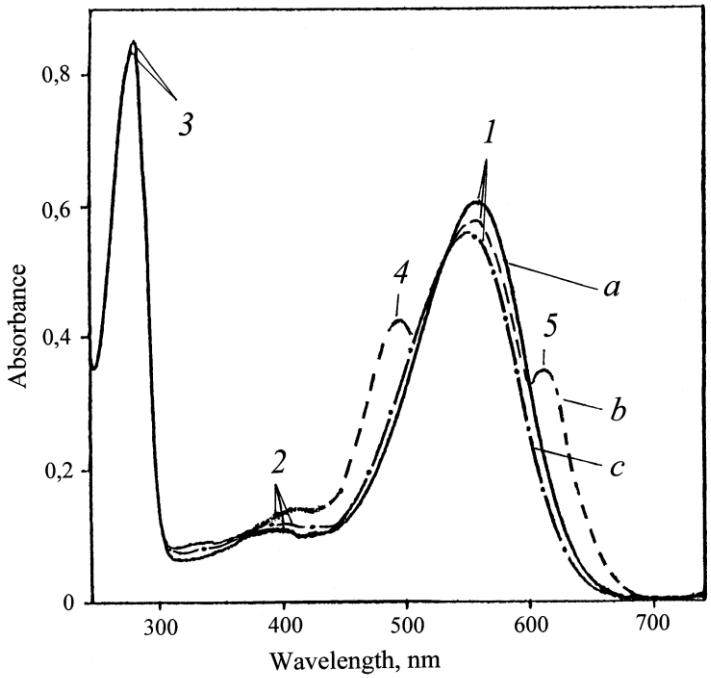

Figure 9. The absorption spectra of PM (50 % (v/v) EtOH) at various stages of processing: (*a*) – natural BR; (*b*) – PM after intermediate treatment; (*c*) – PM purified from carotenoids. The bandwith (1) is the spectral form of BR_{568}, (2) – impurity of spectral form of *meta*-bacteriorhodopsin M_{412}, (3) – the total absorption bandwith of aromatic amino acids, (4) and (5) – extraneous carotenoids. As a control used the native BR.

The final stage of purification involved the crystallization of the solubilized in 0,5 % (w/v) SDS-Na solution protein by MeOH and further separation of the protein from low-molecular-weight impurities by GPC. For this purpose the fractions containing BR were passed twice through a column with dextran Sephadex G-200 balanced with 0.09 M Tris buffer (pH = 8,35) containing 0,1 % (w/v) SDS-Na and 2,5 mM EDTA.

The homogeneity of isolated BR satisfies to the requirements for reconstruction of native membranes, and was confirmed by electrophoresis in 12,5 % (w/v) PAAG with 0,1 % (w/v) SDS-Na and *in vitro* regeneration of AP with 13-*trans*-retinal. The degree of regeneration of PM was determined by the ratio: $D_{nat.280} \cdot D_{nat.568} / D_{reg.280} \cdot D_{reg.568}$ (D_{280} and D_{568} – the absorbance of a suspension of native and regenerated PM at λ = 280 and λ = 568 nm) was 65 mol.%. Output of crystalline protein makes up approximately 5 mg. The total level of deuterium enrichment of the BR molecule, calculated on deuterium enrichment levels of amino acids of the protein hydrolyzate was 95,7 atom% ^2H.

Discussion

Our studies indicated that the ability of adaptation to ^2H_2O for different taxonomic groups of microorganisms is different, and stipulated by taxonomic affiliation, metabolic characteristics, pathways of assimilation of substrates, as well as by evolutionary niche occupied by the object. Thus, the lower the level of evolutionary organization of the organism, the easier it adapted to the

presence of deuterium in growth media. Thus, most primitive in evolutionary terms (cell membrane structure, cell organization, resistance to environmental factors) of the studied objects are photo-organotrophic halobacteria related to archaebacteria, standing apart from both prokaryotic and eukaryotic microorganisms, exhibiting increased resistance to ^2H_2O and practically needed no adaptation to ^2H_2O, contrary to blue-green algae, which, being eukaryotes, are the more difficult adapted to ^2H_2O and, therefore, exhibit inhibition of growth at 70–75 % (v/v) D_2O.

The composition of growth media evidently also plays an important role in process of adaptation to ^2H_2O, because the reason of inhibition of cell growth and cell death can be changes of the parity ratio of synthesized metabolites in ^2H_2O-media: amino acids, proteins and carbohydrates. It is noted that adaptation to ^2H_2O occures easier on complex growth media than on the minimal growth media with full substrates at a gradual increasing of deuterium content in the growth media, as the sensitivity to ^2H_2O of different vital systems is different. As a rule, even highly deuterated growth media contain remaining protons ~0,2–10,0 atom.%. These remaining protons facilitate the restructuring to the changed conditions during the adaptation to ^2H_2O, presumably integrating into those sites, which are the most sensitive to the replacement of hydrogen by deuterium. The evidence has been obtained that cells evidently are able to regulate the $^2H/^1H$ ratios, while its changes trigger distinct molecular processes. One possibility to modify intracellular $^2H/^1H$ ratios is the activation of the H^+-transport system, which preferentially eliminates H^+, resulting in increased $^2H/^1H$ ratios within cells. Furthermore deuterium induces physiological, morphological and cytological alterations on the cell. There were marked the significant differences in the morphology of the protonated and deuterated cells of blue-green algae *C. vulgaris*. Cells grown on ^2H_2O-media were ~2–3 times larger in size and had thicker cell walls, than the control cells grown on a conventional protonated growth media with ordinary water, the distribution of DNA in them was non-uniform. In some cases on on the surface of cell membranes may be observed areas consisting of tightly packed pleats of a cytoplasmic membrane resembling mezosoms – intracytoplasmic bacterial membrane of vesicular structure and tubular form formed by the invasion of cytoplasmic membrane into the cytoplasm (Figure 10). It is assumed that mezosoms involved in the formation of cell walls, replication and segregation of DNA, nucleotides and other processes. There is also evidence that the majority number of mezosoms being absent in normal cells is formed by a chemical action of some external factors – low and high temperatures, fluctuation of pH and and other factors. Furthermore, deuterated cells of *C. vulgaris* were also characterized by a drastic change in cell form and direction of their division. The observed cell division cytodieresis did not end by the usual divergence of the daughter cells, but led to the formation of abnormal cells, as described by other authors [30]. The observed morphological changes associated with the inhibition of growth of deuterated cells were stipulated by the cell restructuring during the process of adaptation to ^2H_2O. The fact that the deuterated cells are larger in size (apparent size was of ~2–4 times larger than the size of the protonated cells), apparently is a general biological phenomenn proved by growing a number of other adapted to ^2H_2O prokaryotic and eukaryotic cells.

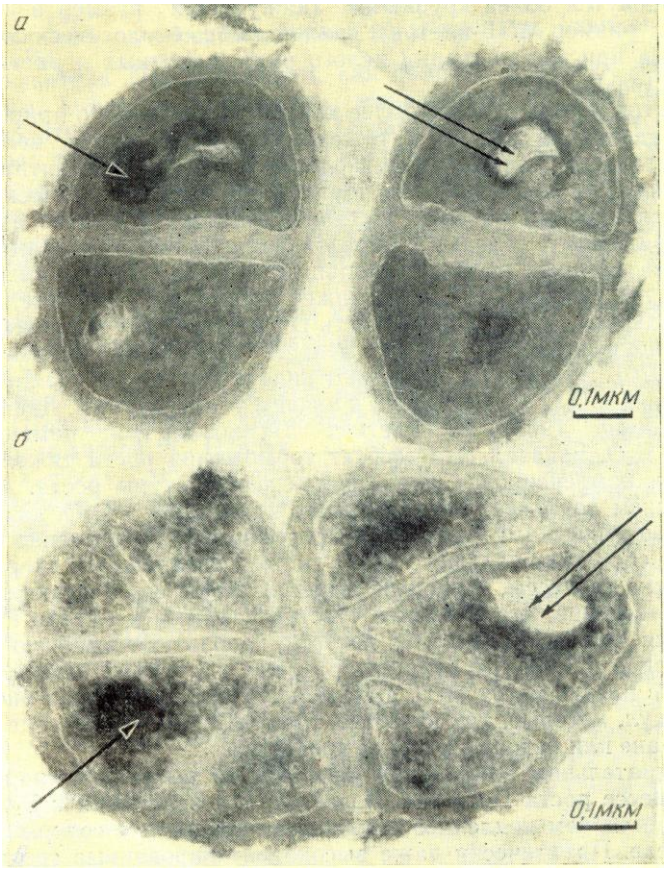

Figure 10. Electron micrographs of *Micrococcus lysodeikticus* cells obtained by SEM method: *a*) – protonated cells obtained on H_2O-medium; *b*) – deuterated cells obtained on ^2H_2O-medium. The arrows indicate the tightly-packed portions of the membranes

Our data generally confirm a stable notion that adaptation to ^2H_2O is a phenotypic phenomenon as the adapted cells eventually return back to the normal growth after some lag-period after their replacement back onto H_2O-medium. However, the effect of reversion of growth on $H_2O/^2H_2O$ media does not exclude an opportunity that a certain genotype determines the manifistation of the same phenotypic attribute in ^2H_2O-media with high deuterium content. At placing a cell onto ^2H_2O-media lacking protons, not only ^2H_2O is removed from a cell due to isotopic ($^1H–^2H$) exchange, but also there are occurred a rapid isotopic ($^1H–^2H$) exchange in hydroxyl (-OH), sulfohydryl (-SH) and amino ($-NH_2$) groups in all molecules of organic substances, including proteins, nucleic acids, carbohydrates and lipids. It is known, that in these conditions only covalent C–H bond is not exposed to isotopic ($^1H–^2H$) exchange and, thereof only molecules with bonds such as C–^2H can be synthesized de novo. Depending on the position of the deuterium atom in the molecule, there are distinguished primary and secondary isotopic effects mediated by intermolecular interactions. In this aspect, the most important for the structure of macromolecules are dynamic short-lived hydrogen (deuterium) bonds formed between the electron deficient $^1H(^2H)$ atoms and adjacent electronegative O, C, N, S- heteroatoms in the molecules, acting as acceptors of H-bond. The hydrogen bond, based on weak electrostatic forces, donor-acceptor interactions with charge-transfer and intermolecular van der Waals forces, is of the vital importance in the chemistry of intermolecular interactions and maintaining the spatial structure of macromolecules in aqueous solutions. Another important property is defined by the three-dimensional structure of ^2H_2O molecule having the tendency to pull together hydrophobic groups of macromolecules to minimize their disruptive effect on the hydrogen (deuterium)-bonded network in ^2H_2O. This leads to stabilization of the structure of protein and nucleic acid macromolecules in the presence of ^2H_2O. That is why, the structure of macromolecules of proteins and nucleic acids in the presence of ^2H_2O is somehow stabilized [31].

Evidently the cell implements a special adaptive mechanisms promoting the functional reorganization of vital systems in ^2H_2O. Thus, for the normal synthesis and function in ^2H_2O of

such vital compounds as nucleic acids and proteins contributes to the maintenance of their structure by forming hydrogen (deuterium) bonds in the molecules. The bonds formed by deuterium atoms are differed in strength and energy from similar bonds formed by hydrogen. Somewhat greater strength of $^{2}H–O$ bond compared to $^{1}H–O$ bond causes the differences in the kinetics of reactions in H_2O and $^{2}H_2O$. Thus, according to the theory of a chemical bond the breaking up of covalent $^{1}H–C$ bonds can occur faster than $C–^{2}H$ bonds, the mobility of $^{2}H_3O^{+}$ ion is lower on 28,5 % than H_3O^{+} ion, and $O^{2}H^{-}$ ion is lower on 39,8 % than OH^{-} ion, the constant of ionization of $^{2}H_2O$ is less than that of H_2O. These chemical-physical factors lead to slowing down in the rates of enzymatic reactions in $^{2}H_2O$ [32]. However, there are also such reactions which rates in $^{2}H_2O$ are higher than in H_2O. In general these reactions are catalyzed by $^{2}H_3O^{+}$ or H_3O^{+} ions or $O^{2}H^{-}$ and OH^{-} ions. The substitution of ^{1}H with ^{2}H affects the stability and geometry of hydrogen bonds in an apparently rather complex way and may, through the changes in the hydrogen bond zero-point vibration energies, alter the conformational dynamics of hydrogen (deuterium)-bonded structures of DNA and proteins in $^{2}H_2O$. It may cause disturbances in the DNA-synthesis during mitosis, leading to permanent changes on DNA structure and consequently on cell genotype [33]. Isotopic effects of deuterium, which would occur in macromolecules of even a small difference between hydrogen and deuterium, would certainly have the effect upon the structure. The sensitivity of enzyme function to the structure and the sensitivity of nucleic acid function (genetic and mitotic) would lead to a noticeable effect on the metabolic pathways and reproductive behaviour of an organism in the presence of $^{2}H_2O$. And next, the changes in dissociation constants of DNA and protein ionizable groups when transferring the macromolecule from H_2O into $^{2}H_2O$ may perturb the charge state of the DNA and protein molecules. All this can cause variations in nucleic acid synthesis, which can lead to structural changes and functional differences in the cell and its organelles. Hence, the structural and dynamic properties of the cell membrane, which depends on qualitative and quantitative composition of membrane's fatty acids, can also be modified in the presence of $^{2}H_2O$. The cellular membrane is one of the most important organelles in the bacteria for metabolic regulation, combining apparatus of biosynthesis of polysaccharides, transformation of energy, supplying cells with nutrients and involvement in the biosynthesis of proteins, nucleic acids and fatty acids. Obviously, the cell membrane plays an important role in the adaptation to $^{2}H_2O$. But it has been not clearly known what occurs with the membranes – how they react to the replacement of protium to deuterium and how it concerns the survival of cells in $^{2}H_2O$-media devoid of protons.

Comparative analysis of the fatty acid composition of deuterated cells of chemoheterotrophic bacteria *B. subtilis*, obtained on the maximum deuterated medium with 99,9 atom.% $^{2}H_2O$, carried out by HPLC method, revealed significant quantitative differences in the fatty acid composition compared to the control obtained in ordinary water (Figure 11a, b). Characteristically, in a deuterated sample fatty acids having retention times at 33,38; 33,74; 33,26 and 36,03 min are not detected in HPLC-chromatogram (Fig. 11b). This result is apparently due to the fact that the cell membrane is one of the first cell organelles, sensitive to the effects of $^{2}H_2O$, and thus compensates the changes in rheological properties of a membrane (viscosity, fluidity, structuredness) not only by quantitative but also by qualitative composition of membrane fatty acids. Similar situation was observed with the separation of other natural compounds (proteins, amino acids, carbohydrates) extracted from deutero-biomass obtained from maximally deuterated $^{2}H_2O$-medium.

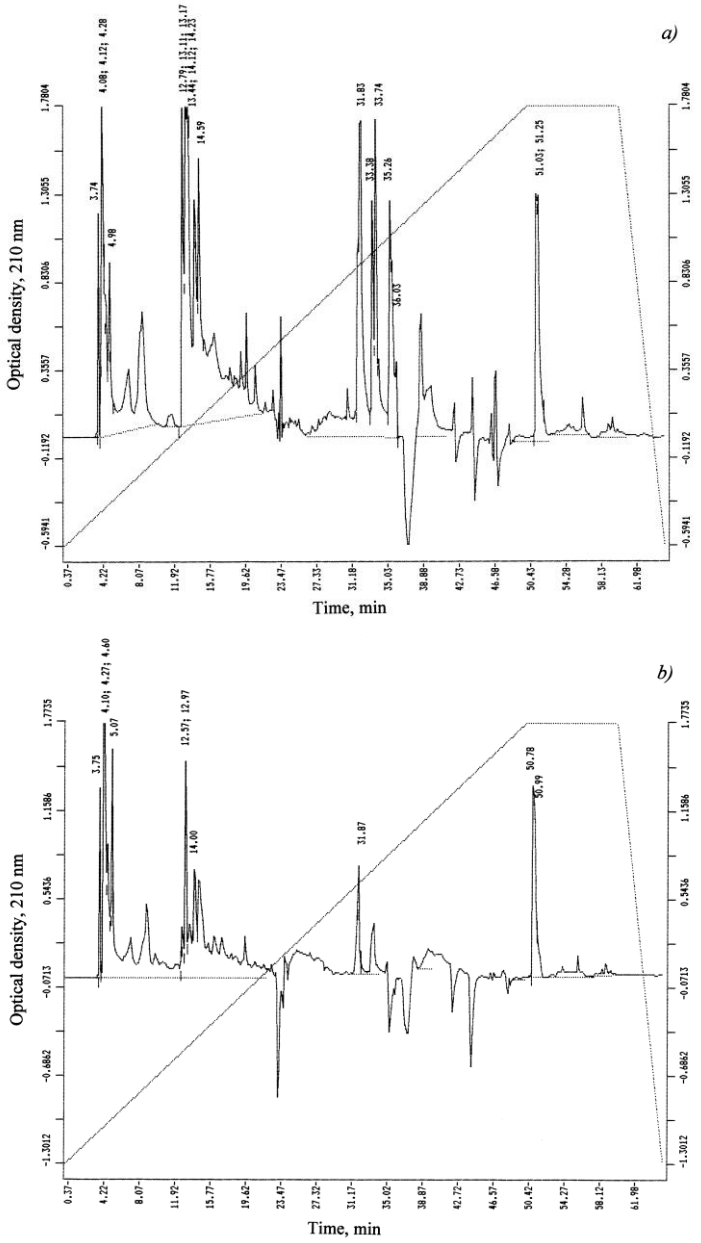

Figure 11. HPLC-chromatograms of fatty acids obtained from protonated (*a*) and deuterated (*b*) cells of *B. subtilis* on the maximally deuterated ^2H_2O-medium: Beckman Gold System (Beckman, USA) chromatograph (4,6×250 mm); stationary phase: Ultrasphere ODS, 5 μm; mobile phase: linear gradient 5 mM KH_2PO_4–acetonitrile (shown in phantom), elution rate: 0,5 ml/min, detection at λ = 210 nm. The peaks with retention time 3,75 min (instead of 3,74 minutes in the control); 4,10; 4,27; 4,60 (instead of 4,08; 4,12; 4,28 in the control), 5,07 (instead of 4,98 in control) 12,57; 12,97 (instead of 12,79; 13,11; 13,17 in control); 14,00 (instead of 14,59 in the control); 31,87 (instead of 31,83 in the control); 33,38; 33,74; 33,26; 36,03; 50,78; 50,99 (instead of 51,03; 51,25 for control) correspond to individual intracellular fatty acids

Amino acid analysis of protein hydrolysates isolated from deuterated cells of B. subtilis, also revealed the differences in quantitative composition of amino acids synthesized in ^2H_2O-medium (Figure 12). Protein hydrolyzates contains fifteen identified amino acids (except proline, which was detected at λ = 440 nm) (Table 5). An indicator that determines a high efficiency of deuterium inclusion into amino acid molecules of protein hydrolyzates are high levels of deuterium enrichment of amino acid molecules, which are varied from 50 atom.% for leucine/isoleucine to 97,5 atom.% for alanine.

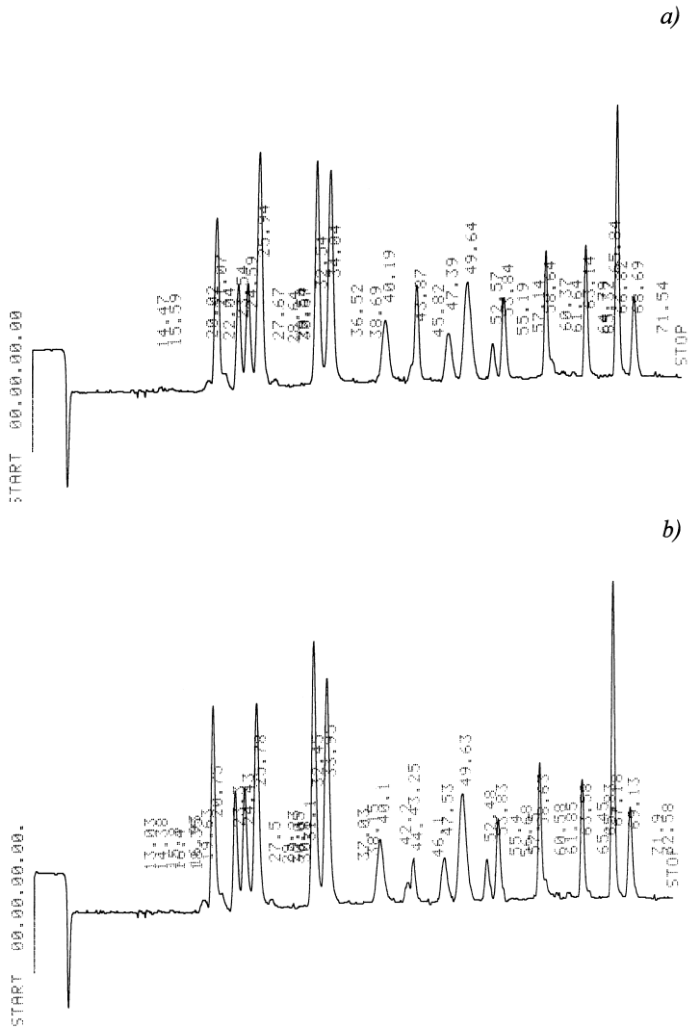

Figure 12. HPLC-chromatograms of amino acids obtained from hydrolizates of protonated (a) and deuterated (b) cells of *B. subtilis* on the maximally deuterated D_2O-medium: Biotronic LC-5001 (230×3,2 mm) column ("Eppendorf–Nethleler–Hinz", Germany); stationary phase: UR-30 sulfonated styrene resin ("Beckman–Spinco", USA); 25 μm; 50–60 atm; mobile phase: 0,2 N sodium–citrate buffer (pH = 2,5); the eluent input rate: 18,5 ml/h; the ninhydrin input rate: 9,25 ml/h; detection at λ = 570 and λ = 440 nm (for proline).

Table 5: Amino acid composition of the protein hydrolysates of *B. subtilis*, obtained on the maximum deuterated medium and levels of deuterium enrichment of molecules*

Amino acid	Yield, % (w/w) dry weight per 1 gram of biomass		Number of deuterium atoms incorporated into the carbon backbone of a molecule**	Level of deuterium enrichment of molecules, % of the total number of hydrogen atoms***
	Protonated sample (control)	The sample obtained in 99,9 atom.% ^2H_2O		
Glycine	8,03	9,69	2	90,0
Alanine	12,95	13,98	4	97,5
Valine	3,54	3,74	4	50,0
Leucine	8,62	7,33	5	50,0

Isoleucine	4,14	3,64	5	50,0
Phenylalanine	3,88	3,94	8	95,0
Tyrosine	1,56	1,83	7	92,8
Serine	4,18	4,90	3	86,6
Threonine	4,81	5,51	–	–
Methionine	4,94	2,25	–	–
Asparagine	7,88	9,59	2	66,6
Glutamic acid	11,68	10,38	4	70,0
Lysine	4,34	3,98	5	58,9
Arginine	4,63	5,28	–	–
Histidine	3,43	3,73	–	–

Notes:

* The data obtained by mass spectrometry for the methyl esters of N-5-(dimethylamino) naphthalene-1-sulfonyl chloride (dansyl) amino acid derivatives.

** While calculating the level of deuterium enrichment protons (deuterons) at the carboxyl (COOH-) and NH_2-groups of amino acid molecules are not taken into account because of their easy dissociation in $H_2O/^2H_2O$

*** A dash means absence of data.

Qualitative and quantitative composition of the intracellular carbohydrates of *B. subtilis* obtained on maximally deuterated ^2H_2O-medium is shown in Table. 6 (the numbering is given to the sequence of their elution from the column) contained monosaccharides (glucose, fructose, rhamnose, arabinose), disaccharides (maltose, sucrose), and four other unidentified carbohydrates with retention time 3,08 min (15,63 %); 4,26 min (7,46 %); 7,23 min (11,72 %) and 9,14 min (7,95 %) (not shown) (Figure 13). Yield of glucose in deuterated sample makes up 21,4 % by dry weight, i.e. higher than for fructose (6,82 %), rhamnose (3,47 %), arabinose (3,69 %), and maltose (11,62 %). Their outputs are not significantly different from the control in H_2O except for sucrose in deuterated sample that was not detected (Table 6). The deuterium enrichment levels of carbohydrates were varied from 90,7 atom.% for arabinose to 80,6 atom.% for glucose.

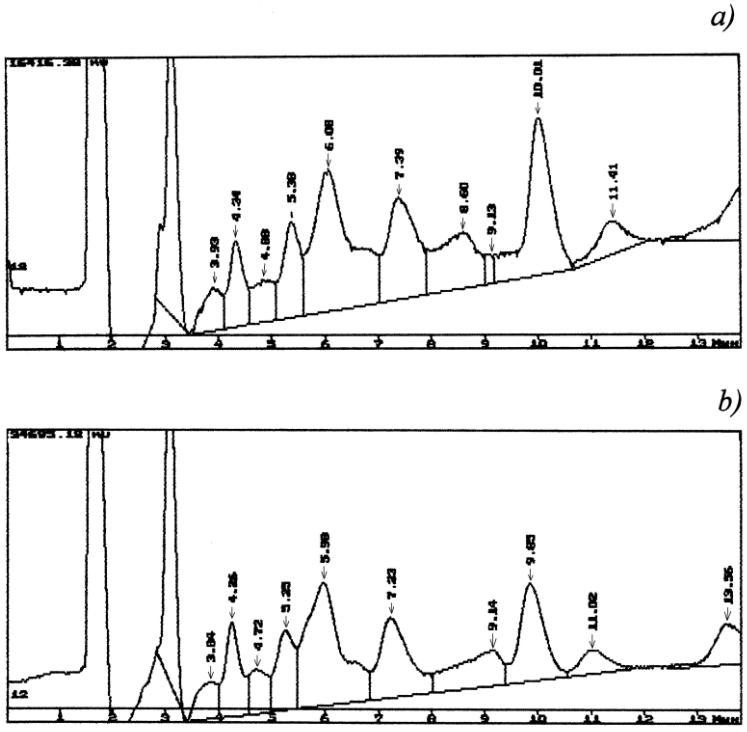

Figure 13. HPLC-chromatograms of intracellular carbohydrates obtained from protonated (a) and deuterated (b) cells of *B. subtilis* on the maximally deuterated ^2H_2O-medium: Knauer Smartline chromatograph (250×10 mm) ("Knauer", Germany); stationary phase: Ultrasorb CN; 10 μm; mobile phase: acetonitrile–water (75:25, % (w/w); the input rate: 0,6 ml/min

Table 6: Qualitative and quantitative composition of intracellular carbohydrates of *B. subtilis* obtained on the maximally deuterated medium and levels of deuterium enrichment of molecules*

Carbohydrate	Content in the biomass, % of the dry weight of 1 g biomass		Level of deuterium enrichment, % of the total number of hydrogen atoms***
	Protonated sample (control)	The sample obtained in 99,9 atom.% ^2H_2O**	
Glucose	20,01	21,40	80,6
Fructose	6,12	6,82	85,5
Rhamnose	2,91	3,47	90,3
Arabinose	3,26	3,69	90,7
Maltose	15,30	11,62	–
Sucrose	8,62	ND	–

Notes:
* The data were obtained by IR-spectroscopy.
** ND – not detected
** A dash means the absence of data.

In conclusion it should be noted that comparative analysis of IR-spectra of H_2O solutions and its deuterated analogues (^2H_2O, H^2HO) is of considerable interest for biophysical studies, because at changing of the atomic mass of hydrogen by deuterium atoms in H_2O molecule their interaction will also change, although the electronic structure of the molecule and its ability to form H-bonds, however, remains the same. The local maximums in IR-spectra reflect vibrational-rotational transitions in the ground electronic state; the substitution with deuterium changes the vibrational-rotational transitions in H_2O molecule, that is why it appear other local maximums in IR-spectra. In the water vapor state, the vibrations involve combinations of symmetric stretch (υ_1), asymmetric stretch (υ_3) and bending (υ_2) of the covalent bonds with absorption intensity (H_2O) $\upsilon_1;\upsilon_2;\upsilon_3$ = 2671; 1178,4; 2787,7 cm^{-1}. For liquid water absorption bands are observed in other regions of the IR-spectrum, the most intense of which are located at 2100, cm^{-1} and 710-645 cm^{-1}. For ^2H_2O molecule these ratio compiles 2723,7; 1403,5 and 3707,5 cm^{-1}, while for H^2HO molecule – 2671,6; 1178,4 and 2787,7 cm^{-1}. H^2HO (50 mole% H_2O + 50 mole% ^2H_2O; ~50 % H^2HO, ~25 % H_2O, ~25 % ^2H_2O) has local maxima in IR-spectra at 3415 cm^{-1}, 2495 cm^{-1} 1850 cm^{-1} and 1450 cm^{-1} assigned to OH^- -stretch, O^2H^- -stretch, as well as combination of bending and libration and H^2HO bending respectively.

In the IR-spectrum of liquid water absorbance band considerably broadened and shifted relative to the corresponding bands in the spectrum of water vapor. Their position depends on the temperature [34]. The temperature dependence of individual spectral bands of liquid water is very complex [35]. Furthermore, the complexity of the IR-spectrum in the area of OH^- stretching vibration can be explained by the existence of different types of H_2O associations, manifestation of overtones and composite frequencies of OH^- groups in the hydrogen bonds, and the tunneling effect of the proton (for relay mechanism) [36]. Such complexity makes it difficult to interpret the spectrum and partly explains the discrepancy in the literature available on this subject.

In liquid water and ice the IR-spectra are far more complex than those ones of the vapor due to vibrational overtones and combinations with librations (restricted rotations, i.g. rocking motions). These librations are due to the restrictions imposed by hydrogen bonding (minor L_1 band at 395,5 cm^{-1}; major L_2 band at 686,3 cm^{-1}; for liquid water at 0 ^oC, the absorbance of L_1 increasing with increasing temperature, while L_2 absorbance decreases but broadens with reduced wave number with increasing temperature [37]. The IR spectra of liquid water usually contain three absorbance bands, which can be identified on absorption band of the stretching vibration of OH^- group; absorption band of the first overtone of the bending vibration of the molecule H^2HO and absorption band of stretching vibration of O^2H^- group. Hydroxyl group OH^- is able to absorb much infrared radiation in the infrared region of the IR-spectrum. Because of its polarity, these groups typically react with each other or with other polar groups to form intra-and intermolecular hydrogen bonds. The hydroxyl groups, which are not involved in formation of hydrogen bonds

usually produce the narrow bands in IR spectrum, while the associated groups – broad intense absorbance bands at lower frequencies. The magnitude of the frequency shift is determined by the strength of the hydrogen bond. Complication of the IR spectrum in the area of OH^- stretching vibrations can be explained by the existence of different types of associations of H_2O molecules, a manifestation of overtones and combination frequencies of OH^- groups in hydrogen bonding, as well as the proton tunneling effect (on the relay mechanism).

Assignment of main absorbtion bands in the IR-spectrum of liquid water is given in the Table. 7. The IR spectrum of H_2O molecule was examined in detail from the microwave till the middle (4–17500 cm^{-1}) visible region and the ultraviolet region – from 200 nm^{-1} to ionization limit at 98 nm^{-1} [38]. In the middle visible region at 4–7500 cm^{-1} are located rotational spectrum and the bands corresponding to the vibrational-rotational transitions in the ground electronic state. In the ultraviolet region (200 to 98 nm^{-1}) are located bands corresponding to transitions from the excited electronic states close to the ionization limit in the electronic ground state. The intermediate region of the IR-spectrum – from 570 nm to 200 nm corresponds to transitions to higher vibrational levels of the ground electronic state**.**

Table 7: The assignment of main frequencies in IR-spectra of liquid water H_2O and ^2H_2O

Main vibrations of liquid H_2O and ^2H_2O				
Vibration(s)	H_2O (t = 25 °C)		^2H_2O (t = 25 °C)	
	υ, cm^{-1}	E_0, M^{-1} cm^{-1}	υ, cm^{-1}	E_0, M^{-1} cm^{-1}
Spinning ν_1 + deformation ν_2	780-1645	21,65	1210	17,10
Composite $\nu_1 + \nu_2$	2150	3,46	1555	1,88
Valence symmetrical ν_1, valence asymmetrical ν_3, and overtone $2\nu_2$	3290-3450	100,65	2510	69,70

At the transition from H_2O monomers to H_2O dimer and H_3O trimer absorption maximum of valent stretching vibrations of the O-H bond is shifted toward lower frequencies (υ_3 = 3490 cm^{-1} and υ_1 = 3280 cm^{-1}) and the bending frequency increased (υ_2 = 1644 cm^{-1}) because of hydrogen bonding. The increased strength of hydrogen bonding typically shifts the stretch vibration to lower frequencies (red-shift) with greatly increased intensity in the infrared due to the increased dipoles. In contrast, for the deformation vibrations of the H-O-H, it is observed a shift towards higher frequencies. Absorption bands at 3546 and 3691 cm^{-1} were attributed to the stretching modes of the dimer [$(H_2O)_2$]. These frequencies are significantly lower than the valence modes of ν_1 and ν_3 vibrations of isolated H_2O molecules at 3657 and 3756 cm^{-1} respectively). The absorbtion band at 3250 cm^{-1} represents overtones of deformation vibrations. Among frequencies between 3250 and 3420 cm^{-1} is possible Fermi resonance (this resonance is a single substitution of intensity of one fluctuations by another fluctuation when they accidentally overlap each other). The absorption band at 1620 cm^{-1} is attributed to the deformation mode of the dimer. This frequency is slightly higher than the deformation mode of the isolated H_2O molecule (1596 cm^{-1}). A shift of the band of deformation vibration of water in the direction of high frequencies at the transition from a liquid to a solid atate is attributed by the appearance of additional force, preventing O-H bond bending. Deformation absorption band in IR-spectum of water has a frequency at 1645 cm^{-1} and a very weak temperature dependence. It changes little in the transition to the individual H_2O molecule at a frequency of 1595 cm^{-1}. This frequency is found to be sufficiently stable, while all other frequencies are greatly affected by temperature changes, the dissolution of the salts and phase transitions. It is believed that the persistence of deformation oscillations is stipulated by processes of intermolecular interactions, i.g. by the change in bond angle as a result of interaction of H_2O molecules with each other, as well as with cations and anions.

Thus the study of the characteristics of the IR spectrum of water allows to answer the question not only on the physical parameters of the molecule and the covalent bonds **at** isotopic

substitution with deuterium, but also **to make a certain conclusion on** associative environment in water. The latter fact is important in the study of structural and functional properties of water assotiates and its isotopomers **at the** isotopic substitution with deuterium.

Conclusions

The experimental data demonstrated that the effects observed at the cellular growth on ^2H_2O-media possess a complex multifactor character stipulated by changes of morpholodical, cytological and physiological parameters – magnitude of the lag-period, time of cellular generation, outputs of biomass, a ratio of amino acids, protein, carbohydrates and fatty acids synthesized in ^2H_2O, and with an evolutionary level of organization of investigated object as well. The cell evidently implements the special adaptive mechanisms promoting functional reorganization of work of the vital systems in the presence of ^2H_2O. Thus, the most sensitive to replacement of ^1H on ^2H are the apparatus of biosynthesis of macromolecules and a respiratory chain, i.e., those cellular systems using high mobility of protons and high speed of breaking up of hydrogen bonds. Last fact allows the consideration of adaptation to ^2H_2O as adaptation to the nonspecific factor affecting simultaneously the functional condition of several numbers of cellular systems: metabolism, ways of assimilation of carbon substrates, biosynthetic processes, and transport function, structure and functions of deuterated macromolecules. It seems to be reasonable to choose as biomodels in these studies microorganisms, as they are very well adapted to the environmental conditions and able to withstand high concentrations of ^2H_2O in growth media.

Referenses:

1. Ignatov I. Possible processes for origin of life and living matter with modeling of physiological processes of bacterium Bacillus subtilis in heavy water as model system / I. Ignatov, O.V. Mosin // Journal of Natural Sciences Research. 2013. V. 3. № 9. P. 65-76.

2. Ignatov I. Modeling of possible processes for origin of life and living matter in hot mineral and seawater with deuterium / I. Ignatov, O.V. Mosin // Journal of Environment and Earth Science. 2013. V. 3. № 14. P. 103-118.

3. Kushner D.J. Pharmacological uses and perspectives of heavy water and deuterated compounds // D.J. Kushner, A. Baker, T.G. Dunstall // Can. J. Physiol. Pharmacol. 1999. V. 77. № 2. P. 79–88.

4. Lis G. High-precision laser spectroscopy D/H and $^{18}O/^{16}O$ Measurements of microliter natural water samples / G. Lis, L.I. Wassenaar, M.J. Hendry // Anal. Chem. 2008. V. 80. № 1. P. 287–293.

5. Lobishev V.N. Isotopic effects of D_2O in biological systems / V.N. Lobishev, L.P. Kalinichenko. – Moscow: Nauka, 2008. 215 p.

6. Vertes A. Physiological effect of heavy water. Elements and isotopes: formation, transformation, distribution / A. Vertes, Ed. – Vienna: Dordrecht: Kluwer Acad. Publ., 2003. 112 p.

7. Mosin O.V. Studying of methods of biotechnological preparation of proteins, amino acids and nucleosides, labeled with stable isotopes ^2H, ^{13}C and ^{15}N with high levels of isotopic enrichment / O.V. Mosin. Autoref. disser. thesis PhD. – Moscow: M.V. Lomonosov State Academy of Fine Chemical Technology, 1996. 26 p.

8. Den'ko E.I. Influence of heavy water (D_2O) on animal, plant and microorganism's cells / E.I. Den'ko // Usp. Sovrem. Biol. 1970. V. 70. № 4. P. 41–49.

9. Stom D.I. Influense of water with varying content of deuterium on red Californian hybride (Eusenia fetida Andrei Bouche) / D.I. Stom, A.K. Ponomareva, O.F. Vyatchina // Bull. RAS. 2006. V. 6. № 52. P. 167–169 [in Russian].

10. Mosin O.V. Isotope effects of deuterium in bacterial and microalgae cells at growth on heavy water (D_2O) / O.V. Mosin, I. Ignatov // Voda: Himia i Ecologija. 2012. V. 3. P. 83–94 [in Russian].

11. Katz J.J. The biology of heavy water / J.J. Katz // Scientific American. 1960. V. 12. P. 106-115.

12. Michel F. Radioprotection by pretreatment with deuterated water: cytokinetic changes in the small intestine of the mouse / F. Michel, H.J. Altermatt, J.O. Gebbers // Virchows. Arch. B. Cell. Pathol. Incl. Mol. Pathol. 1988. V. 54. № 4. P. 214–220.

13. Laeng R.H. Radioprotection of cultured cells by preincubation in medium containing deuterium oxide / R.H. Laeng, R.L. Mini, J.A. Laissue, R. Schindler // Int. J. Radiat. Biol. 1991. V. 59. № 1. P. 165–173.

14. Somlyai G. The Biological Effect of Deuterium Depletion / G. Somlyai, Ed. – Budapest: Akademiai Klado, 2002. 130 p.

15. Mosin O.V. Studying of isotopic effects of heavy water in biological systems on example of prokaryotic and eukaryotic cells / O.V. Mosin, I. Ignatov // Biomedicine, Moscow. 2013. V. 1. № 1–3. P. 31–50 [in Russian].

16. Mosin O.V. Biological influence of deuterium on procariotic and eukaryotic cells / O.V. Mosin, I. Ignatov // European Journal of Molecular Biotechnology. 2014. V. 3. № 1. P. 11–24.

17. Crespi H.L. Fully deuterated microorganisms: tools in magnetic resonance and neutron scattering. Synthesis and applications of isotopically labeled compounds. in: Proceedings of an International Symposium / H.L. Crespi, T. Baillie, J.R. Jones (eds.). Amsterdam: Elsevier, 1989. pp. 329–332.

18. LeMaster D.M. Uniform and selective deuteration in two-dimensional NMR studies of proteins / D.M. LeMaster // Ann. Rev. Biophys. Chem. 1990. V. 19. P. 243–266.

19. MacCarthy P. Infrared spectroscopy of deuterated compounds: an undergraduate experiment / P. MacCarthy // J. Chem. Educ. 1985. V. 62. № 7. P. 633–638.

20. Mosin O.V. Mass-spectrometric determination of levels of enrichment of ^{2}H and ^{13}C in molecules of amino acids of various bacterial objects / O.V. Mosin, D.A. Skladnev, T.A. Egorova, V.I. Shvets // Bioorganic Chemistry. 1996. V. 22. № 10–11. P. 856–869.

21. Mosin O.V. Incorporation of [2,3,4,5,6-^{2}H]phenylalanine, [3,5-^{2}H]tyrosine, and [2,4,5,6,7-^{2}H]tryptophan into bacteriorhodopsin molecule of *Halobacterium halobium* / O.V. Mosin, D.A. Skladnev, V.I. Shvets // Applied Biochemistry and Microbiology. 1999. V. 35. № 1. P. 34–42.

22. Mosin O.V. Studying physiological adaptation of microorganisms to heavy water / O.V. Mosin, D.A. Skladnev, V.I. Shvets // Biotechnologya. 1999. № 8. P. 16–23.

23. Mosin O.V. Biosynthesis of photochrome transmembrane protein bacteriorhodopsin of *Halobacterium halobium* labeled with deuterium at aromatic amino acids residues of 2,3,4,5,6-2H5]Phe, [3,5-2H2]Tyr and [2,4,5,6,7 -2H5]Trp / O.V. Mosin, I. Ignatov // Chemistry and Materials Research. 2014. V. 6. № 3. P. 38-48.

24. Mosin O.V. Studying of the biosynthesis of ^{2}H-labeled inosine by a Gram-positive chemoheterotrofic bacterium *Bacillus subtilis B-3157* on heavy water ($^{2}H_2O$) medium / O.V. Mosin, I. Ignatov // Chemical and Process Engineering Research. 2013. V. 15. P. 32–45.

25. Mosin O.V. Studying of biosynthesis of amino acids by a strain of *Brevibacterium methylicum* at growth on media, containing heavy water and deuteron-methanol / O.V. Mosin, D.A. Skladnev, T.A. Egorova, A.M. Yurkevitch, V.I. Shvets // *Biotechnologija. 1996. №* 3. P. 3–12.

26. Mosin O.V. Studying of microbic synthesis of deuterium labeled L-phenylalanine by methylotrophic bacterium *Brevibacterium methylicum* on media with different content of heavy water // O.V. Mosin, V.I. Shvets, D.A. Skladnev, I. Ignatov // Russian Journal of Biopharmaceuticals. 2012. V. 4. № 1. P. 11–22.

27. Mosin O.V. Microbiological synthesis of ^{2}H-labeled phenylalanine, alanine, valine, and leucine/isoleucine with different degrees of deuterium enrichment by the Gram-positive facultative methylotrophic bacterium Brevibacterium methylicum / O.V. Mosin, I. Ignatov // International Journal of Biomedicine. 2013. V. 3. № 2. P. 132–138.

28. Mosin O.V. Biosynthesis of ^{2}H-labeled phenylalanine by a new methylotrophic mutant *Brevibacterium methylicum* / O.V. Mosin, D.A. Skladnev, V.I. Shvets // Bioscience, biotechnology and biochemistry. 1998. V. 62. № 2. P. 225–229.

29. Mosin O.V. Microbial synthesis of ^{2}H-labelled L-phenylalanine with different levels of isotopic enrichment by a facultive methylotrophic bacterium Brevibacterium methylicum with RuMP assimilation of carbon / O.V. Mosin, V.I. Shvets, D.A. Skladnev, I. Ignatov // Biochemistry (Moscow) Supplement Series B: Biomedical Chemistry. 2013. V. 7. № 3. P. 249-260.

30. Eryomin V.A. Growth of Micrococcus lysodeikticus on a deuterated medium / V.A. Eryomin, L.N. Chekulayeva, F.F. Kharatyan // Microbiologia. 1978. V. 14. P. 629–636 [in Russian].

31. Cioni P. Effect of heavy water on protein flexibility / P. Cioni, G.B. Strambini // Biophysical J. 2002. V. 82. № 6. P. 3246–3253.

32. Cleland W.N. Isotope effects on enzyme-catalyzed reactions / W.N. Cleland, M.N. O'Leary & D.D. Northrop (eds.). – Baltimore, London, Tokyo: University Park Press, 1976. 303 p.
33. Lamprecht I. Disorganization of mitosis in HeLa cells by deuterium oxide / I. Lamprecht, D. Schroeter, N. Paweletz // European journal of cell biology. 1989. V. 50. № 2. P. 360-369.
34. Ignatov I. Structural mathematical models describing water clusters / I. Igantov, O.V. Mosin // Journal of Mathematical Theory and Modeling. 2013. V. 3. № 11. P. 72-87.
35. Zelsmann H.R. Temperature dependence of the optical constants for liquid H_2O and D_2O in the far IR region / H.R. Zelsmann // J. Mol. Struct. 1995. V. 350. P. 95–114.
36. Yakhnevitch G.B. Infrared spectroscopy of water / G.B. Yakhnevitch. – Moscow: Nauka, 1973. 207 p. [in Russian].
37. Brubach J.B. Signatures of the hydrogen bonding in the infrared bands of water / J.B. Brubach, A. Mermet, A. Filabozzi, A. Gerschel, P. Roy, P. (2005). J. Chem. Phys., 122: 184509.
38. Walrafen, G.E. (1972) Raman and infrared spectral investigations of water structure. In Water a Comprehensive Treatise, F. Franks, Ed., Vol. 1, Plenum Press, New York, pp. 151–214.

УДК 579.871.08

Исследование феномена биологической адаптации к тяжелой воде

[1] Олег Викторович Мосин
[2] Игнат Игнатов
[3] Дмитрий Анатольевич Складнев
[4] Виталий Иванович Швец

[1] Московский государственный университет прикладной биотехнологии, Российская Федерация
Старший научный сотрудник кафедры биотехнологии, канд. хим. наук
103316, Москва, ул. Талалихина, 33
E-mail: mosin-oleg@yandex.ru
[2] Научно-исследовательский центр медицинской биофизики (РИЦ МБ), Болгария
Профессор, доктор наук Европейской академии естественных наук (ФРГ), директор НИЦ МБ
1111, София, ул. Н. Коперника, 32/6
E-mail: mbioph@dir.bg
[3] Государственный научно-исследовательский институт генетики и селекции промышленных микроорганизмов ГосНИИГенетика, Российская Федерация
Профессор, доктор биол. наук, ведущий научный сотрудник ГосНИИГенетика
117545, Москва, 1-й Дорожный пр., 1.
E-mail: genetika@genetika.ru
[4] Московский государственный университет тонких химических технологий им. М.В. Ломоносова, Российская Федерация
Академик РАН, доктор химических наук, заведующий кафедрой биотехнологии и нанобиотехнологии
117571, Москва, Вернадского просп., 86
E-mail: mitht@mitht.ru

Аннотация. Исследовано биологическое влияние дейтерия на клетки различных таксономических групп прокариотических и эукариотических микроорганизмов, реализующих метилотрофный, хемогетеротрофный, фото-органотрофный и фотосинтетический способы ассимиляции углеродных субстратов (метилотрофные бактерии *Brevibacterium methylicum*, хемогетеротрофные бактерии *Bacillus subtilis*, фото-органотрофные галобактерии *Halobacterium halobium* и синезеленая микроводоросль *Chlorella vulgaris*) при росте на питательных средах с тяжелой водой (^2H_2O). Для исследуемых микрооорганизмов представлены данные по росту и адаптации на питательных средах, содержащих в качестве источников дейтерированных субстратов ^2H_2O, [^{2}H]метанол и гидролизаты дейтерированного биомассы метилотрофных бактерий *B.*

methylicum, полученных в условиях многоступенчатой адаптации к ^2H_2O. Приведен качественный и количественный состав внутри-и межклеточных аминокислот, белков, углеводов и жирных кислот в условиях адаптации к ^2H_2O. Показано, что эффекты, наблюдаемые при адаптации к ^2H_2O, имеют сложный многофакторный характер и связаны с цитологическими, морфологическими и физиологическими изменениями в клетке – величины лаг-периода, времени клеточной генерации, выходах биомассы, соотношении синтезированных аминокислот, белков, углеводов и липидов, а также с эволюционным уровнем организации исследуемого объекта и путями ассимиляции углерода субстратов.

Ключевые слова: дейтерий; тяжелая вода; адаптация; изотопные эффекты; бактерии; микроводоросли.

Published in the Russian Federation
European Journal of Molecular Biotechnology
Has been issued since 2013.
ISSN: 2310-6255
E-ISSN 2409-1332
Vol. 6, No. 4, pp. 210-222, 2014

DOI: 10.13187/ejmb.2014.6.210
www.ejournal8.com

UDC 616.72-018.3 : 577.3

Different Phenotype of Chondrocytes in Articular Cartilage: Mapping, Possible Mechanisms, and Impact to Implant Healing

[1] Valery V. Novochadov
[2] Kristina A. Bovol'skaya
[2] Sof"ya A. Lipnitzkaya
[2] Ekaterina V. Perevalova
[2] Ekaterina Yu. Shuvalova
[2] Zoya N. Zagrebina
[3, 4] Valery G. Zaytzev

[1] Volgograd State University, Russian Federation
Universitetskiy Avenue 100, Volgograd city, 400062
MD, Professor
E-mail: novovv@rambler.ru
[2] Volgograd State University, Russian Federation
Universitetskiy Avenue 100, Volgograd city, 400062
Senior Student
E-mail: biobio@volsu.ru
[3] Volgograd State University, Russian Federation
Universitetskiy Avenue 100, Volgograd city, 400062
PhD, Ass.-Professor
E-mail: biobio@volsu.ru
[4] Volgograd State Medical University, Russian Federation
Pavshikh Bortsov Sq 1, Volgograd city, 400131
PhD, Ass.-Professor
E-mail: valeryzaitsev@gmail.com

Abstract

A remodelling of articular cartilage due to damage or pathological state development is characterized by an alteration in cartilage homeostasis including distribution of the chondrocytes. Said alteration can be determined by cellular response changes during cartilage regeneration and remodelling. However, features of cellular distrubution in native cartilage is not yet clear. This study was undertaken to select representative set of regulatory molecules and their receptors related to the formation of mosaic structures in the native cartilage. We used bioinformatical approaches and mapping of the chondrocyte phenotype markers in different areas of the intact articular cartilage. Differences in the phenotype markers expression as like as in cellular density gradient from tidemark to articular surface were observed. Additionaly, we have found specific order of lateral cellular distribution in the intact cartilage. The database of molecular processes in

chondrocytes have been obtained, seems to be suitable for further investigation of the articular cartilage remodeling. The hypothetical model of scaffold to satisfy the conditions of mosaic structure formation in cartilage after substitution of full-layer defects and stimulation of colonization by cells from the bone marrow, have been proposed.

Keywords: articular cartilage; osteoarthritis; cartilage tissue engineering; scaffolds; molecular mapping.

Introduction

Articular cartilage has unique structural features and control mechanisms of its tertiary functions to provide noninvasive stress distribution due to joint movements. These features, as a minimum, include visco-elastic and, the same time, very sough characteristics of extracellular matrix (ECM), monomorphic cellular composition, full avascularity, and absence of innervations. The trophic and molecular control the chondrocyte phenotype are carried out by molecules diffused from the underlying bone and synovial fluid [1, 2]. These features are the biological foundations of extremely low ability of articular cartilage to full regeneration, therefore, different post-traumatic problems in large joints and chronic pathology of degenerative and inflammatory genesis, osteoarthritis (OA), are wide-spread in the human population [3-6].

Despite the chondrocytes are the only cell population composed of cartilage, the tissue forming the articular surface is not seems to be homogeneous in its volume. In addition to the classic subdivision into loaded and not loaded areas, as well as deep, middle, and superficial zones [3, 7], an articular cartilage, as shown recently in rats and rabbits [8, 9], has distinct structural heterogeneity. The revealed phenomenon concluded in a presence of mosaic plots (microclusters), different from the environment by the numerical density of chondrocytes, structure and optical density of ECM. Those microclusters took about 40% of cartilage volume and could be described as a polygon-based truncated pyramids with a diameter cross section about 60-120 microns near the tidemark and extending to 100-150 microns by superficial zone of the cartilage, and they were critically altered in experimental osteoarthritis [10].

Currently, there are over forty biologically active molecules being able to actively influence over the chondrocyte phenotype. Basically, they represent cytokines (TNF-α, interleukin 1), growth and/or differentiation factors (TGF-β, BMP-2, IIS-7, IGF-1 etc.), although the effects of a number of hormones (in particular, the number of thyroid, insulin and metabolites were described in [11-15]). Recently there have been published the evidence of involvement of some signaling molecules, as growth factor and differentiation 5 (GDF-5) [20] and connective tissue growth factor (CCN2) [21, 22] in the regulation of chondrocyte phenotype. The participation hypoxia-inducible factor HIF-1α [23], and integrin α1β1 in this process has been substantially revised [24, 25].

That is the reason to make significant changes in scaffold technology for cartilage tissue engineering. Based on the of biomimetic principle, such scaffolds should have such structure and properties that the maximum extent close to the one of intact cartilage [26]. Tissue regenerates in the scaffold replacement site should be remodel into native cartilage in natural manner within some reasonable period, including all the nuances of zonal and mosaic organization [27, 28]. In order to achieve the results it is necessary to construct the scaffold being able to form zonal and mosaic heterogeneity of cartilage after implantation, based on engineering principles and bioinformatics approach.

The goal of this work, based on the above, is an attempt to develop principles for the fabrication of new scaffolds for cartilage tissue engineering.

Material and Methods

The first step in our study is an attempt to connect the imaginations about structural irregularity of cartilage with differences in chondrocyte phenotype. The samples of cartilage in the knee and elbow joints of six male Chinchilla rabbits weight of from 2.4 to 3.2 kg have been used for mapping the phenotype of the chondrocytes. Removing the animals from experiment was carried out in accordance within the context of Directive 2010/63/EU on the protection of animals used for scientific purposes.

Histological specimens were prepared after fixation in 10% solution of neutral buffered formalin (pH = 7.4) and decalcification in Cal-Ex® solution (Fisher Scientific). The sections were stained with hematoxylin, eosin, and with safranin O, to identify ECM. Primary phenotype

identification included such characteristics of chondrocytes, as the average size on the section (μm²) after visualization of their nuclei by fluorescent DAPI staining, and the average optical density of their territorial matrix (con. U/μm²), correlated to the distance between cell and articular surface (μm). The measurement was carried out in 4 or 5 slides from each specimen, 5-6 visual fields in each slide, so that the total number was of the order of 10^3.

Identification of the phenotype of chondrocytes was performed by sensitive immunohistochemical assays. Using the monoclonal antibodies against the proliferation marker Ki-67 (DakoCytomation, Denmark), TNF-related apoptosis-inducing ligand (TRAIL, Novocastra, UK) and the key enzyme of apoptosis cascade, caspase-3 (Novocastra, UK) we obtained the opportunity to reveal proliferative and apoptotic potential of chondrocytes. The antibodies against aggrecan (Santa Cruz Biotechonogy, USA) and lubricin (Santa Cruz Biotechonogy, USA), matrix metalloproteinases MMP-9 (Leica Mycrosystems, Germany) and MMP-13 (Santa Cruz Biotechonogy, USA), and their tissue inhibitors TIMP-1 (DakoCytomation, Denmark) and TIMP-3 (Santa Cruz Biotechonogy, USA) one used following the manufacturer's instructions to identify specific synthetic activity of cells. We also used temperature method of antigen demasking, secondary antibodies labeled with alkaline phosphatase with Fast Red visualization direct fluorescent label, negative control antigens and antibodies were used.

To examine visually and obtain digitized images we used research microscopes BIMAM R-13 (LOMO, Russia) with JCM camera (Japan) and AxioPlan 2 Imaging (Carl Zeiss, Germany) with visualization system AxioVision LE. We evaluate the expression immunopositive material in cells and/or territorial matrix as negative (-), very low, low, moderate and high. The most frequent variant of the conclusion was assigned to the specific site of the specimen.

Quantitative data were processed using Statistica 10.0 (StatSoft Inc., USA) with the calculation of the indices adopted to characterize the non-parametric samples in biomedical research: median [1st quartile ÷ 3rd quartile]. To prove the validity of differences the non-parametric Friedman criterion for multiple groups was applied. *P* values less than 0.05 were considered significant.

The next step was to build a scheme of genes encoding key proteins. It is required to determinate the chondrocyte phenotype. We used routine bioinformatics techniques, including the search free access NCBI resources (PubMed, PubMed Central, Gene, Protein, BioSystems), UniProtKB, PDB, KEGG, and SRS. We used comprehensive pool of synonymous constructs to success in data mining. As a result, genes from the operational database were associated with metabolism and the regulation of the functional activity of the chondrocyte (signaling molecules and their receptors, transcription factors). Representation of the signaling pathways controlling chondrocyte metabolism in the form of intellectual schema allowed to transform the information from the database, into a set of necessary properties of the chondrocyte environment in each compartment of articular cartilage: the surface area (1), the microclusters (2) and between them (3), and also near to the tidemark (4).

The final step was to establish a working model of scaffold for tissue engineering, taking into account the necessity of forming a cartilage with a three-dimensional heterogeneity of cellular setting and ECM density.

Results

Morphological analysis confirmed that the chondrocytes in the articular cartilage had quite heterogeneous phenotype; this heterogeneity cannot be reduced to the differences caused by different loads on specific areas of joint or different zonal location. Typical chondrocyte columns formed by chondrocyte isogroups in the deep and middle zones of cartilage are additionally aggregated into specific microclusters the size of about 100 μm (fig. 1a).

In the horizontal scanning the cartilage, we found distinct areas of more dense settlement of cells, usually about 5-8 in cross section (fig. 1b). When you restore the volume structure of microclusters they consisted generally up to a couple hundred of chondrocytes. As a detailed morphological description had been given in previous publications [8, 9], we specify only key features of the chondrocyte phenotype in the description of the cartilage under this perspective.

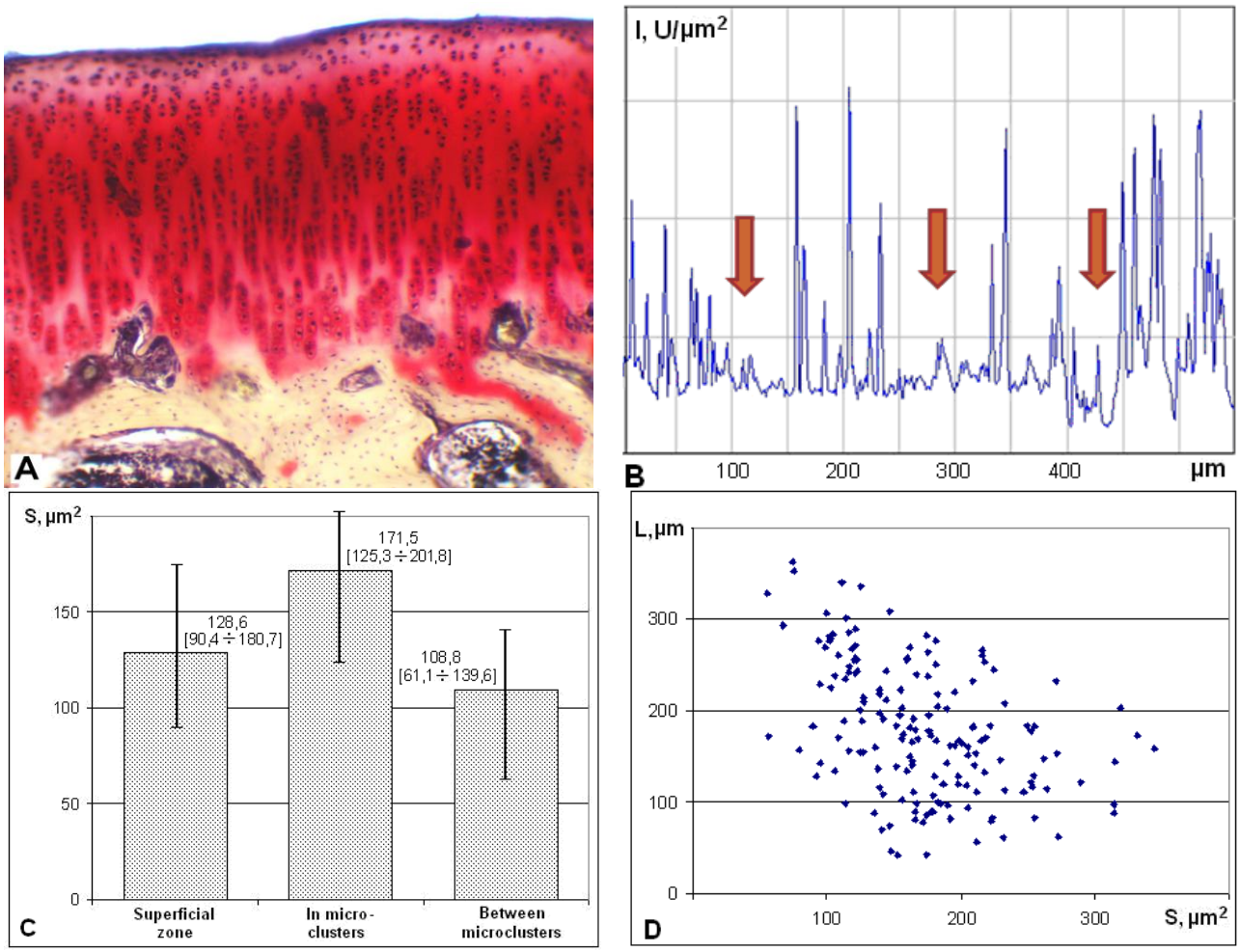

Figure 1. Chondrocytes in the cartilage of rabbit knee joint particularly group into microclusters different from surrounding areas of cartilage by cellular phenotype and denser ECM. A. Chondrocyte microclusters are presented by groups of several columns, spreading and widening from deep to superficial zone of cartilage. Safranin O staining, x 240. B. The characteristic distribution of DAPI fluorescence intensity in the articular cartilage reflects the presence of microclusters and intermediate areas (shown as arrows). C. Average sizes of chondrocytes, presented as Median [25% ÷ 75%], are different in superficial zone of cartilage, in microclusters of middle zone, and between them. D. Average size of chondrocytes in microclusters depends on the distance to articular surface in inversely proportional manner. The sample image contains about 200 cells in sight (estimation using Image J program).

First, the size and shape of the chondrocytes differed not only in the comparative study the superficial, middle and deep zones of cartilage. The size of chondrocytes in microclusters is much larger than the similar one between microclusters. The chondrocytes of the superficial zone, as well known, characterizing by a more elongated shape, had intermediate size in this list (fig. 1c). Then, the size of chondrocytes in microclusters was largely depended on their distance from the articular surface, this dependence was close to inversely proportional (fig. 1d). Finally, the density of the territorial matrix of the chondrocytes in the structure of microclusters was significantly higher than the similar one between microclusters.

These differences already suggest the existence of metabolic phenotype heterogeneity for chondrocytes, including their relation to synthesis, proliferation, and apoptosis.

Table 1 summarizes our findings in respect of these phenotypic traits. For ease of comparisons, we subdivided the chondrocytes in accordance with their position in the cartilage into 4 groups: surface area (1), in microclusters (2), between them (3) and in areas of deep zone near the tidemark (4).

Table 1: The distribution of phenotypic markers in chondrocytes and territorial matrix of the rabbit articular cartilage in the concept of its mosaic structure

Marker	Location of chondrocytes			
	Superficial zone	In microclusters	Between microclusters	Near tidemark
Ki-67	-	Very low	Very low	Moderate
TRAIL	Moderate	Low	Low	High
Caspase-3	Low	Low	Low	Moderate
Aggrecan	Low	High	Moderate	Low
Lubricin	High	Very low	-	-
MMP-9	Moderate	Low	Moderate	Very low
MMP-13	Moderate	Low	Moderate	-
TIMP-1	Low	Moderate	Low	Low
TIMP-3	Very low	Moderate	Low	Low

Besides the obvious marker findings, such as high lubricin expression of almost exclusively in the superficial zone of the cartilage, and the presence of proliferative potential in the deep zone, we discover several interesting findings. Pre-apoptotic and apoptotic potentials, estimated balance TRAIL and caspase-3 have been quite high in the deep zone of cartilage and moderate in the surface zone. These markers almost never appears in the middle zone's chondrocytes of native cartilage. The aggrecan expression was higher in chondrocytes of microclusters, less in chondrocytes localized between clusters, and it was tending to zero as it approached the surface. The chondrocytes in microclusters were characterized by a higher expression of TIMP-1 and TIMP-3, whereas chondrocytes between the microclusters and in surface area were characterized by the prevalence of MMP-9 and MMP-13 expression and low expression of TIMPs.

The received data specify the number of mechanisms associated with relatively higher ECM density in microclusters of articular cartilage. They, at least, are in the presence of high synthetic potential of chondrocytes, their resistance to apoptosis, and in MMP/TIMP balance preventing any intensive destruction of the matrix.

Bioinformatics approach allows particularly explain structural irregularity of cartilage using a metabolic map creation. Key bonds between signal molecules and specific synthesis in chondrocyte is considered a control network for chondrocyte phenotype.

A first control circuit for the control chondrocyte phenotype is a set of signaling molecules coming from the bloodstream and bone marrow through the underlying bone. In accordance with the diffusion mechanism of receipt such molecules increasingly act to young cells near the tidemark and, in a much lesser extent, to the middle zone chondrocytes. Necessary information about intake of almost all known cytokines and growth factors, as well as a number of hormones and other regulatory molecules to the cartilage has been found in open access databases.

The second control circuit is in a pool of molecules coming from the synovial fluid. Similar to the first one, as is clear from the revealed cartilage structure, this pool is able to influence the chondrocytes of the superficial zone and cells between microclusters in middle zone. Many cytokines were found in the synovial fluid: more than ten interleukins (IL-1β, IL-6, IL-8, IL-10, IL-17 etc.), TNF-α, interferon γ, interferon-inducible protein 10, cell-derived factor-1, oncostatin M, monocyte chemoattractant proteins 1 and 2, and RANTES. Also growth factors such as transforming growth factors (TGF-α and TGF-β1-3), granulocyte colony-stimulating factor, insulin-like growth factors (IGF-1 and IGF-2), platelet-derived growth factor (PDGF-BB), vascular endothelial growth factor (VEGF), connective tissue growth factor (also known as CCN2) were detected in the synovial fluid. A number of hormones, including leptin, were also identified there. In addition, synovial fluid contains many products of disintegrating cartilage, and therefore it is possible to discover in it a variety of glycosaminoglycans, their sulfated fragments, glycoconjugates, polygalacturonase acid, fibronectin-aggrecan complexes, fractalkine, cartilage oligomeric matrix protein, osteopontin, and matrix metalloproteases 1, 3, 9, and 13. Collectively, they represent an additional pool of substances seems to regulate composition and properties of the superficial zone in articular cartilage.

Directly in the middle zone the paracrine and autocrine regulation mechanisms are probably prevalent particularly stimulating by mechanical loads on articular surface. Such factors can

include hyaluronic acid and its derivatives, matrix metalloproteinases and their inhibitors, a number of transcription factors capable of intercellular transfer (for example, Nupr1, NF-kB), etc.

The most important of all these regulators and their possible receptor-dependent involvement in the formation of the chondrocyte phenotype we group in table 2.

Table 2: Proved presence of regulatory molecules in the environments supplying articular cartilage and their influence on the chondrocyte phenotype

Regulatory molecule	Evidence of presence		Impact to processes in chondrocytes			
	Synovial fluid	Bone and bone marrow	Proliferation and differentiation	Apoptosis	ECM synthesis	ECM degradation
Cytokines						
Growth regulated oncogene	+++	+	+++			+
Interferon γ	+++	+++		+		+++
Interferon-inducible protein 10	+++	+++	+	+		+++
Interleukin 1α, 1β	+	+++		+++	-	+++
Interleukin 6	+++	+++	+++	+	+	+
Interleukin 8	+	+++		+	-	+++
Interleukin 10	+++	+++	+	-	+	-
Interleukin 17	+	+++		+++	-	+++
Monocyte chemoattractant protein 1, 2	+++	+++	+++	+		+
Oncostatin M	+++	+++	-			-
RANTES	+	+++		+++		+++
Tumor necrosis factor α	+++	+++		+++		+
Growth factors						
Connective tissue growth factor	+++	+++	+++		+++	
Bone morphogenetic protein 2	+	+++	+++	-	+++	+
Bone morphogenetic protein 4	-	+++	+		+++	+
Bone morphogenetic protein 6	-	+++	+		+++	+
Bone morphogenetic protein 7	-	+	+		+++	+
Granulocyte colony-stimulating factor	+++	+++	+++			
Growth differentiation factor 5	-	+++	+++		+	
Insulin-like growth factor 1, 2	+++	+++	+++		+++	
Platelet-derived growth factor	+++	+++	+++		+	
Transforming growth factor β1-3	+++	+++	+++	-	+++	+++
Vascular endothelial growth factor	-	+++	+++			+
Hormones and other regulatory molecules						
Angiotensin 1, 2	-	+++	+++			
Hyaluronic acid	+++	-	+++		+++	
Leptin	+	+++	+++		+++	
Lipoplysaccharide	+	+		+++	+	
Osteopontin	+	+++	+		+	+
Prostaglandin E-2	+	+++	+			+++

Note: Note: the sign '+++' indicates the presence of information in multiple sources and reflects the established view this molecule, '+' denotes a single source on this fact, '-' indicates evidence of a negative effect. Blank cells indicate absence of information.

Based on these data, a list of genes encoding key proteins for the chondrocyte phenotype was compiled. Factors connected to strong pro-apoptotic stimuli are not included. With respect to

future plans to research the possible effectiveness of new scaffolds for tissue engineering in rats, data about genes of human and rat have been included into table 3.

Table 3: Common characteristics of the genes encoding key proteins involved in the differentiation and phenotypic expression of articular chondrocytes

Coding protein	Gene	Gene ID		Function of coding protein
		Human	Rat	
Encoding chondrocyte receptors				
TGF-βR1	*tgfbr2*	7046	29591	Reception of relevant molecules from transforming growth factor β super family.
TGF-βR2	*tgfbr2*	7048	81810	
BMPR-1	*bmpr1a*	657	81507	Reception of bone morphogenetic proteins 2, 4, 6, 7, and growth differentiation factor 5 (BMP-14)
BMPR-2	*bmpr2*	659	140590	
IGFR-1	*igfr1*	3480	25718	Reception of insulin-like growth factor
PDGFR-α	*pdgfra*	5156	25267	Reception of platelet-derived growth factor
PDGFR-β	*pdgfrb*	5159	24629	
FGFR2	*fgfr2*	2263	25022	Reception of connective tissue growth factor (CCN2)
FGFR3	*fgfr3*	2261	84489	
IL-6R	*il6r*	3570	24499	Reception of interleukin 6
CXCR1	*cxcr1*	3577	54258	Reception of interleukin 8
CXCR2	*cxcr2*	3579	29385	
CD44	*cd44*	960	25406	Reception of hyaluronic acid
LEPR	*lepr*	3953	24536	Reception of leptin
Encoding common ECM components				
Aggrecan	*acan*	176	58968	Base proteoglycan of cartilage ECM
Collagen type II	*col2a1*	1280	25412	Base protein of cartilage ECM
MMP-3	*mmp3*	4314	171045	Common matrix metalloproteinases of cartilage involving to its remodeling and ECM degradation
MMP-13	*mmp13*	4322	171052	
TIMP1	*timp1*	7076	116510	The specific inhibitors of matrix metalloproteinases involving to ECM protection
TIMP3	*timp3*	7078	25358	
Encoding autocrine and paracrine regulators				
Intergin β1	*itgb1*	3688	24511	Key protein of cell adhesion in skeletal tissues
Hypoxia inducible factor 1α	*hif1a*	3091	29560	The inducible regulator of cellular metabolism by activating transcription
Nuclear protein 1	*nupr1*	26471	100912108	Stress-inducible protein involved in gene transcription including MMP-13 expression
Tenascin C	*tnc*	3371	116640	Extracellular matrix protein, controlling the spatial and temporal distribution of ECM

The data presented in table, in our opinion, could be used to design DNA probes for mapping the gene expression in native and altered cartilage, to detail the mechanisms of its formation and remodeling under the physiological and pathogenic conditions. Secondly, this information is useful to connect elements of gene therapy to replacement technology of cartilage defects in clinical practice.

In order to choose the main directions in modification of existing scaffolds for cartilage tissue engineering, it is necessary to map them to current structure with general organization of the surrounding cartilage. Ideally, the cartilage, formed at the site of implantation after scaffold remodeling, should have a similar structure. Figure 2A presents a schematic structure of articular cartilage, taking into account the presence of zones, distinguished by the morphology of chondrocytes and ECM, as well as microclusters presence.

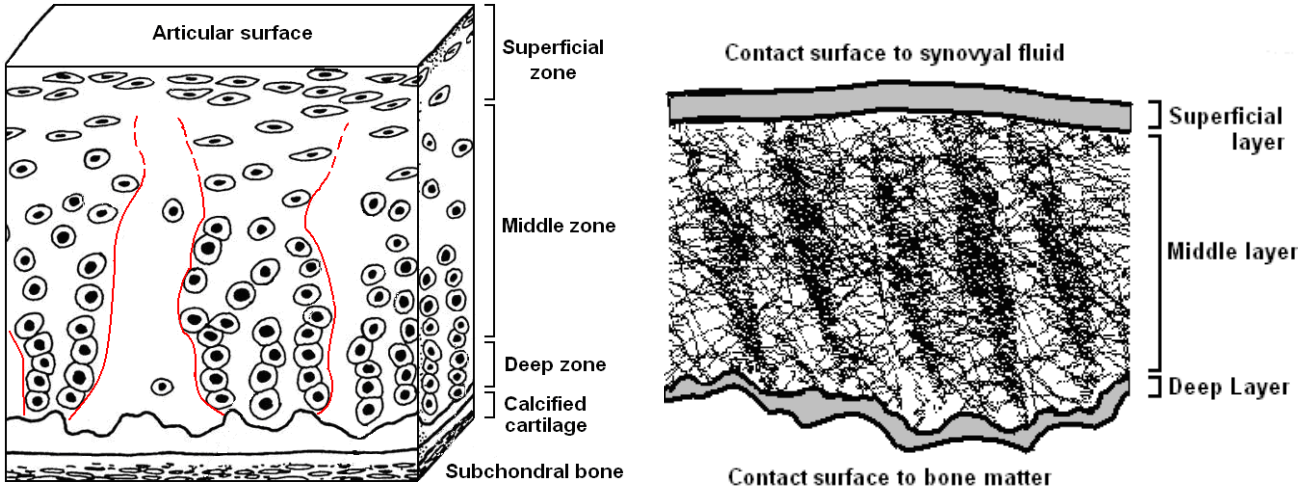

Figure 2. A. Scheme illustrates zonal organization of the articular cartilage with the selection of microclusters (bordered by red lines). B. Hypothetic model of scaffold for cartilage tissue engineering based on principles of zonal and mosaic organization of natural articular cartilage. Explanations are in the text.

Based on these representations, it is not sufficient for bulk of scaffold to have the three-dimensional porous structure for cell seeding (1), and certain strength to ensure early load on the articular surface after implantation (2). This part of scaffold should initially contain certain irregularities look like seal columns the size of about 100-150 microns. They should become the basis for microcluster formation in the remodeling matter scaffold into cartilage ECM (fig. 2b).

To ensure the specific properties of scaffold surface layer ought to be an important aspect of scaffold building. In most existing tissue engineering constructions, this task is left to nature, so that surface lubricants were formed by the active function of the synovial fluid. It seems appropriate to provide neo-formed articular surface of the lubricating layer with a thickness of about 50 μm in the first few days after implantation. For example, it can be done by applying hyaluronate gel on the outer scaffold surface.

Structural features of the scaffold deep layer depend on the depth of the defect, they should provide strong fixation to the underlying bone and, at the same time, the possibility of cell seeding and diffusion of necessary substances in remodeling area. It is here, in our opinion, should be placed microspheres containing the required number of growth factors for the successful trigger of cellular differentiation and providing the necessary chondrocyte phenotype.

Discussion

Thinking about the need to provide adaptability to environmental changes for a certain area through the formation of irregular structures with conditional repetitive elements is a consequence of the cellular principle of Life organization and general biological principle of mosaicism. In this sense, our findings are not inconsistent with recent detailed studies of the articular cartilage, including the use of computer-conversion and modeling [2, 7, 29].

Microcluster described in our study, should be distinguished from pathological clusters of chondrocytes in osteoarthritis. These structures are formed with long-term progression of the disease, they are mainly located in the deep zone of the cartilage, and not surrounded by a dense ECM [30].

Possible mechanisms for the formation of such clusters from cellular columns, most likely conclude in the spatial characteristics of molecular signal distribution near tidemark in connection to the heterogeneity of underlying bone surface. One of the mechanisms leading to the advanced differentiation of some cellular groups may be earlier deprivation of oxygenation. As the formation of dense territorial and extraterritorial ECM, the mechanical stimuli, as a result of total redistribution of mechanical loads from the articular surface, are connected to these mechanisms.

Such switching and mechanisms of mechanic signal reception have been recently described directly in the cartilage [29].

Range markers of chondrocyte phenotype, formed in this research, meet the tasks used to improve and monitor the results of the cartilage tissue engineering. They could change significantly if, for example, we are talking about the cultivation of chondrocytes on artificial media. The results of mapping the lubricin, metalloproteinases, their inhibitors, the characteristics of the chondrocyte receptors, as well as the role of these differences in functioning and remodeling of ECM appeared very recently [13, 31-33]. In relation to apoptosis of chondrocytes the discussion is still ongoing due to the ambiguity of the propagation mechanisms of molecular signals in the thickness of the cartilage [15, 34].

The elaboration of new principles for the scaffold fabrication in cartilage tissue engineering was practical objective of this research. Articles, where the authors focused on creating scaffolds with zonal structure for these tasks, only appear in the open access [26, 28, 35], but attempts to create structures reproducing the horizontal irregularity of ECM, has not yet been undertaken. This study proves the relevance of this approach in cartilage tissue engineering.

Conclusion

The study suggests that native articular cartilage had a mosaic structure, which was provided by differences in chondrocyte phenotype. Based on bioinformatics approach and mapping the actual chondrocyte phenotype in different areas of articular cartilage it is possible to explain this structural mosaicism. As a result, the intellectual map and database of molecular processes in chondrocytes have been obtained, seems to be suitable for further investigation of the articular cartilage remodeling. The hypothetical model of scaffold to satisfy the conditions of mosaic structure formation in cartilage after substitution of full-layer defects and stimulation of colonization by cells from the bone marrow, may be a basis for future elaboration of scaffold technologies.

Acknowledgements

The reported study was particularly supported by Russian Foundation for Basic Research (Russian Federation), research project No. 4-04-01679 a.

References:

1. Becerra J., Andrades J.A., Guerado E., et al. (2010) Articular cartilage: structure and regeneration. *Tissue Eng Part B Rev*. 16(6), pp. 617-627.

2. Goldring M. B. (2012) Chondrogenesis, chondrocyte differentiation, and articular cartilage metabolism in health and osteoarthritis. *Ther. Adv. Musculoskelet. Dis*. 4 (4), pp. 269-285.

3. Bhosale A.M. (2008) Articular cartilage: structure, injuries and review of management / A.M. Bhosale, J.B. Richardson. *Br. Med. Bull*. 87, pp. 77–95.

4. Tchetina E.V. (2011) Developmental mechanisms in articular cartilage degradation in osteoarthritis. *Arthritis*. ID 683970, 16 pp.

5. Stupina T.A., Schoudlo N.A., Petrovskaya N.V., Stepanov M.A. (2013) Histomorphometric analysis of the knee articular cartilage and synovium for metadiaphyseal leg lengthening (experimental-and-morphological study). Russian Traumatology and Orthopedics *[Travmatologia i Ortopedia Rossii]*. (1), pp.80-86. [in Rus.].

6. Makushin V.D., Stupina T.A. (2014) To the problem of activating the processes regulating articular cartilage structure recovery (Review of literature and our own data). *Genius of Orthopedics [Geniy Ortopedii]*. (1), pp. 82-88. [in Rus.].

7. Mootanah R., Imhauser C.W., Reisse F., et al. (2014) Development and validation of a computational model of the knee joint for the evaluation of surgical treatments for osteoarthritis. *Comput. Methods Biomech. Biomed. Engin*. 17(13), pp. 1502–1517.

8. Novochadov V.V., Alekseenko A.Yu., Krylov P.A., Shuvalova E.Yu. Mosaicism of hyaline cartilage: quantitative morphological study on rabbit elbow joint. *I.P. Pavlov Russian Medical Biological Herald [Rossiyskiy Mediko-Biologicheskiy Vestnik imeni Akademika I.P. Pavlova]*. (3), pp. 33-39. [in Rus.].

9. Novochadov V.V., Krylov P.A. (2014) Heterogeneity of hyaline cartilage matrix density of rabbit knee joint. *J. Clin. Exp. Morphol. (Moscow) [Klinicheskaya i Eksperimental'naya Morfologiya]*. (3), pp. 33-39. [in Rus.].

10. Novochadov V.V., Krylov P.A., Zaytzev V.G. (2014) Clusterization of knee hyaline cartilage in rat with and without experimental osteoarthritis. *J. Volgograd State Univ. 11: Natural Sciences [Vestnik Volgogradskogo Gosudarstvennogo Universiteta. 11: Estestvennye Nauki]*. (4), pp. 6-15. [in Rus.].

11. Wang P., Zhu F., Konstantopoulos K. (2010) Prostaglandin E_2 induces interleukin-6 expression in human chondrocytes via cAMP/protein kinase A- and phosphatidylinositol 3-kinase-dependent NF-κB activation. *Cell Physiol.* 298(6), pp. 1445–1456.

12. Montaseri A., Busch F. (2011) IGF-1 and PDGF-bb Suppress IL-1β-Induced Cartilage Degradation through Down-Regulation of NF-κB Signaling: Involvement of Src/PI-3K/AKT Pathway. *PLoS One.* 6(12), e28663.

13. Doyle J.J., Gerber E.E., Dietz H.C. (2012) Matrix-dependent perturbation of TGF-beta signaling and disease. *FEBS Lett.* 586, pp. 2003–2015.

14. Papathanasiou I., Malizos K.N., Tsezou A. (2012) Bone morphogenetic protein-2-induced Wnt/β-catenin signaling pathway activation through enhanced low-density-lipoprotein receptor-related protein 5 catabolic activity contributes to hypertrophy in osteoarthritic chondrocytes. *Arthritis Res Ther.* 14(2), R82.

15. Byun S., Sinskey Y.L., Lu Y.C., et al. (2013) Transport and binding of tumor necrosis factor-α in articular cartilage depend on its quaternary structure. *Arch. Biochem. Biophys.* 540 (1-2), pp. 1-8.

16. Takahashi N., Knudson C.B., Thankamony S., et. al. (2010) Induction of CD44 cleavage in articular chondrocytes. *Arthritis Rheum.* 62(5), pp. 1338–1348.

17. Chen Y.J., Sheu M.L., Tsai K.S., et al. (2013) Advanced glycation end products induce peroxisome proliferator-activated receptor and down-regulation-related inflammatory signals in human chondrocytes via toll-like receptor-4 and receptor for advanced glycation end products. *PLoS One.* 8(6), e66611.

18. Tsukamoto I., Inoue S., Teramura T., et. al. (2013) Activating types 1 and 2 angiotensin II receptors modulate the hypertrophic differentiation of chondrocytes. *FEBS Open Biol.* 3, pp. 279–284.

19. Krylov P.A. (2014) The grouping of chondrocyte receptors according to their control over cartilage tissue remodeling. *Eur. J. Mol. Biotech.* 2(1), pp. 4-10.

20. Gruber H.E., Hoelscher G.L., Ingram J.A., et al. (2014) Growth and differentiation factor-5 (GDF-5) in the human intervertebral annulus cells and its modulation by IL-1ß and TNF-α in vitro. *Exp. Mol. Pathol.* 96(2), pp. 225-229.

21. Takigawa M. (2013) CCN2: a master regulator of the genesis of bone and cartilage. *J. Cell Commun. Signal.* 7(3), pp. 191-201.

22. Abd El Kader T., Kubota S., Nishida T., et al. (2014) The regenerative effects of CCN2 independent modules on chondrocytes in vitro and osteoarthritis models in vivo. *Bone.* 59, pp. 180-188.

23. Tran C.M., Fujita N., Huang B.L., et al. (2013) Hypoxia-inducible factor (HIF)-1α and CCN2 form a regulatory circuit in hypoxic nucleus pulposus cells: CCN2 suppresses HIF-1α level and transcriptional activity. *J Biol Chem.* 288(18), pp. 12654-12666.

24. Gardner H. (2014) Integrin α1β1. *Adv. Exp. Med. Biol.* 819, pp. 21-39.

25. Jablonski C.L., Ferguson S., Pozzi A., Clark A.L. (2014) Integrin α1β1 participates in chondrocyte transduction of osmotic stress. *Biochem Biophys Res Commun.* 445(1), pp. 184-190.

26. Shen J., Chen D. (2014) Recent progress in osteoarthritis research. *J. Am. Acad. Orthop. Surg.* 22(7), pp. 467–468.

27. Novochadov V.V. (2013) The control of the cell settlement and scaffold remodeling in cartilage tissue engineerng: a review. *J. Volgograd State Univ. 11: Natural Sciences [Vestnik Volgogradskogo Gosudarstvennogo Universiteta. 11: Estestvennye Nauki]*. (1), pp. 19-28. [in Rus.]

28. Steele J.A.M., McCullen S.D., Callanan A., et al. (2014) Combinatorial scaffold morphologies for zonal articular cartilage engineering. *Acta Biomater.* 10(5), pp. 2065–2075.

29. Hubmacher D., Apte S. S. (2013) The biology of the extracellular matrix: novel in-sights. *Curr. Opin. Rheumatol.* 25 (1), pp. 65-70.

30. Lotz M.K., Otsuki Sh., Grogan Sh.P., et al. (2010) Cartilage cell clusters. *Arthritis Rheum.* 62 (8), pp. 2206–2218.

31. Wu G., Zhu L., Dent J.E., Nardini C. (2010) A comprehensive molecular interaction map for rheumatoid arthritis. *PLoS ONE* 5(4), e10137.

32. Andrades J.A., Motaung S.C., Jiménez-Palomo P. (2012) Induction of superficial zone protein (SZP)/lubricin/PRG 4 in muscle-derived mesenchymal stem/progenitor cells by transforming growth factor-β1 and bone morphogenetic protein-7. *Arthritis Res. Ther.* 14(2), R72.

33. Wang J., Lü D., Mao D., Long M. (2014) Mechanomics: an emerging field between biology and biomechanics. *Protein Cell.* 5(7), pp. 518–531.

34. Wang Y., de Li L., Zhang X. B., et al. (2013) Increase of TNF-α-stimulated osteoarthritic chondrocytes apoptosis and decrease of matrix metalloproteinases-9 by NF-κB inhibition. *Biomed. Environ. Sci.* 26, pp. 277-283.

35. Meszaros E., Malemud C. J. (2012) Prospects for treating osteoarthritis: enzyme–protein interactions regulating matrix metalloproteinase activity. *Ther. Adv. Chronic Dis.* 3. pp. 219-229.

Примечания:

1. Becerra J., Andrades J.A., Guerado E., et al. Articular cartilage: structure and regeneration // Tissue Eng Part B Rev. – 2010. – Vol. 16, № 6. – P. 617-627.

2. Goldring M.B. Chondrogenesis, chondrocyte differentiation, and articular cartilage metabolism in health and osteoarthritis // Ther. Adv. Musculoskelet. Dis. – 2012. – Vol. 4, № 4. – P. 269-285.

3. Bhosale A.M., Richardson J.B. Articular cartilage: structure, injuries and review of management // Br. Med. Bull. – 2008. – Vol. 87. – P. 77–95.

4. Tchetina E.V. Developmental mechanisms in articular cartilage degradation in osteoarthritis // *Arthritis.* – 2011. – ID 683970, 16 pp.

5. Ступина Т.А., Щудло Н.А., Петровская Н.В., Степанов М.А. Гистоморфометрический анализ суставного хряща и синовиальной оболочки коленного сустава при метадиафизарном удлинении голени (экспериментально-морфологическое исследование) Травматология и ортопедия России. – 2013. – № 1 (67). – С. 80-86.

6. Макушин В.Д., Ступина Т.А. К вопросу об активизации процессов, регулирующих восстановление структуры суставного хряща (обзор литературы и собственные данные) // Гений ортопедии. – 2014. – № 1. – С. 82-88.

7. Mootanah R., Imhauser C.W., Reisse F., et al. Development and validation of a computational model of the knee joint for the evaluation of surgical treatments for osteoarthritis // Comput. Methods Biomech. Biomed. Engin. – 2014. – Vol. 17, № 13. – P. 1502–1517.

8. Новочадов В.В., Алексеенко А.Ю., Крылов П.А., Шувалова Е.Ю. Признаки мозаичного строения гиалинового хряща: количественное морфологическое исследование локтевого суставов кролика // Российский медико-биологический вестник им. академика И.П. Павлова. – 2014. – № 3. – С. 33-39.

9. Новочадов В.В., Крылов П.А., Зайцев В.Г. Неоднородность строения гиалинового хряща коленного сустава у интактных крыс и при экспериментальном остеоартрозе // Вестник Волгоградского государственного университета. Серия 11: Естественные науки. – 2014. – № 4. – С. 6-15.

10. Новочадов В.В., Крылов П.А. Гетерогенность распределения плотности матрикса в гиалиновом хряще: доказательства при исследовании коленного сустава кролика // Клиническая и экспериментальная морфология. – 2014. – № 3. – С. 33-39.

11. Wang P., Zhu F., Konstantopoulos K. Prostaglandin E_2 induces interleukin-6 expression in human chondrocytes via cAMP/protein kinase A- and phosphatidylinositol 3-kinase-dependent NF-κB activation // Cell Physiol. – 2010. – Vol. 298, № 6. – P. 1445–1456.

12. Montaseri A., Busch F. IGF-1 and PDGF-bb suppress IL-1β-induced cartilage degradation through down-regulation of NF-κB signaling: involvement of Src/PI-3K/AKT pathway // PLoS One. – 2011. – Vol. 6, № 12. – e28663.

13. Doyle J.J., Gerber E.E., Dietz H.C. Matrix-dependent perturbation of TGF-beta signaling and disease // FEBS Lett. – 2012. – Vol. 586. – P. 2003–2015.

14. Papathanasiou I., Malizos K.N., Tsezou A. Bone morphogenetic protein-2-induced Wnt/β-catenin signaling pathway activation through enhanced low-density-lipoprotein receptor-related protein 5 catabolic activity contributes to hypertrophy in osteoarthritic chondrocytes // Arthritis Res Ther. – 2012. – Vol. 14, № 2. – R82.

15. Byun S., Sinskey Y.L., Lu Y.C., et al. Transport and binding of tumor necrosis factor-α in articular cartilage depend on its quaternary structure // Arch. Biochem. Biophys. – 2013. – Vol. 540, № 1-2. – P. 1-8.

16. Takahashi N., Knudson C.B., Thankamony S., et. al. Induction of CD44 cleavage in articular chondrocytes // Arthritis Rheum. – 2010. – Vol. 62, № 5. – P. 1338–1348.

17. Chen Y.J., Sheu M.L., Tsai K.S., et al. Advanced glycation end products induce peroxisome proliferator-activated receptor and down-regulation-related inflammatory signals in human chondrocytes via toll-like receptor-4 and receptor for advanced glycation end products // PLoS One. – 2013. – Vol. 8, № 6. – e66611.

18. Tsukamoto I., Inoue S., Teramura T., et. al. Activating types 1 and 2 angiotensin II receptors modulate the hypertrophic differentiation of chondrocytes. *FEBS Open Biol.* (2013) 3, pp. 279–284.

19. Krylov P.A. The grouping of chondrocyte receptors according to their control over cartilage tissue remodeling // Eur. J. Mol. Biotech. – 2014. – Vol. 2, № 1. – P. 4-10.

20. Gruber H.E., Hoelscher G.L., Ingram J.A., et al. Growth and differentiation factor-5 (GDF-5) in the human intervertebral annulus cells and its modulation by IL-1ß and TNF-α in vitro // Exp. Mol. Pathol. – 2014. – Vol. 96, № 2. – P. 225-229.

21. Takigawa M. CCN2: a master regulator of the genesis of bone and cartilage // J. Cell Commun. Signal. – 2013. – Vol. 7, № 3. – P. 191-201.

22. Abd El Kader T., Kubota S., Nishida T., et al. The regenerative effects of CCN2 independent modules on chondrocytes in vitro and osteoarthritis models in vivo // Bone. – 2014. – Vol. 59. – P. 180-188.

23. Tran C.M., Fujita N., Huang B.L., et al. Hypoxia-inducible factor (HIF)-1α and CCN2 form a regulatory circuit in hypoxic nucleus pulposus cells: CCN2 suppresses HIF-1α level and transcriptional activity // J. Biol. Chem. – 2013. – Vol. 288, № 18. – P. 12654-12666.

24. Gardner H. Integrin α1β1 // Adv. Exp. Med. Biol. – 2014. – Iss. 819. – P. 21-39.

25. Jablonski C.L., Ferguson S., Pozzi A., Clark A.L. Integrin α1β1 participates in chondrocyte transduction of osmotic stress // Biochem. Biophys. Res. Commun. – 2014. – Vol. 445, № 1. – P. 184-190.

26. Shen J., Chen D. Recent progress in osteoarthritis research // J. Am. Acad. Orthop. Surg. – 2014. – Vol. 22, № 7. – P. 467–468.

27. Новочадов В.В. Проблема управления клеточным заселением и ремоделированием тканеинженерных матриц для восстановления суставного хряща (обзор литературы). Вестник Волгоградского государственного университета. Серия 11: Естественные науки. – 2013. – № 1. – P. 19-28.

28. Steele J.A.M., McCullen S.D., Callanan A., et al. Combinatorial scaffold morphologies for zonal articular cartilage engineering // Acta Biomater. – 2014. – Vol. 10, № 5. – P. 2065–2075.

29. Hubmacher D., Apte S. S. The biology of the extracellular matrix: novel in-sights // Curr. Opin. Rheumatol. – 2013. – Vol. 25, № 1. – P. 65-70.

30. Lotz M.K., Otsuki Sh., Grogan Sh.P., et al. Cartilage cell clusters // Arthritis Rheum. – 2010. – Vol. 62, N8. – P. 2206–2218.

31. Wu G., Zhu L., Dent J.E., Nardini C. A comprehensive molecular interaction map for rheumatoid arthritis // PLoS ONE. – 2010. – Vol. 5, № 4. – e10137.

32. Andrades J.A., Motaung S.C., Jiménez-Palomo P. Induction of superficial zone protein (SZP)/lubricin/PRG 4 in muscle-derived mesenchymal stem/progenitor cells by transforming growth factor-β1 and bone morphogenetic protein-7 // Arthritis Res. Ther. – 2012. – Vol. 14, № 2. – R72.

33. Wang J., Lü D., Mao D., Long M. Mechanomics: an emerging field between biology and biomechanics // Protein Cell. – 2014. – Vol. 5, № 7. – P. 518–531.

34. Wang Y., de Li L., Zhang X. B., et al. Increase of TNF-α-stimulated osteoarthritic chondrocytes apoptosis and decrease of matrix metalloproteinases-9 by NF-κB inhibition // Biomed. Environ. Sci. – 2013. – Vol. 26. – P. 277-283.

35. Meszaros E., Malemud C.J. Prospects for treating osteoarthritis: enzyme–protein interactions regulating matrix metalloproteinase activity // Ther. Adv. Chronic Dis. – 2012. – Vol. 3. – P. 219-229.

УДК 616.72-018.3 : 577.3

Различия фенотипа хондроцитов в составе суставного хряща: картирование, возможные механизмы и влияние на приживление имплантатов

[1] Валерий Валерьевич Новочадов
[2] Кристина Александровна Бовольская
[2] Софья Алексеевна Липницкая
[2] Екатерина Владимировна Перевалова
[2] Екатерина Юрьевна Шувалова
[2] Зоя Николаевна Загребина
[3, 4] Валерий Геннадьевич Зайцев

[1] Волгоградский государственный университет, Российская Федерация
400062, г. Волгоград, пр. Университетский, 100
Доктор медицинских наук, профессор
E-mail: novovv@rambler.ru
[2] Волгоградский государственный университет, Российская Федерация
400062, г. Волгоград, пр. Университетский, 100
Студент
E-mail: biobio@volsu.ru
[3] Волгоградский государственный университет, Российская Федерация
400062, г. Волгоград, пр. Университетский, 100
Кандидат биологических наук, доцент
E-mail: biobio@volsu.ru
[4] Волгоградский государственный медицинский университет, Российская Федерация
400131, г. Волгоград, пл. Павших борцов, 1
Кандидат биологических наук, доцент
E-mail: valeryzaitsev@gmail.com

Аннотация

На основании биоинформационного поиска и сопоставления с реальным фенотипом хондроцитов выбран спектр биологически активных молекул-регуляторов и их рецепторов, имеющих отношение к формированию мозаичных структур в неизмененном хряще и их ремоделированию при развитии экспериментального остеоартроза. Как итог, получена интеллектуальная карта молекулярных процессов в хондроците, сопряженная с базой знаний об этих молекулах, пригодная для дальнейшего исследования процессов ремоделирования суставного хряща. Предложена гипотетическая модель скаффолда, удовлетворяющая условиям формирования мозаичной структуры хряща после имплантации на место полнослойных дефектов хряща в условиях стимуляции заселения клетками из костного мозга.

Ключевые слова: суставной хрящ; тканевая инженерия; скаффолды; остеоартроз; молекулярное картирование.

Published in the Russian Federation
European Journal of Molecular Biotechnology
Has been issued since 2013.
ISSN: 2310-6255
E-ISSN 2409-1332
Vol. 6, No. 4, pp. 223-228, 2014

DOI: 10.13187/ejmb.2014.6.223
www.ejournal8.com

UDC 616

Determination of Effect of Substrate Concentration and Dilution of Inoculums on Population Dynamics of *Pseudomonas Fluorescens*

[1]* Ajay Tomer
[2] Ramji Singh,
[3] Manoj Kumar Maurya

[1-3] Sardar Vallabhbhi Patel University of Agriculture & Technolody, Meerut, India
250110 (UP)
Department of Plant Pathology
*Corresponding Author's E-mail: ajaytomer1489@gmail.com

Abstract

Deoiled cakes of Neem and Jatropha served as source of diversified nutrition for Pseudomonas flourescens when used as substrate for mass culturing of antagonist. The present investigation were undertaken to test the suitability of neem and Jatropha cakes for liquid Concentration and longevity of Pseudomonas flourescens in vitro. Increasing the dilution of stock of initial inoculums resulted in decrease of total viable counts of Pseudomonas flourescens was comparatively highest population (64.67×10^5) and (201.67×10^5) lesser after 15 days than after 7 days of inoculation on Neem and Jatropha cake concentration respectively.

Keywords: Deoiled Neem cake; Jatropha cake concentration; moisture level; *Pseudomonas flourescens*.

Introduction

Many agro-industrial bioproducts such as deoiled cakes of tree born oils seeds (TBOs) like Neem and Jatropha which are either going waste or being used as a less profitable and usable products since quite long time. The oils extracted from Neem and Jatropha, are either directly used as bio-fuel or as raw material for industrial inputs in various manufacturing industries like cosmetics, agrochemicals and pharmaceuticals (Tiwari, et.al. 2007). Deoiled cakes of these trees remain either unexploited or poorly exploited. These deoiled cakes contains lot of carbohydrates, proteins, fatty acids, minerals and many more biochemical constituents which are served as source of nutrition for beneficial micro-organisms (growth promoting and biocontrol agents) in crop cultivation, Patolia *et al.* (2007), hence might being exploited as substrate for mass multiplication of bacterial bio-control agents such as *Pseudomonas flourescens*. Mass multiplication of *Pseudomonas flourescens* on deoiled cakes of these TBOs may be a boon for popularization of bio-control of plant diseases and thereby for crop cultivation, utilization and popularization of Neem and Jatropha as well. Mass multiplication of *Pseudomonas fluorescens* will not only leads to value added products development from deoiled cakes of Neem and Jatropha; rather it will prevent huge wastage and misuse of these by-products.

Mass culture available in the market generally shows poor efficacy after application in the crop field. This is probably due to long duration taken in transportation from manufacturing unit

to the users (farmers). The mass cultures made at industrial scale are generally talc based, with no nutritional background to support the life of BCAs during storage, transportation and other stress. Deoiled cakes of TBOs may serve as source of diversified nutrition for BCAs when used as substrate for mass culturing of antagonists.

Material and Methods

Collection of soil samples and isolation of biocontrol agent

To isolate the biocontrol agent *i.e.*, *Pseudomonas fluorescens* from tomato crop rhizosphere, soil samples were collected from crop research centre (CRC) of university. For isolation, one gm of soil sample was placed in a 250 ml conical flask containing 100 ml of sterilized distilled water (SDW) and mixed thoroughly. Different dilutions of working samples were prepared by serially diluting the stock solution (10^{-8}). 1 ml of last serial dilution *i.e.*, 10^{-8} was spread on *Pseudomonas fluorescens* Selective king's B Medium (King's et.al 1954) for isolation of *Pseudomonas fluorescens*. The plates were incubated for 2 days at 37±2°C and after incubation, pure culture was grown; colour of bacterial colony was initially yellow but turned yellow green as pigmentation were produced (Bonds 1957).

Composition of Culture media:
Pseudomonas fluorescens (Selective) King's B Medium (King et, al, 1954)
Composition:

Peptone	20gm
Agar-agar	20gm
Potassium monophosphate (k2Hpo4)	1.5gm
Magnesium sulphate (Mgso4)	1.5gm
Glycerol	10ml
Distilled water	1000 ml

Preparation:

After mixing all the ingredients with distilled water, media was placed into a stainless steel pan and steered with glass rod for proper mixing of all the ingredients. Now the medium was filtered through a muslin cloth by squeezing out whole liquid. 200 ml medium was placed in each 500 ml capacity flasks. Flasks were tightly plugged with non-absorbent cotton plug and wrapped with butter paper and rubber band. Medium was autoclaved at 1.1 kg/cm² pressure for 20 min at 121.6°C and cooled before pouring into Petri plates.

Maintenance of the culture

The Bacteria initially isolated in a pure culture on King's B media and sub cultured on PDA slants were allowed to grow at 28±2°C temperature. The culture thus obtained was stored in refrigerator at 5°C for further studies and was sub cultured periodically.

Determination of effect of substrate concentration and dilution of inoculums on Population dynamics of *Pseudomonas fluorescens*

Initially the *Pseudomonas fluorescens* cultures were grown in King,s B broth medium at 28 ±2°C for 2 days. After 2 days of incubation, a serial dilution of 10^{-5}, 10^{-6}, 10^{-7} and 10^{-8} were prepared by the method given at above.

Results and Discussion

Present studies entitled "Longevity and Survival of *Pseudomonas fluorescens* on neem and jatropha cakes" were conducted under laboratory and pot conditions with the objectives to determine the suitability of deoiled cakes of Neem and Jatropha for mass multiplication of *P .fluorescens in vitro* and to determine the longevity of *P .fluorescens* grown on two deoiled cakes in the rhizosphere of tomato at the Department of Plant Pathology, S.V.P. University of Agriculture & Technology, Meerut.

Effect of substrates concentration on population of *Pseudomonas fluorescens:* Population of *Pseudomonas fluorescens* on different concentration of Neem cake extract after 7 days:

The colony forming unit (CFUs) of *Pseudomonas fluorescens* showed variation in different concentration of substrates i.e deoiled Neem cake extract and deoiled Jatropha cake extract after 7 days and 15 days interval as given in table 1, 2, 3 and 4 respectively. It is evident from table-1.1 that with the inoculation of 10^{-5} dilution of *Pseudomonas flourescens* stock of initial inoculums, recovery of *Pseudomonas fluorescens CFUs* were towards increasing with increasing concentration of substrate which were 42.33×10^5, 72.00×10^5, 80.00×10^5, 171.67×10^5, 193.67×10^5, and 201.67×10^5 CFUs of *P .fluorescens* at 5%, 10%, 15%, 20%, 25% and 30% concentration respectively of Neeem cake extract after 7 days of inoculation. With the inoculation of 10^{-6}. dilution of *P .fluorescens* cfus stock of initial inoculums in the different concentration of Neem cake extract population of *Pseudomonas fluorescens* recovered after 7 days of inoculatin also showed increasing trends which were 39.00×10^6, 63.00×10^6, 70.33×10^6, 118.00×10^6, 156.00×10^6 and 184.67×10^6 at 5%, 10%, 15%, 20%, 25% and 30% concentration respectively of Neem cake extract.

Table 1: Longevity and survivability of *Pseudomonas fluorescens* in Neem cake extract of different concentration at various dilution point with different moisture level for 7 and 15 days

Concentration Dilution	0%	5%	10%	15%	20%	25%	30%
10^5	22.00	42.33	72.00	80.00	171.67	193.67	201.67
10^6	21.00	39.00	63.00	70.33	118.00	156.00	184.67
10^7	20.00	30.67	48.00	54.00	96.33	145.00	175.00
10^8	19.00	23.33	34.33	41.00	76.00	133.67	165.00
CD @ 5% Dilution =1.3523 Concentration= 1.6563 DxC= 3.313							

7 Days

With inoculation of 10^{-7} dilution of *P .fluorescens* CFUs stock into different concentration of Neem cake extract, there was recovery of 30.67×10^7 48.00×10^7 54.00×10^7, 96.33×10^7, 145.00×10^7 and 175.00×10^7 CFUs at 5%, 10%, 15%, 20%, 25% and 30% concentration respectively of Neem cake extract after 7 days. With the inoculation at 10^{-8} dilution of *Pseudomonas fluorescens* CFUs stock, recovery of *P. flourescens* population recorded were 23.33×1010^8, 34.33×10^8, 41.00×10^8, 76.00×10^8, 133.67×10^8 and 165.00×10^8 at 5%, 10%, 15%, 20%, 25% and 30% concentration respectively of neem cake extract after 7 days of inoculation. It was observed that the level of CFUs, get increased with increasing in substrates concentration i.e from 5% to 30%. Unless mentioned otherwise level of CFUs recorded with different dilution of initial inoculums of *P.flourescens* i.e 10^{-5} to 10^{-8} and from different concentration of substrate i.e. from 5% to 30% at each 5% interval were significantly different from each other. In plain PDA (Check) no of cfus were quite less (24, 24, 24 and 23) than the PDA added with different concentration of substrate.

Table 2: Population of *Pseudomonas fluorescens* after 15 days:

As given in table 1, it was observed that level of *P.flourescens* population density was comparatively less after 15 days of inoculation than after 7 days. However rest of the trends of population dynamics were same as it was observed after 7days. With the inoculation of 10^{-5} dilution of *Pseudomonas flourescens* stock of initial inoculum, recovery of CFUs, were, 27.00×10^5, 34.67×10^5, 41.00×10^5, 45.67×10^5, 52.23×10^5 and 64.67×10^5 from 5%, 10%, 15%, 20%, 25% and 30% concentration respectively of Neem cake extract. With inoculation of 10^6 dilution of *P .fluorescens* stock of initial inoculums, recovery of CFUs, were. 27.00×10^6, 21.67×10^6, 33.67×10^6, 38.00×10^6, 44.00×10^6, and 56.00×10^6 from 5%, 10%, 15%, 20%, 25% and 30% concentration respectively of Neem cake extract after 15 days of inoculation.

Concentration Dilution	0%	5%	10%	15%	20%	25%	30%
10^5	20.00	27.00	34.67	41.00	45.67	52.33	64.67
10^6	18.00	27.00	21.67	33.67	38.00	44.00	56.00
10^7	17.00	27.00	17.00	27.00	32.67	38.33	45.67
10^8	16.00	27.00	16.00	23.00	26.00	31.00	42.00
CD @ 5% Dilution = 0.9931 Concentration= 1.2163 DxC= 2.433							

15 days

With the inoculation of 10^{-7} dilution of *P .fluorescens* stock of initial inoculums, recovery of CFUs were, 27.00×10^7, 17.00×10^7, 27.00×10^7, 32.67×10^7, 38.33×10^7 and 45.67×10^7 from 5%, 10%, 15%, 20%, 25% and 30% concentration respectively of neem cake extract after 15 days of inoculation.

With inoculation of 10^{-8} dilution of *P .fluorescens* stock of initial inoculum recovery of CFUs, were 27.00×10^8, 16.00×10^8, 23.00×10^8, 26.00×10^8, 31.00×10^8 and 42.00×10^8 from 5%, 10%, 15%, 20%, 25% and 30% concentration respectively of Neem cake extract. Unless mentioned otherwise level of CFUs recorded with different dilution of initial inoculums of *P.flourescens* i.e 10^{-5} to 10^{-8} and from different concentration of substrate i.e. from 5% to 30% at each 5% interval were significantly different from each other except at 5% moisture after where all dilution resulted in similar level of population density. In check plates the cfus of *P.flourescens* were 15,15,14 and 13 at all four dilutions respectively.

Population of *Pseudomonas fluorescens* on different concentration on Jatropha cake extract after 7 days:

Inoculation of 10^{-5} dilution of *Pseudomonas fluorescens* stock of initial inoculum in the different concentration of Jatropha cake extract it resulted in increasing population density of *Pseudomonas fluorescens* with increasing concentration of Jatropha cake extract (Table-3). Population densities recovered were 74.67×10^5, 110.33×10^5, 138.33×10^5, 166.33×10^5, 214.67×10^5 and 245.00×10^5 CFUs of *P .fluorescens* from 5%, 10%, 15%, 20%, 25% and 30% concentration respectively of Jatropha cake extract after 7 days of inoculation.

Table 3: Longevity and survivability of *Pseudomonas fluorescens* in Jatropha cake extract of different concentration at various dilution point with different moisture level for 7 and 15 days

Concentration Dilution	0%	5%	10%	15%	20%	25%	30%
10^5	40.00	74.67	110.33	138.33	166.33	214.67	245.00
10^6	38.00	108.67	123.00	116.33	142.67	192.67	213.3
10^7	34.00	63.00	71.00	92.00	127.00	162.33	194.67
10^8	30.00	56.67	66.33	88.67	113.67	144.33	183.00
CD @ 5% Dilution = 4.5911 Concentration= 5.6229 DxC= 11.246							

7 days

With the inoculation of 10^{-6} dilution of *P .fluorescens* stock of initial inoculum into different concentrations of Jatropha cake extract there was recovery of 108.67×10^6, 123.00×10^6, 116.33×10^6,

142.67×10⁶, 192.67×10⁶ and 213.33××10⁶ CFUs of *P .fluorescens* from 5%, 10%, 15%, 20%, 25% and 30% concentration respectively of Jatropha cake extract after 7 days of inoculation. With inoculation of 10^{-7} dilution of *P .fluorescens* stock of initial inoculum to different concentration of Jatropha cake there was recovery of 63.00×10⁷, 71.00×10⁷, 92.00×10⁷, 127.00×10⁷, 162.33×10⁷ and 194.67×10⁷ CFUs of *P .fluorescens* from 5%, 10%, 15%, 20%, 25% and 30% concentration respectively of Jatropha cake extract after 7 days of inoculation.

With inoculation of 10^{-8} dilution of *P .fluorescens* stock of initial inoculum into different concentration of Jatropha cake extract, there was recovery of 56.67×10⁸, 66.33×10⁸, 88.67×10⁸, 113.67×10⁸, 144.33×10⁸ and 183.00×10⁸ CFUs of *P .fluorescens* from 5%, 10%, 15%, 20%, 25% and 30% concentration respectively of Jatropha cake extract after 7 days of inoculation. In this case also the level of population of *P .fluorescens* get increased with the increasing concentration of substrates, whereas increasing the dilution of *P .fluorescens* for inoculation resulted in decreasing level of population of *P .fluorescens*. Unless mentioned otherwise level of CFUs recorded with different dilution of initial inoculums of *P.flourescens* i.e 10^{-5} to 10^{-8} and from different concentration of substrate i.e. from 5% to 30% at each 5% interval, were significantly different from each other.

Table 4: Population of *Pseudomonas fluorescens* after 15 days:

As already observed in case of neem cake extract, here also level of *P.flourescens* population density was comparatively less after 15 days of inoculation than after 7 days (Table 4). After 15days of inoculation of a stock dilution of 10^{-5} of initial inoculums resulted in increasing number of CFUs of *Pseudomonas fluorescens* with increasing concentration of substrates. There was recovery of 31.33×10⁵, 42.67×10⁵, 52.67×10⁵, 59.00×10⁵, 73.33×10⁵ and 78.00×10⁵ number of CFUs of *Pseudomonas fluorescens* from 5%, 10%, 15%, 20%, 25% and 30% concentration respectively of Jatropha cake extract after 15 days of inoculation.

Concentration Dilution	0%	5%	10%	15%	20%	25%	30%
10^5	17.00	31.33	42.67	52.67	59.00	73.33	78.00
10^6	16.00	25.67	31.00	39.00	43.33	52.33	56.00
10^7	15.00	14.00	17.00	21.00	24.00	28.00	34.00
10^8	14.00	11.00	14.00	19.33	22.00	25.00	31.00
CD @ 5% Dilution = 1.0600 Concentration= 1.2982 DxC= 2.596							

15 days

With inoculation of 10^{-6} dilution of *P .fluorescens* stock of initial inoculum there was recovery of 25.67×10⁶, 31.00×10⁶, 39.00×10⁶, 43.33×10⁶ 52.33×10⁶ and 56.00×10⁶ number of *P .fluorescens* CFUs from 5%, 10%, 15%, 20%, 25% and 30% concentration respectively of Jatropha cake extract after 15 days of inoculation.

With inoculation of 10^{-7} dilution of *P .fluorescens* stock of initial inoculums, there was recovery of 14.00×10⁷, 17.00×10⁷, 21.00 ×10⁷, 24.00×10⁷, 28.00×10⁷, and 34.00×10⁷, number of CFUs of *P .fluorescens* from 5%, 10%, 15%, 20%, 25% and 30% concentration respectively of Jatropha cake extract after 15 days of inoculation. With the inoculation 10^{-8} dilution of *P .fluorescens* stock of initial inoculums, there was recovery of 11.00×10⁸, 14.00×10⁸, and 19.33×10⁸, 22.00×10⁸, 25.00×10⁸ and 31.00×10⁸ number of CFUs of *P .fluorescens* from 5%, 10%, 15%, 20%, 25% and 30% concentration respectively of Jatropha cake extract after 15 days of inoculation. Unless mentioned otherwise level of CFUs recorded with different dilution of initial inoculums of *P.flourescens* i.e 10^{-5} to 10^{-8} and from different concentration of substrate i.e. from 5% to 30% at

each 5% interval were significantly different from each other. Level of cfus in plain PDA were 15, 15, 14 and 13 with inoculation of different dilution of inoculums of *P .fluorescens*

Effect of substrates concentration on population of *Pseudomonas fluorescens*

Colony forming units of *Pseudomonas fluorescens* showed variation in different concentration of two substrate i.e. neem cake and Jatropha cake. Total viable count was highest (245.00) for the Jatropha cake at 30% concentration after 7 days of inoculation. At the similar concentration of neem cake the total viable count was comparatively less (201.67) after 7 days .Increasing in substrate concentration was directly proportional to total viable count of *Pseudomonas fluorescens*. Increasing in inoculums dilution was universally proportional to total viable count of *Pseudomonas fluorescens*. Total viable count of *Pseudomonas fluorescens* after 15 days were comparatively quite less at all concentration of two substrates and four dilution of inoculums than total viable counts of *Pseudomonas fluorescens* recovered after 7 days. Abhinav *et al.* (2011) evaluates PGPR strain of *Pseudomonas fluorescens PS1* to formulate carrier based bioformulations. The viability of *Pseudomonas fluorescens PS1* was monitored at different time intervals during the period of storage at room temperature in different carriers such as soil, charcoal, sawdust and sawdust-soil. The substrate concentration and therefore medium viscosity would influence the growth of *Pseudomonas fluorescens* Solomon (1983) has also reported that substrate concentration affects the yield of *Saccharomyces cerevisiae* when grown on an assimilable carbohydrate such as glucose or sucrose. Possibly richness of potassium, protein and carbohydrate content in deoiled cakes of neem and jatrofa may be responsible for enhanced growth of *Pseudomonas fluorescens*. Murugalakshmi and Sudha (2010) concluded that agricultural residues rich in carbohydrates can be utilized in fermentation process to produce microbial protein which in turn can be used to determine the factors influencing cell biomass production *Pseudomonas fluorescens* was cultivated using banana peel out, watermelon skin, and Cane molasses showed that the strain was capable of meeting its components required for growth. The organism was capable of growth at 28^{o} C, when supplemented with agricultural wastes in different concentration mixed with agar. The number of colony forming unit were more when compared with nutrient agar. Thus the present findings are well supported by the findings of these workers.

Conclusion

Increasing the dilution of stock of initial inoculums resulted in decrease of total viable counts of *Pseudomonas flourescens*. Population of *Pseudomonas flourescens* was comparatively lesser after 15 days than after 7 days of inoculation.

To achieve comparatively higher population dynamics, of *Pseudomonas fluorescens*, it should be initially grown in king'sB medium and transferred to a basal medium containing 30% concentration of either jatropha cake extract or 30% concentration of neem cake extract.

References

1. Abhinav, A.; Dubey, R.C.; Maheshwari, D.K.; Pandey, P.; Bajpai, K.; Vivek. and Kang and Sun Chul, 2011. PGPR strain *Pseudomonas fluorescens* PS1 was evaluated to formulate carrier based bioformulations.*European Journal of Plant Pathology* l: 81-93.

2. Augustus, G.D.P.S.; Jayabalan, M. and G.J. Seiler. 2002. Evaluation and bioinduction of energy components of Jatropha curcas. *Biomass and Bioenergy*. 23: 161-164.

3. King, E.O.; Ward, M.K. and Raney, D.E., 1954. Two simple media for the demonstration of Pyocyanin and fluorescin. *Journal of Laboratory and Clinical Medicine*, 36: 100-102.

4. Solomons, G. L. 1983. Single Cell Protein. In CRC Critical Reviews in Biotechnology 1: 21-58.

5. Murugalakshmi, C.N. and Sudha, S.S., 2010. The Efficacy of agrowaste on cultivation of *Pseudomonas fluorescens*. A potential biocontrol agent *International Journal of Biological Technology,* 1: 32-34.

6. Patolia, J. S., A. Ghosh., J. Chikara., D. R. Chaudharry., D. R. Parmar., and H. M. Bhuva. 2007. "Response of *Jatropha curcas* L. Grown on Wasteland to N and P Fertilization." Paper presented at the FACT Seminar on *Jatropha curcas* L. Agronomy and Genetics, March 26–28, Wageningen. Article No.34.

7. Tiwari, AK.; Kumar, A, and Raheman, H. 2007. Biodiesel production from jatropha oil (Jatropha curcas) with high free fatty acids: an optimized process. Biomass Bioenergy; 31:569–75.